Institut für Nutzpflanzenwissenschaften und Ressourcenschutz
Pflanzenernährung

Ready for regrowth

A physiological and metabolic characterization of young sugar beets under temporary drought

Dissertation

zur Erlangung des Grades

Doktorin der Agrarwissenschaften (Dr. agr.)

der Landwirtschaftlichen Fakultät

der Rheinischen Friedrich-Wilhelms-Universität Bonn

von

Rita Wedeking

aus

Waldbröl

Bonn 2018

Referent	Prof. emerit. Dr. Heiner E. Goldbach
1. Korreferent	PD Dr. Jürgen Schellberg
2. Korreferent	Prof. Jens Léon
Tag der mündlichen Prüfung	4. Juni 2018

Angefertigt mit der Genehmigung der landwirtschaftlichen Fakultät der Universität Bonn.

Jedes Ding hat seine Zeit.

William Shakespeare
1564-1616

In liebevoller Erinnerung an meinen Vater.

SUMMARY

Although the sugar beet belongs to the rather drought relevant species, water availability plays a crucial role in terms of plant development and yield formation, hence water deficits can lead to adverse consequences. Aim of this work was the physiological and metabolic characterization of young temporarily drought-stressed sugar beets with special emphasis of the recovery process of shoots and roots under rewatering and possible differences thereby. In this work the analysis of the chronological order of physiological and metabolic alterations under drought and rewatering was studied and further how these changes were related to a phenotypic approach, namely infrared thermography (IRT). Besides this, an untargeted ^{1}H nuclear magnetic resonance spectroscopy (^{1}H-NMR) and targeted enzyme based metabolite assays were used for the identification and characterization of major metabolites of the primary metabolism aiming at the identification of the metabolic strategy of temporarily drought-stressed sugar beets. While the experimental setup allowed reproducible greenhouse experiments, the analytic approach has been optimized for both, small scale and high throughput analysis. Within the phenotypic approach using IRT the initial impairment of transpiration as first reaction to drought. However, stress-induced metabolic adaptations with subsequent membrane-destabilization and cellular damage were only detectable by the combined application of invasive and non-invasive methods. Only the combination of both techniques allowed the holistic analysis of drought-induced alterations with close attention to plant water status and osmotic adjustment. The untargeted ^{1}H-NMR-analysis revealed clear stress-induced changes of the primary metabolism and its reprogramming under rewatering. While drought lead rather to a downregulation of glycolysis and TCA-cycle in shoots and roots, amino acids generally increased. The observed distinct dynamics of shoots and roots under rewatering might be ascribed to the different functions of both organs. It can be concluded that the reactions to drought and rewatering are distinct and organ-specific processes that are actively driven by the plant. Moreover, the recovery process does not seem to be only the de-acclimation of the stress and is thus not the simple return to initial control conditions. The presented results contribute to a better understanding of the physiological and metabolic alterations under temporary drought-stress and rewatering in sugar beet and they provide valuable information for the breeding of drought-tolerant species while the applied analytical methods enables a quick and reliable high-throughput metabolite analysis.

KURZFASSUNG

Obwohl die Zuckerrübe zu den eher trockentoleranten Spezies zählt, spielt Wasser bezüglich Entwicklung und Ertragsbildung dennoch eine entscheidende Rolle und eine Limitierung kann zu erheblichen negativen Folgen führen. Ziel dieser Arbeit war die physiologische und metabolische Charakterisierung von jungen Zuckerrüben unter temporärem Trockenstress mit besonderem Fokus auf den Recovery-Prozess von Spross und Wurzel unter Wiederbewässerung und mögliche Unterschiede dabei. Es erfolgte eine Analyse der chronologischen Abläufe von physiologischen und metabolischen Veränderungen unter Trockenstress und Wiederbewässerung, und wie diese im Zusammenhang mit einem phänotypischen Ansatz, der Infrarot-thermographie (IRT), stehen. Darüber hinaus wurde eine Identifizierung und Charakterisierung von Hauptmetaboliten des Primärstoffwechsels zur Untersuchung der metabolischen Strategie von temporär gestressten Zuckerüben mittels Kernspinresonanzspektroskopie (^{1}H nuclear magnetic resonance spectroscopy, ^{1}H-NMR) und enzymbasierten Metabolitanalysen durchgeführt. Der experimentelle Ansatz ermöglichte robuste und reproduzierbare Versuche unter Gewächshausbedingen und die Analytik wurde so optimiert, dass sie sowohl für den Einsatz von kleineren Probenmengen als auch für die Hochdurchsatzanalytik geeignet war. In dem phänotypischen Ansatz, konnte mittels IRT die initiale Beeinträchtigung der Transpiration als erste Reaktion auf Trockenstress festgehalten werden. Die metabolischen Anpassungen auf den Stress mit anschließender Membran-Destabilisierung und Zellschädigung konnten jedoch nur durch die Kombination aus invasiven und nicht-invasiven Verfahren aufgedeckt werden. Nur die Kombination beider Techniken ermöglichte eine ganzheitliche Beurteilung trockenstress-induzierter Veränderungen mit Fokus auf den Wasserhaushalt und die osmotische Anpassung. Die ^{1}H-NMR Analyse legte eindeutige stress-induzierte Veränderungen des Primärstoffwechsels und dessen Umprogrammierung unter Wiederbewässerung offen. Während Trockenheit eher zu einer Herabregulation von Glykolyse und Citratzyklus in Spross und Wurzel führte, reagierten die Aminosäuren mit einem generellen Anstieg. Unter Wiederbewässerung zeigten beide Organe jedoch eine unterschiedliche Dynamik in der Erholungsreaktion, die vermutlich auf die unterschiedlichen Funktionen von Spross und Wurzel zurückzuführen sind. Es handelt sich bei den Reaktionen auf Trockenheit und Wiederbewässerung offenbar um unterschiedliche und organ-spezifische Prozesse. Darüber hinaus scheint der Erholungsprozess keine simple De-Akklimatisierung des Stresses zu sein und ist damit nicht nur die Rückkehr zu Kontrollbedingungen. Die Ergebnisse dieser Arbeit tragen zu einem verbesserten Verständnis der physiologischen und metabolischen Veränderungen unter temporärem Trockenstress und Wiederbewässerung bei und liefern wertvolle Informationen für die Züchtung trockentoleranter Sorten. Die angewendeten Methoden bieten die Möglichkeit auch im Hochdurchsatzverfahren eine schnelle und zuverlässige Analyse durchzuführen.

TABLE OF CONTENTS

LIST OF ABBREVIATIONS

α	Alpha
AA	Amino acids
AA_t	Total amino acid content
AAA	Aromatic amino acid
ADP	Adenosine diphosphate
ATP	Adenosine triphosphate
BBCH	Biologische Bundesanstalt, Bundessortenamt and Chemical Industry
BCAA	Branched chain amino acid
BSA	Bovine serum albumin
Blk	Blank
BioRef	Biological reference
C	Carbon
DAR	Days after rewatering
D_2O	Deuterium oxide
DW	Dry weight
EC	Electrical conductivity
EL	Electrolyte leakage
EL_S	Electrolyte leakage shoot
EDTA	Ethylenediaminetetraacetic acid
EtOH	Ethanol
F6P	Fructose-6-phosphate
FW	Fresh weight
G1P	Glucose-1-phosphate
G6P	Glucose-6-phosphate
G6PDH	Glucose-6-phosphater dehydrogenase
HEPES	4-(2-hydroxyethyl)-1-piperazineethanesulfonic acid
HexP	Hexose phosphates
HNO_3	Nitric acid
HCl	Hydrogen chloride
IRT	Infrared thermography
K	Potassium
KOH	Potassium hydroxide
l	Length
MDA	Malondialdehyde
Mg	Magnesium
$MgCl_2$	Magnesium chloride
MTT	Thiazol blue tetrazolium bromide
N	Nitrogen
Na	Sodium
NAD	Nicotinamide adenine dinucleotide
NADP	Nicotinamide adenine dinucleotide phosphate sodium salt

Table is continued on the next page

LIST OF ABBREVIATIONS - continued

^{1}H-NMR	Proton nuclear magnetic resonance spectroscopy
NNEDA	N(1-Naphtyl)ethylemdiamine dihydrochloride
NO_{3-}	Nitrate
NR	Nitrate reductase
OA	Osmotic adjustment
OD	Optical density
OP	Osmotic potential
OP_S	Osmotic potential shoot
OP_R	Osmotic potential root
PCA	Principal component analysis
PES	Phenazine ethosulfate
PGI	Phosoglucoisomerase
PGM	Phophoglucosmutase
RGB	Red green blue
RH	Relative humidity
RT	Room temperature
RWC	Relative water content
RWC_S	Relative water content shoot
SD	Standards
SPL	Sample
TCA	Trichloroacetic acid
TCA-cycle	Tricarboxylic acid cycle
TSP	Sodium trimethylsilyl [2,2,3,3-d4] propionate
TW	Turgid weight
WC	Water content
WC_{max}	Water capacity maximum
WC_{sub}	Water capacity substrate
YEL	Youngest fully expanded leaf

MEASUREMENT UNITS

%	Percent
Δ	Delta
ε	Extinction coefficient
°C	Degree Celsius
µL	Microliter
µM	Micromolar
cm	Centimeter
g	Gram
kg	Kilogram
L	Liter
m	Meter
M	Mol
mg	Milligram
mL	Milliliter
mm	Millimeter
MPa	Mega Pascal
nm	Nanometer
Ø	Diameter
Osmol kg^{-1}	Osmolality
pF	Soil moisture tension
pH	Pondus hydrogenii
s	Second
u	Unit
v/v	Volume to volume
w/v	Weight to volume
w/w	Weight to weight

LIST OF FIGURES

LIST OF TABLES

GENERAL INTRODUCTION

SUGAR BEET

The sugar beet, *Beta vulgaris* L. *subsp. vulgaris var. altissima* Döll, is the main sugar producing crop in European temperate climates and of high economic importance. The crop account for 25% of the world sugar production (Draycott 2006). In addition, raw sugar plays a crucial role in the chemical industry and extraction residues like beet pulp are used as animal feed and serve as base for quite a number of other products. Since a couple of years, the sugar beet is used for biogas production due to its good fermentation properties compared to other energy crops. The origin of the biennial crop, which belongs to the family of the *Amaranthaceae (formerly Chenopodiaceae)* (Kadereit *et al.* 2003), are the Mediterranean North Sea coastal areas. The oldest findings of the halophytic plant (Marschner *et al.* 1981) are dated to the Neolithic period and were made in the northern part of Holland (Knörzer 1991). The usage of the beet residues found there is not quite clear, but probably only the leaves were used for consumption. In the 16th century, it was discovered that the extract of the sugar beet pulp delivers a sweet syrup and afterwards, in 1747, the chemist Andreas Sigismund Marggraf showed that sugar crystals obtained from the Runkelrübe (*B. vulgaris* L*. var. crassa*), a fodder beet with only 4% sugar content, are chemically identical with the crystals gained from sugar cane (*Saccharum officinarum* L.). Since the Runkelrübe contained less sugar, planters tried to increase the sucrose content by selection. In 1802, the first sugar factory was built by Franz Carl Achard in Kunern (Prussia). Although the main breakthrough for the sugar beet was the Continental Blockade by Napoleon (1809-1814), the low sugar content of 8% was still a reason for the import of sugar cane. Systematic breeding in the following centuries lead to a continuously increasing of sugar contents. Nowadays, the sucrose content of current cultivars reaches 17-22% (fresh weight, w/w) and the sugar beet is still the plant with the highest sugar content for sugar production in Europe.

Despite the broad and continuous changes in the European sugar sector during the recent years and the sugar market worldwide, sugar beet cultivation still provides the base for the German sugar production since more than 200 years. In Europe, approx. 14.9 million tons of sugar were produced in the business year 2015/16, where France is the most important producer with 12.9 t/ha followed by Germany and Poland with 11.3 t/ha and 8.5 t/ha respectively (WZV and VdZ 2016). Main growing regions in Germany are Lower Saxony (Braunschweiger und Hillesheimer Börde), the Rhineland between Bonn and Krefeld (Köln-Aachener Bucht) as well as regions along the rivers Main, Danube and the Lower Rhine region. Further growing areas are located in Württemberg, Saxony, Saxony-Anhalt and Mecklenburg-Western Pomerania. Since environmental and climate change takes place since the

last decades, new breeding approaches and altered needs for cultivation were needed. Thus, breeding strategies do not aim any longer only for an increasing sugar yield.

Due to changes in precipitation and temperature patterns, breeding and research are now aimed more towards drought (e.g. Štajner *et al.* 1995; Ober *et al.* 2005; Romano *et al.* 2012) and cold tolerant cultivars (e.g. Ober and Rajabi 2010; Loel and Hoffmann 2014). In addition, breeding strategies are still targeting on e.g. *Rhizomania* and *Cercospora* resistance (Scholten and Lange 2000; Weiland and Koch 2004) as well as nematode resistance (Stevanato *et al.* 2015). Regarding the improvement of mechanical harvest techniques, automated fertilization and plant protection with the aid of optical sensors or cameras, breeding for different growth forms of shoot and the sugar beet tuber plays a further major role (e.g. Loel *et al.* 2014; Metzner *et al.* 2014; Thomas *et al.* 2017). All these factors taken together illustrate the diversity of old and new traits for breeding. Thus, breeding usually aimed at optimizing several complex traits simultaneously which are in addition under multigenic control. Sugar content, technical quality and the improvement of biomass partitioning are only a few parameters, but to advance breeding more requires searching for diverse phenotypic and genotypic traits are necessary.

WATER DEFICIT IN SUGAR BEET

Sufficient precipitation during the main growing period from June until September is the base for efficient growth and development of the sugar beet. Due to its halophytic traits, the biennial crop is quite drought tolerant, especially in comparison to other spring sown crops (McKersie and Leshem 1994). Since there is no clearly defined decisive period during the vegetative growth in the first year, e.g. flowering or fruit development, and due to the relatively good water use efficiency (WUE) of the beet (Ehlers and Goss 2016), the root crops ability to withstand drought over a certain period of time is rather good. Established with a deep and widely branched root system, that can reach depths up to 110 cm (Brown and Biscoe 1985), this chenopod species can extract and utilize large amounts of soil water as shown by Windt and Märlander (1994). However, its ability to regulate transpiration is limited (Hanson and Hitz 1982) and wilting is thus one of the first symptoms, that can be observed nearly regularly during temporary periods of drought often combined with high irradiance, e.g. around noon during the summer. But this phenomenon is also observed at noon under regular water supply; therefore, wilting sugar beet leaves are not only a consequence of drought, but is also a trait of insufficient water uptake and utilization of the beet even under regular water supply.

Although the sugar beet recovers as soon as the evaporative demand is decreasing, Lawlor and Milford (1975) stated that the plants ability to cope with a decreasing soil water deficit is restricted and that the leaf water potential tends to decrease faster compared to the soil water potential. In tem-

perate climates, the amount of precipitation year of approx. 600 mm is crucial for a high sugar yield with the main precipitation within in the second part of the season (June-September). However, this is not the common case, especially during long and extensive summer periods in Southern Europe. Here, sugar beet growing is only possible with irrigation. But also in main growing regions like Russia, Ukraine, Poland, Germany and England, where usually enough precipitation during the year occurs, yield losses between 15-40% due to drought were observed (Pidgeon *et al.* 2001).

A better understanding of physiological and metabolic changes during temporary or constant drought periods would improve established approaches in the development of drought tolerant cultivars, would deliver contributing insights for the development of new breeding strategies and provide new options for selection criteria for drought tolerance. Since adaptation mechanisms under drought stress are similar to other abiotic stresses, such as cold stress or salinity, tolerance against drought would also raise tolerance against other stresses. To reach these goals, an early and exceptionally differentiated picture of the drought induced alterations is needed which might be achieved by the combination of classical destructive methods as well as non-destructive approaches, e.g. thermal imaging.

RECOVERY PROCESS

Recovery describes the time period after termination of a stress until a new physiological and metabolic homeostasis is set, and is a decisive step in the plant metabolism. As stress response, physiological adaptations of the metabolism allow the synthesis of metabolites, including protective compounds, e.g. sugars or quaternary ammonium compounds, that can confer tolerance or resistance to drought stress (Bhargava and Sawant 2013). When the stress is terminated, recovery processes set in, and the plant must strike a balance between the investment of resources into damage repair, maintained acclimation (priming for upcoming stress events), or into new growth/reproduction (resetting) (Crisp *et al.* 2016). While resetting maximizes growth and yield under favorable conditions, it carries the risk of major and possibly fatal damage if the stress recurs. Maintained acclimation, on the other hand, makes the plant “alert” for upcoming stress events, but comes at the cost of reduced growth or development and reduced yield (Crisp *et al.* 2016).

During the recovery process, metabolic energy flows into preparation and adjustment for the reactivation of photosynthesis, respiration and lipid biosynthesis (Souza *et al.* 2004; Galmes *et al.* 2007; Flexas *et al.* 2009), highly-synchronized and sensitive processes that are delicate to manage. For *B. vulgaris*, available studies of recovery processes after a drought stress event are mainly restricted to describe changes of the chemical composition and sucrose accumulation of the taproot (Bloch *et al.* 2006a; Hoffmann 2010), or handle the effect of transient and continuous drought on yield, photosyn-

thesis and carbon discrimination (Monti *et al.* 2006). What is still not available, and might be of specific interest in root yielding plant species such as sugar beet, is a better understanding of the similarities and differences specificities of roots and shoots in metabolic adjustment and recovery after a transient drought. This is relevant because for a high yield, it is of particular importance that the taproot recovers quickly to warrant water and nutrient uptake and is not lastingly impaired in sugar accumulation after a transient drought event in order to prevent yield loss.

PHENOTYPING

The current use of the word *phenome* (acient greek: φαίνω *phaino* "I appear" and τύπος *týpos* "shape") refers to the entire phenotype as stated by Soule (1967). The phenotype describes the composition of observable traits of a certain being. In case of plants, this includes growth and development, morphology, tolerance, yield as well as physiological and biochemical characteristics. The phenotype of an organism is the result of the genome expression, which can be influenced by external and internal factors, like environmental influences e.g. abiotic or biotic stress (external) or the interaction between external factors and the genome itself e.g. mutations due to abiotic impacts (internal). Hence, the interaction between genome x environment determines the phenotypic plasticity of a plant. Phenotyping takes place since thousands of years, initially, intuitively performed by the grower who observed his field during the season. Today, phenotyping is done by farmers, breeders, agricultural industry and academia - not only aiming at high yields, but also to improve growing techniques for the enhancement of desirable traits, e.g. water use efficiency or biomass, or the early detection of abiotic and biotic stress. Phenotyping is a research that developed rapidly within the last decades. What began as pure observation by the human eye, is today supported by different, complex and often automated high-throughput systems in phenotyping facilities at research institutes, unmanned aerial vehicles (UAVs) used for observation and monitoring of growing areas as well as in agricultural industry. But although there was enormous development of non-invasive techniques for the observation of the external phenotype in the recent years, the analysis and interpretation of the *internal* phenotype, that includes physiological, biochemical and thus metabolomic changes, which finally determine the external phenotype, lag behind (Großkinsky *et al.* 2015). To close this gap, it is definitely needed to combine the external approach with the highly dynamic internal processes on the biochemical and physiological level. Only this approach can result in a picture of the *real and holistic* phenotype which is the result of genotype x environment interaction.

AIM OF THE WORK

The main objective of thesis work was the physiological and metabolic characterization of young sugar beet plants under temporary drought and recovery with a special emphasis on the differences between the responses of shoots and roots.

To this end, the following aims were addressed:

i. The development of a reliable and reproducible test system, that allows the controlled implementation of progressive drought and rewatering of sugar beets under greenhouse conditions as well as a sufficient and cost-effective analysis of physiological and metabolic changes.

ii. The investigation of the chronological order of physiological and metabolic changes of young sugar beets under progressive drought and rewatering, with special emphasis on plant water status and osmotic adjustment assessed by invasive and non-invasive techniques.

iii. A detailed metabolic approach using untargeted ^{1}H-NMR and targeted metabolites assays for the analysis of the underlying metabolic mechanisms in temporarily drought-stressed and rewatered sugar beets with close attention to differences in the recovery process in shoots and roots.

BACKGROUND

The current work was in part carried out with the support of the Federal Ministry of Education and Research (BMBF) in the context of the network project CROP.SENSe. The aim of this interdisciplinary network was to develop, to apply, and to promote new as well as established phenotyping methodologies for crop management and improvement of breeding strategies. The two model plants used throughout the network were *Beta vulgaris* and *Hordeum vulgaris*.

1 EXPERIMENTAL SETUP AND METHODICAL APPROACH

Introductory remarks

The development of a functional and reproducible test system was an essential and major part of this work. This chapter is presented in form of a handbook, which can be used in the daily laboratory work providing detailed background information. Parts of the following subchapters were used for published and submitted articles included in this thesis.

CONTRIBUTORS

- Dr. Yves Gibon and team INRA UMR 1332, Biologie du Fruit et Pathologie – High throughput enzyme based metabolite assays
- PD Dr. Anne Mahlein, PD Dr. Erich-Christian Oerke and PD Dr. Ulrike Steiner INRES Phyto-medicine Plant Diseases and Plant Protection
- Dr. Annick Moing and team INRA UMR 1332, Biologie du Fruit et Pathologie
- Dr. Manfred Trimborn INRES Plant Nutrition
- PD Dr. Gerd Welp INRES Soil Science and Soil Ecology
- Inge Neumann, INRES Phytomedicine Plant Diseases and Plant Protection
- Eva Schulze-Varnholt, Waltraud Köhler INRES Plant Nutrition
- Libeth Schwager INRES Horticulture
- Brigitte Überbach, Angelika Glogau and Angelika Veits INRES Plant Nutrition

1.1 PLANTS

For all experiments the sugar beet cultivar Pauletta were used. Pauletta, a nematode and rhizomaina-tolerant cultivar, that is recommended for challenging growing areas that suffer under drought and weeds (esp. *Mercurialis annua* L.), is characterized by a good youth development. Seeds were kindly provided by Dr. Britta Schulz, KWS Saat AG, Einbeck.

Phenological plant development

The phenological plant development was determined according the BBCH scale (Enz and Dachler 1997), that distinguishes between 9 principal growth stages (Table 1-1).

Table 1-1: BBCH scale (in parts) of the phenological sugar beet development.
Table is based on Enz and Dachler (1997). Pictures (modified) by Klett®.

Code	Description
PRINCIPAL GROWTH STAGE 0: GERMINATION	
00 - 09	Dry seed until emergence of the shoot
PRINCIPAL GROWTH STAGE 1: LEAF DEVELOPMENT (YOUTH STAGE)	
10	First leaf visible (pinhead size): cotyledons horizontally unfolded
11	First pair of leaves visible, not yet unfolded (pea size)
12	2 leaves (1st pair of leaves) unfolded
14	4 leaves (2nd pair of leaves) unfolded
15	5 leaves unfolded
1…	Stages continuous until
19	9 and more leaves unfolded
PRINCIPAL GROWTH STAGE 3: ROSETTE GROWTH (CROP COVER)	
31	Beginning of crop cover: leaves cover 10% of ground
32	Leaves cover 20% of ground
33	Leaves cover 30% of ground
3…	Stages continuous until
39	Crop cover is complete: leaves cover 90% of ground
PRINCIPAL GROWTH STAGE 4: DEVELOPMENT OF THE HARVESTABLE VEGETATIVE PLANT PARTS (BEET ROOT)	
49	Beet root has reached harvestable size

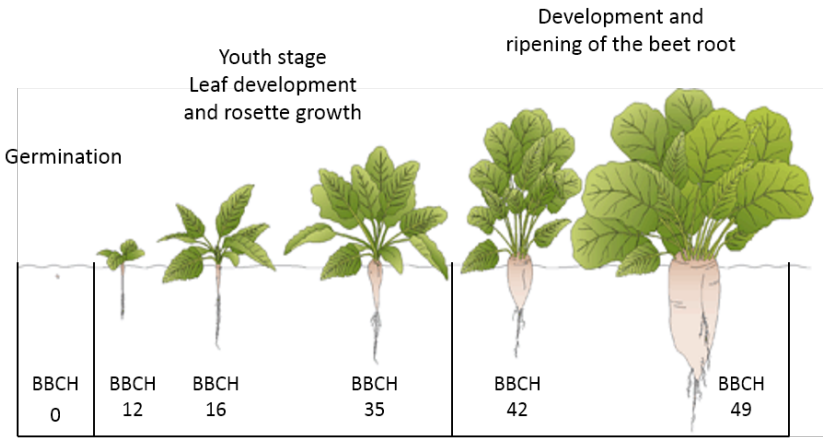

The growth stages can be divided in two sections. The first 4 growth stages are referred to the first year of the development, from germination (BBCH 0) until the development of the vegetatively propagated organs, the rosette stage (BBCH 4), and the subsequent growth stages are denoted to the second year, from the emergence of inflorescences (BBCH 5) until the plant senescence (BBCH 9).

1.2 PLANT CULTIVATION

Plants were pre-grown in prick out trays containing a mixture of sandy soil (quartz sand / prick out soil, v/v 1:1). Seedlings were cultivated under greenhouse conditions and piqued until the primary leaves were fully emerged and developed. During vegetative growth, plants grew in 2 Liter plastic pots
(11.3 x 11.3 x 21.5 cm) filled with 850 g of a substrate mix (70% white peat, 20% loam, 10% perlite, Gepac, Type VM, Sinntal-Jossa, Germany). Substrate properties are given in Figure 1-1 and Table 1-2. Day/night temperature was 24/18°C with a relative humidity (RH) of approx. 75% and a photoperiod of 16 h with >250 µmol m^{-2} s^{-1} light intensity (Philips SON-T Agro 400W).

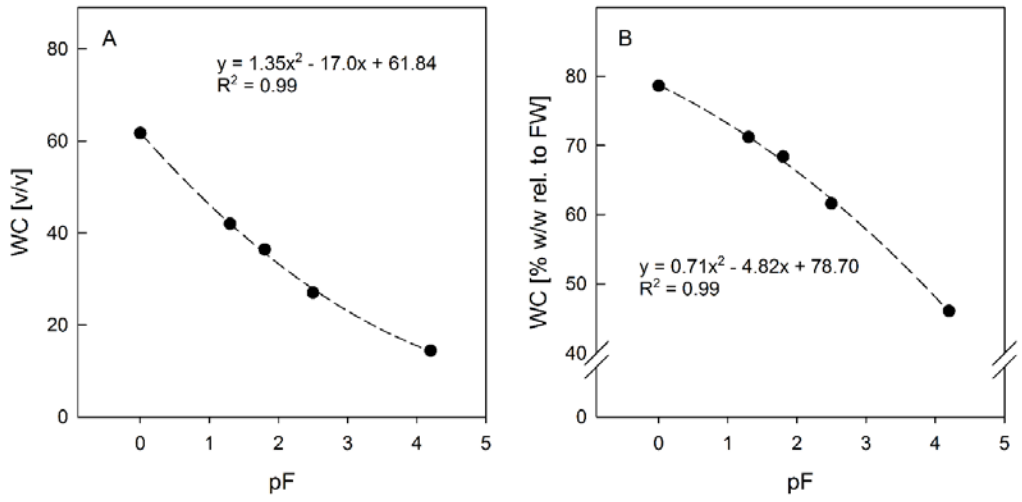

Figure 1-1: Substrate properties Gepac Typ VM.
A: Water content (WC) in % v/v, B: Water content in % w/w relative to the fresh weight.

Sugar beet plants were watered three times a day for 3 minutes each, using a time controlled, automated table flooding system. Watering resulted in a water content (WC) of approx. 65-69% w/w based on the fresh weight during pre-treatment growth. This corresponded to a substrate pF (log_{10} of the absolute value of the soil matrix potential, unitless) values between 1.8 and 2.3 (Figure 1-1, Table 1-2).

Table 1-2: Substrate characteristics of Gepac Anzuchterde, Typ VM.

Bulk density	0.169 ± 0.008	g cm^{-3}
Total pore volume	61.7 ± 0.4	%

pF-curve			
pF	Water content [v/v]	Water content [% w/w] rel. to FW	Water content [% w/w] rel. to DW
0.0	61.7	78.6	367
1.3	42.0	71.2	250
1.8	36.4	68.4	216
2.5	27.0	61.6	161
4.2	14.4	46.1	86

To minimize the statistical error and provide a representative batch of independent samples for each harvest day and treatment, plants were arranged in a complete randomized block design (Figure 1-2). For each harvest date, 4 biological replicates were used.

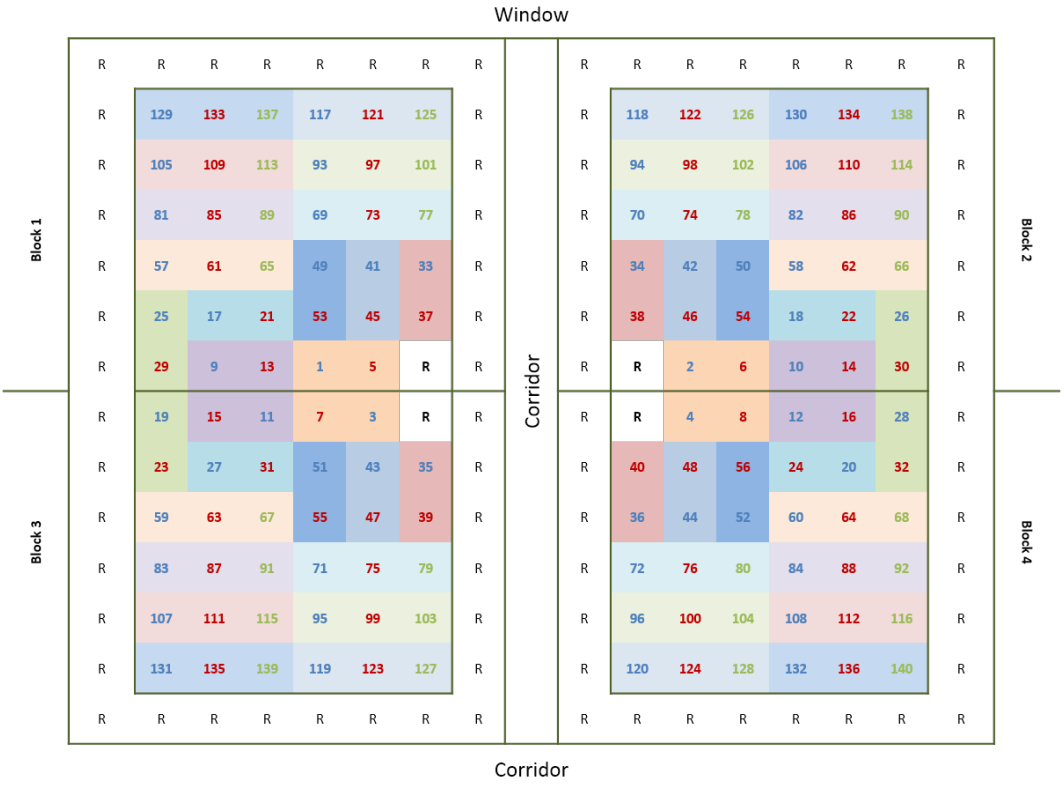

Figure 1-2: Randomized block design for the greenhouse experiments.

Shown are 2x2 plots surrounded by additional plants to avoid side effects during the experiment. R: additional plants to minimize side effects. Colored numbers represent the pot number, whereas the color represents the treatments: blue: control plants, red: drought stressed plants, green: temporary drought stressed plants (recovery).

1.3 PLANT PROTECTION

During the entire experimental period, plants were kept free of pests and diseases with integrated plant protection (Table 1-3).

Table 1-3: Actions of plant protection.
Overview of the applied plant protection actions during the experimental period.

Pest / Disease	Beneficial Insect / Active ingredient	Trade name	Application / Use pattern	Supplier
Fungus gnats	*Bacillus thuringiensis*	BioMückk®	5 g L^{-1}	Proagro GmbH
Thrips	*Amblyseius curcumeris*		as recommended	Sauter und Stepper
White fly	*Encarsia formosa*		as recommended	Sauter und Stepper
Spider mites	*Amblyseius californicus*		as recommended	Sauter und Stepper
Powdery mildew	250 g L^{-1} Quinoxyfen	Fortress 250®	0.625 µL L^{-1}	DowAgro

1.4 STRESS TREATMENTS

Treatments were started when plants reached approx. BBCH 15-17. Then, plants were either kept under regular water supply (control) or were subjected to drought or to temporary drought with subsequent rewatering (Figure 1-3).

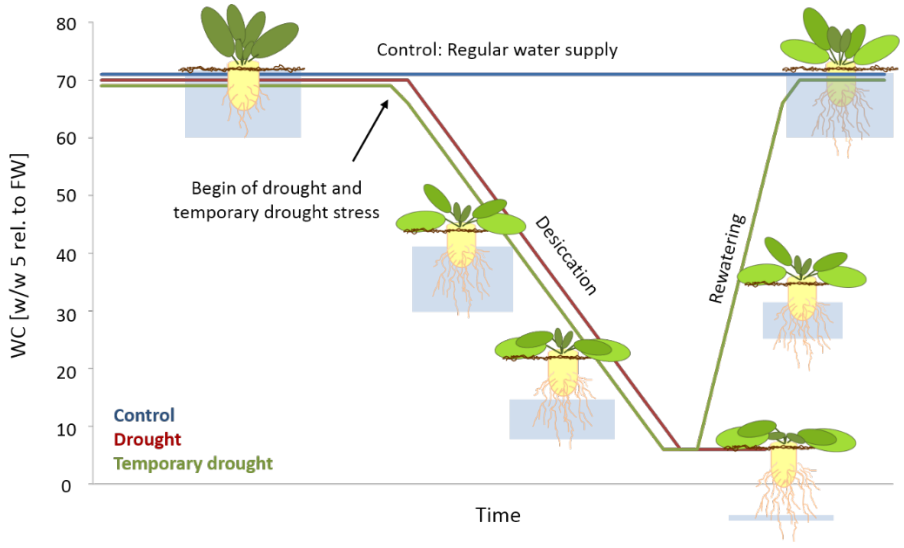

Figure 1-3: Illustration of the stress treatment: drought and temporary drought with subsequent rewatering.
Control plants (blue) under regular water supply during the experiment. Drought stress is implemented by cutting off the irrigation. Drought stressed plants (red) desiccate for up to 17 days, whereas the temporary stressed plants are rewatered for up to 13 days.

In all experiments, the water content of the soil (w/w based on FW) was in average 65 ± 5 % and was maintained during the experimental period. This WC corresponds to a substrate suction of 3.4 that can be considered as optimal water supply (Table 1-2).

Drought stress was implemented by cutting off the irrigation. Roots growing outside the pot were placed like this, that contact to the flooding system was impossible. The desiccation period of drought stress plants was up to 17 days. The implementation of temporary drought and drought stress began simultaneously (Figure 1-3). The duration of the rewatering period was up to 12 depending on the experiment.

1.5 HARVEST, SAMPLE PREPARATION AND STORAGE

To gather information about possible correlations between metabolic, physiological and sensor data under drought and rewatering, plants were harvested every other day or daily during the first 3-4 days of the rewatering period. To avoid uncontrolled side effects by the circadian rhythm of the plant water status and metabolite concentrations, plants were always harvested 4 h after beginning of the photoperiod. Before further processing, all plants were photographed by a RGB camera (Panasonic, Lumix DMC-FZ18, Osaka, Japan) and measured with a Stirling-cooled infrared scanning camera in case of the approach described in 1.14.

Metabolic and physiological measurements

Metabolic and physiological analyses of the shoot were performed at the first youngest fully expanded leaf pair (YEL) (Figure 1-4). Physiological measurements included osmotic potential (OP), relative water content of the leaf (RWC), electrolyte leakage (EL), the determination of malondialdehyde (MDA) as well as microscopic investigations. For root analysis, the thickest part below the crown was used (Figure 1-4). This part was divided in 2 pieces. One piece was used for the determination of the OP and the other was used for the targeted enzyme based metabolite analysis and ion determination. Plant material of both organs for the metabolite analysis was immediately shock frozen in liquid nitrogen until further sample preparation and analysis to prevent any metabolic activity. Leaf and root material for the metabolite and ^{1}H-NMR were treated different due to technical issues. The metabolite analysis in the shoot was done with fresh (frozen) plant material whereas ^{1}H-NMR analysis was done with lyophilized material. In case of taproot analysis (both techniques) only lyophilized plant material was used due to better handling.

Before metabolite and MDA analysis, leaf material was mortared to a fine powder and stored at -80°C while leaf parts for physiological measurements (RWC; EL, microscopy) were immediately ana-

lyzed or frozen at -20°C (OP). The root part for metabolite analysis was cut into fine pieces, was subsequent shock frozen in liquid nitrogen and also stored at -80°C until lyophilization. After lyophilization, root material was stored vaccumized at -20°C until analysis. Storage at -80°C and at -20°C in case of vaccumized plant material is obligatory to prevent the samples from degradations processes.

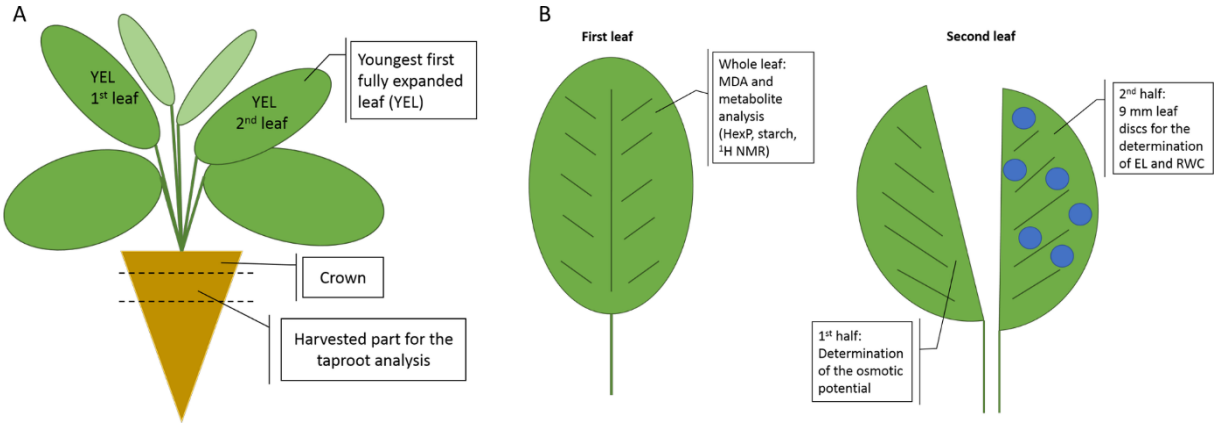

Figure 1-4: Harvest scheme of sugar beet shoot and root.
A: Overview of the sugar beet plant and the harvested plant parts of shoot and taproot. **B**: Harvest scheme of the leaf. Abbreviations: YEL, youngest fully expanded leaf; MDA, malondialdehyde; HexP, hexose phosphates; ^{1}H-NMR, proton nuclear magnet resonance; EL, electrolyte leakage; RWC, relative water content.

1.6 GROWTH AND DEVELOPMENT

Biomass was determined by fresh and dry weight (FW, DW) of shoot and taproot. Shoot and taproot FW were determined before plant parts for the respective analysis were taken. Dry weight was determined after oven drying at 70°C until no change of DW was observed. Plant material which was used for physiological and metabolic analysis was excluded to the DW, since this amount was negligible.

1.7 PLANT WATER STATUS

The plant water status is described by the parameters water content (WC), RWC and OP. These parameters provide the base for the osmotic adjustment (OA) described in 1.8.

Water content

Based on the FW and DW data obtained from the analysis of growth and development the WC in g H_2O per g DW was calculated based on Barrs and Wheaterly (1962):

$$WC\ (g\ H_2O\ /\ g\ DW) = (FW - DW) / DW.$$

Relative water content

The RWC was calculated according the following formula and refers to the relative amount of water to their fully hydrated status:

$$RWC\ (\%)\ = \left(\frac{FW - DW}{TW - DW}\right) * 100$$

The RWC of sugar beet leaves was determined with 6 leaf discs (Ø 9 mm) of the YEL. Leaf veins were avoided. Before rehydration, FW of the discs was determined and the punched discs were briefly rinsed in ultrapure water to get rid of the cell sap at the cutting areas. Leaf discs where than rehydrated in 30 ml ultrapure water at room temperature (RT). To avoid the reduction of the soluble sugars due to respiration and carbohydrate metabolism, samples were not floated longer than 4 h. Afterwards, leaf discs were dried carefully with a paper towel and turgid weight (TW) was determined. For DW determination leaf discs were oven dried at 60°C for 48 h.

For an improved workflow, the determination of RWC and the measurement of EL can be combined (see 1.9). For this, the conductivity measurement can take place after floating the leaf discs. Instead of drying the leaf discs afterwards, discs are frozen at -20°C for at least 24 h to destroy all membrane structures. Thereafter, the conductivity is measured again. Dry weight determination can take place as described above after the second leakage measurement.

1.8 OSMOTIC POTENTIAL, OSMOTIC ADJUSTMENT AND METABOLITE CONTRIBUTION

Osmotic potential was derived from the osmolality (Osmol kg^{-1}) of the leaf or root cell sap using a cryoscopic osmometer (Osmomat 030, Gonotec GmbH, Berlin, Germany). After thawing and equilibration of the frozen samples to RT, cell sap was extracted using a manual press. Mixed aliquots of 100 µL were centrifuged at 10.000 rpm for 5 min (leaves) or 10 min (taproots) to remove debris. The OP (in MPa) was calculated by multiplying the osmolality with -2.479 (conversion factor at 25 °C; Pariyar *et al.* 2013).

Osmotic adjustment (OA) is defined as the difference in OP (ΔOP) between well-watered and stressed plants. DW-based metabolite concentrations ($conc_{metab\ DW}$) were transformed into tissue water-based concentrations ($conc_{metab\ H2O}$) according to the following formula

$$conc_{metab\ H2O}\ = \frac{conc_{Metab\ DW} \times (1 - WC_{leaf})}{\mathrm{WC}_{leaf}}$$

where WC_{leaf} represents the leaf water content.

The contribution to the OP was then calculated as follows

$$Contribution\ _{metab}(\%) = \frac{\text{conc}\ _{metab\ H2O}\ * 100}{\text{OP}}$$

The contribution to OA was calculated accordingly by using the difference in water-based concentrations between control and stressed plants, and ΔOP, respectively.

1.9 MEMBRANE STABILITY

Membrane stability is described by electrolyte leakage (EL) and the determination of the MDA concentration and was supplemented by microscopic investigations (see 1.10).

Electrolyte leakage

The measurement of EL was based on the protocol of Sukumaran and Weiser (1972). Six leaf discs (Ø 9 mm) were punched out with a cork borer avoiding the veins. Subsequently, discs were rinsed in ultrapure water to wash off electrolytes from the cutting edge. Samples were then rehydrated in 30 ml ultrapure water for 4 h at RT. The conductivity (EL1) of the rehydration solution was measured with an EC-meter (WTW 340i, WTW, Weilheim, Germany). Thereafter, discs were blotted dry, weighed for determination of TW, and frozen in the rehydration solution for 24 h at -20°C. Next day, solutions were thawed, equilibrated to RT for 4 h and the final conductivity was measured (EL2). Finally, discs were oven dried for 24 h at 70°C to determine the DW. Electrolyte leakage was determined using the formula

$$EL\ (\%) = \left(\frac{EL1}{EL2}\right) * 100$$

Malondialdehyde

The determination of MDA, a secondary end product of the oxidation of polyunsaturated fatty acids, is based on the thiobarbituric acid assay of Hodges *et al.* (1999), and was adapted for the use of a 96-well microplate system. All reagents were prepared fresh daily and samples were determined in duplicate. For the extraction, 20 mg of frozen ground plant material were homogenized with 500 µL 0.1 % trichloroacetic acid (TCA) by shaking the vials containing one 3 mm tungsten bead each for 45 s at 30 Hz in a tissue lyzer (Quiagen, Hilden, Germany). After centrifugation at 5000 rpm for 15 min, a 150 µL aliquot of the supernatant was thoroughly mixed with 150 µL of either reagent 1 (RS1: 0.01% 2,6-di-tert-butyl-4-methylphenol in 20% (w/v) TCA, or reagent 2 (RS2: RS1 plus 0.65% 2-thiobarbituric acid), heated at 95°C in a water bath for 30 min, cooled on ice, and centrifuged again. The absorbance (Abs) of the supernatant was read at 440, 532 and 600 nm (BioTek PowerWave, Bad

Friedrichshall, Germany), 0.1% TCA was used as blank and MDA equivalents in nmol mL^{-1} were calculated according the following equations:

$$A = [(Abs\ 532_{RSII} - Abs\ 600_{RSII}) - (Abs\ 532_{RSI} - Abs\ 600_{RSI})]$$

$$B = [(Abs\ 440_{RSII} - Abs\ 600_{RSII}) * 0.0571]$$

$$MDA\ (nmol\ mL^{-1}) = \frac{[(A-B)]}{41448} * 10^6$$

Where 0.0571 corresponds to the ratio of the molar absorbance of 1^{-10} mM sucrose at 532 nm and 440 nm and, 41448 refers to the molar extinction coefficient (ε) of MDA calculated for $d_{100\mu L} = 0.264$.

1.10 MICROSCOPIC INVESTIGATIONS

Monitoring of the histological changes of sugar beet leaves under drought and rehydration were observed with with a Leitz DMR 6000B photomicroscope. For the investigation 3-5 mm x 3-5 mm tissue samples were fixed with 8% paraformaldehyde and 8% glutaraldehyde in 0.2 M sodium cacodylate buffer (pH 7.3) under vacuum for 4 h at RT (Karnovsky 1965). Samples were then rinsed 3 times in cacodylate buffer for 20 min each, subsequent dehydrated in a graded ethanol series, and finally embedded in London Resin white medium. The embedded tissue was semi-thin sectioned with a diamond knife on an ultra-microtome (Reichert Ultracut E; Leica Microsystems, Nussloch, Germany) and stained in 1% toluidine blue. Stained samples were observed with the photomicroscope. Digital photos were taken with a digital camera (JVC, Ky-F75U) and the software Discus, 4.6 (Technical Office Hilgers, Königswinter, Germany) as used for image analysis.

1.11 ELEMENT ANALYSIS

Pressure digestion

The determination of sodium (Na^+), potassium (K^+) and magnesium (Mg^{2+}) was performed with oven dried plant material. Before, the plant material was grinded (disc mill) and pressure digested (0.5 mg shoot, 0.25 mg root) with 4 ml HNO_3 in a Teflon vessel (180 °C, 13 h). Six blank tests and six internal references were included for each element. When samples reached RT after digestion, they were filled up with 25 ml (volumetric flask). To remove undigested material samples were filtered and stored in a 50 ml PE bottle at RT until analysis.

Sodium and potassium

Flame emission spectroscopy was used for the quantification of Na^+ and K^+ using an Eppendorf ELEX 6361 (Eppendorf, Hamburg, Germany, detection limit 20 mg L^{-1} for both elements). Samples of both elements as well as standards were diluted according Table 1-4. The concentration of each sample was calculated using the equation derived from a calibration curve of standards for each element. The standard for Na^+ was 0.5/1/2.5/5/10 mg Na^+ L^{-1} (CertiPUR Na-calibration solution, Merck Chemicals, Darmstadt) and for K^+ 0/2.5/5/10/20 mg K^+ L^{-1} (CertiPUR K-calibration solution, Merck Chemicals, Darmstadt).

Table 1-4: Sample, standard and dilution of the internal references for element analysis.
Leaf and root samples, standards and the internal references for each element were diluted before the determination by flame emission spectroscopy (Na^+, K^+) or atom absorption spectrometry (Mg^{2+}) was done.

Element	Leaf	Root
Na^+	1:200	1:10
K^+	1:200	1:50
Mg^{2+}	1:1000	1:50

Standard	Dilution
Na^+	-
K^+	1:50
Mg^{2+}	1:50

Internal reference	Na	Mg
Dilution	-	1:100

Magnesium

The sample preparation for the determination of Mg^{2+} was the same as described for Na^+ and K^+. The measurement was done by atom absorption spectrometry (AAS 1100 B, Perkin Elmer, MA, United States, detection limit for Mg^{2+} up to 0.5 mg L^{-1}). The standards were 0/0.1/0.3/0.5 mg L^{-1} (CertiPUR Mg^{2+}-calibration solution, Merck Chemicals, Darmstadt). Samples and standards were diluted according Table 1-4.

1.12 TARGETED METABOLITE ANALYSIS

The metabolite analysis was performed in a 96-well Micronic® system (Micronic Europe, Berlin, Germany) which can be also used for automated liquid handling systems. All samples, accept the total amino acid content (AA_t), were analyzed with multiplate readers (M96, Safas, Monaco; Power Wave XS2, BioTek, Vermont, USA) using 96-well flat bottom microplates (Starlab, Hamburg, Germany). The AA_t was measured with a spectrofluormeter (Xenius XC, Safas, Monaco). Pipetting was either done manually with single- or multichannel pipettes (Eppendorf, Hamburg, Germany) or in case of large sample size (> 200) with a pipetting robot (Hamilton, Bonaduz, Switzerland). Samples in small vessels (1.5, 2.0 mL) or enzymes were centrifuged with an Eppendorf centrifuge (Model 5418 R, Rotor FA-45-18-11) and microplates were centrifuged with the Eppendorf centrifuge 5920 R (swing-out-rotor A-4-81).

T*ypes of assays*

For the metabolite analysis of shoot and root material different types of assays were used. Chlorophyll a and b were determined by the measurement of the absorbance of the diluted extract. Proline was determined using a colometric reaction (ninhydrine reaction), whereas the determination of AA_t was analysed by measurement of the fluorescence (fluorescamine method). For the determination of Hexose phosphates (HexP) continuous assays were performed. All other assays were stopped assays. The advantage of stopped assays are that they are quite flexible because the determination of the products of the enzymatic reactions of interest can be studied separately. Furthermore, they provide a higher sensitivity when products of enzymes are being measured with kinetic or fluorometric methods. Another benefit is the low amount of extract of, e.g. 20 µL in a 96-well microplate, which reduce costs compared to continuous assays which usually need about 100 µL in a 96-well microplate for optical reasons. Although one of the big disadvantage of stopped assays is the high number of pipetting steps, this can be compensated by using electronic multichannel pipettes or liquid handling robots to decrease time and errors (Gibon *et al.* 2002; Rogers and Gibon 2009).

Reagents

All chemicals and enzymes which were used for the metabolite analysis were ordered by Roche, Sigma Aldrich and Applichem. Assay mixes which did not contain an electron donator like thiazolyl blue tetrazolium bromide (MTT) or electron carriers like phenazine metosulphate (PMS) or phenazine ethosulphate (PES) were stable and were prepared in advantage (storage -20°C). This was also the case of the used buffers. As long none of them contained enzymes and/or cofactors, stocks were stored at -20°C, otherwise they were stored at -80°C to minimize enzymatic degradation.

Handling of samples

Given that most enzymes are not stable after extraction and that they can be damaged in freeze-thawing cycles, all steps of enzyme preparation for the assays were performed on ice. If needed, enzyme solutions were diluted and were frozen in small aliquots at -80°C.

Fresh plant material for the metabolite analysis was prepared by grinding tissue with mortar and pestle or tungsten carbide beads in a Retsch mill (Retsch, Haan, Germany). Due to degradation processes grinding and weighing of aliquots were done within seconds under liquid nitrogen. Fresh samples were always stored at -80°C until extraction. Lyophilized sample material was stored in vacuum bags filled with silica gel at -20°C until extraction.

Ethanolic extraction

For the analysis, grinded material (20 mg FW shoot, 10 mg DW root) was weight into 1.1 mL Micronic® tubes containing one, 3 mm tungsten carbide bead (Quiagen GmbH, Hilden, Germany). To inhibit metabolite and enzyme degradation, fresh samples were kept in liquid nitrogen and lyophilized samples were kept at RT in a desiccator until extraction buffer was added. If the determination of chlorophyll a and b was the first measurement, pooled extracts were kept in the dark (on ice) to avoid the chlorophyll degradation.

The extraction was carried out in 3 steps. In the first step 250 µL 80 % ethanol (EtOH) (v/v) in 10 mM HEPES KOH, pH 7 was added, vials were closed and shaken for 30 s at 20 Hz (Retsch mill MM400). After samples were heated in a water bath (80 °C, 20 min) and subsequently centrifuged (10 min, 4000 rpm, RT), approx. 200 µL of the supernatant was transferred into a new tube and kept on ice. The second extraction step followed pipetting 150 µL 80 % EtOH (v/v) in 10 mM HEPES KOH, pH 7. After 20 s of shaking, heating (80 °C, 20 min) and centrifugation (10 min, 4000 rpm, RT) approx. 150 µL supernatant were transferred again. The final step was done with 250 µL 50 % EtOH (v/v) in 10 mM HEPES KOH, pH7 and the complete supernatant was added to the previously collected extract. The remaining pellet should be frozen (-20°C) for starch and protein determination.

Extraction volumes, biological references, standards and blanks

Before extraction of the sampled material took place, the needed extraction volumes for the respective assays were determined. Further, biological references (BioRef) were prepared. The idea of BioRefs into the analysis was to have an internal reference for each analyzed metabolite. The BioRef can be seen as an internal reference or standard made of pooled plant material from different studies. Additionally, analytical standards (if needed) as well as blanks were included.

Before analysis took place, experience had shown that the preparation of a sample sheet for the final plate layout was valuable in two ways. Firstly, to enhance the pipetting steps, if this wasn't performed by an automated liquid handling system and secondly, for the subsequent data analysis with e.g. Excel (Microsoft, Redmond, USA). Generally, all samples were placed randomized on a 96-well Micronic® rack, containing 6 blanks and 6 BioRefs and standards. Standards, if needed, were prepared in duplicate (Figure 1-5).

	1	2	3	4	5	6	7	8	9	10	11	12
A	SD0	SD0	SPL	SPL	SPL	SPL	SPL	SPL	SPL	SPL	SPL	BLK
B	SD1	SD1	SPL	SPL	BioRef	SPL	BLK	SPL	SPL	BioRef	SPL	SPL
C	SD2	SD2	SPL	SPL	SPL	SPL	SPL	SPL	SPL	SPL	BLK	SPL
D	SD3	SD3	SPL	BLK	BioRef	SPL	SPL	BioRef	SPL	SPL	SPL	SPL
E	SD4	SD4	SPL	SPL	SPL	SPL	SPL	SPL	SPL	SPL	SPL	SPL
F	SD5	SD5	BioRef	SPL	SPL	SPL	SPL	SPL	SPL	SPL	SPL	SPL
G	SD6	SD6	SPL	SPL	SPL	BLK	SPL	SPL	SPL	SPL	SPL	SPL
H	BLK	SPL	SPL	SPL	SPL	SPL	SPL	SPL	SPL	SPL	SPL	BioRef

Figure 1-5: **Example of a sample sheet (plate layout) for the metabolite analysis.**
Samples (SPL), blanks (BLK) and biological references (BioRef) were placed completely randomized on the 96-well microplate. Standards (SD) were placed in the first 2 columns of the rack.

1.12.1 Chlorophyll a and b

The analysis of chlorophyll a and b was immediately done after the ethanolic extraction. For this, 40 µL of the ethanolic extract was diluted with 120 µL of 96 % EtOH. The optical density (OD) was determined at 645 and 665 nm. For the interpretation of the results ODs should not exceed 0.3 at 645 nm and 0.6 at 665 nm. The amount of chlorophyll in µg per well was calculated according the following equations based on Lichtenthaler (1987).

$$\text{Chlorophyll a } (\mu g\ well^{-1}) = 5.48 * OD_{665} - 2.16 * OD_{645}$$

$$\text{Chlorophyll b } (\mu g\ well^{-1}) = 9.67 * OD_{645} - 3.04 * OD_{665}$$

1.12.2 Hexose phosphates

Principle of the measurements

In the presence of glucose-6-phosphate dehydrogenase (G6PDH) and NADP (nicotinamide adenine dinucleotide phosphate), G6P is converted into 6-phosphogluconate and NADPH (nicotinamide adenine dinucleotide phosphate, reduced). After having destroyed the remaining NADP, NADPH is quantified via a cycling assay for NADPH described in Gibon *et al.* (2002). Due to precipitation processes hexose phosphates (HexP) were determined right after the analysis of chlorophyll. See also Cross *et al.* (2006). It is possible to measure the HexP with fresh *and* freeze-dried material. In both cases, the turnover esp. for glucose-1-phospahte (G1P), is quite fast. Samples should be kept on ice and not at RT during sample preparation. For lyophilized samples the harvest and sample storage in vacuum bags or a desiccator is obligatory to prevent metabolic activities.

Glucose-6-phosphate

Glucose-6-phosphate was analyzed with 5 µL extract (shoot, root) and, 10 µL were used for the calibration curve (0/0.4/1/2/4/10 µM G6P in 0.2 M Tricine/KOH, pH 9, 10 mM $MgCl_2$). After adding 75 µL of mix 1 the samples were homogenized. After 20 min of incubation at RT, 20 µL of 0.5 M sodium hydroxide (NaOH) was added, samples were mixed again and subsequent incubated in a sealed microplate for 10 min at 98.5 °C in a dry bath. After cooling down, samples were centrifuged (1 min, 400 rpm, RT) and 20 µL of 0.1 M Tricine/KOH, pH 9 containing 0.5 M hydrogen chloride (HCl) was added. Finally, mix 2 was pipetted and the samples were immediately measured at 570 nm (37 °C, kinetics: one read every 30 s) in the microplate reader. When preparing mix 2, phenazine methosulfate (PMS) and thiazol blue tetrazolium bromide (MTT) were added last, because of their light sensitivity.

Mix 1

1.8 mL	0.2 M Tricine/KOH, pH 9, 10 mM $MgCl_2$
200 µL	100 u mL^{-1} G6PDH grade II (EC: 1.1.1.49)
200 µL	2.5 mM NADP
5.3 mL	Ultrapure water

Mix 2

3.3 mL	0.2 M Tricine/KOH, pH 9, 10 mM $MgCl_2$
100 µL	500 u mL^{-1} G6PDH grade I (EC: 1.1.1.49)
400 µL	200 mM EDTA pH 8
200 µL	250 mM G6P
200 µL	10 mM PMS – light sensitive!!
1 mL	10 mM MTT – light sensitive!!

The amounts of chemicals for both mixes refer to one microplate (96-well).

Fructose-6-phosphate

Fructose-6-phosphate (F6P) was analyzed with 10 µL extract (shoot, root) and, 10 µL were used for the calibration curve (0/0.4/1/2/4/10 µM F6P in 0.2 M Tricine/KOH, pH 9, 10 mM $MgCl_2$). After adding 30 µL of mix 1 the samples were homogenized. After 20 min of incubation at RT, 10 µL of 0.25 M HCl was added and samples were mixed again. After incubation for another 5 min at RT, 10 µL of 0.1 M Tricine/KOH, pH 9 containing 0.25 M NaOH was added. Then, 10 µL of mix 2 was added and samples were incubated for 20 min at RT. In the next step, 20 µL of 0.5 M NaOH was added, the microplate was sealed and samples subsequently incubated for 10 min at 98.5 °C in a dry bath. After cooling down, samples were centrifuged (1 min, 400 rpm, RT) and 20 µL of 0.1 M Tricine/KOH, pH 9 containing 0.5 M HCl was added and mixed. Finally, 52 µL of mix 3 was added and samples were immediately measured at 570 nm (37 °C, kinetics: 1 read every 30 s). When preparing mix 2, PMS and MTT were added last, because of their light sensitivity.

Mix 1

800 µL	0.2 M Tricine/KOH, pH 9, 10 mM $MgCl_2$
200 µL	100 u mL^{-1} G6PDH grade II (EC: 1.1.1.49)
200 µL	2.5 mM NADP
1.8 mL	Ultrapure water

Mix 2

200 µL	100 u mL^{-1} G6PDH grade II (EC: 1.1.1.49)
200 µL	20 u mL^{-1} phosphoglucoisomerase (PGI) (EC: 5.3.1.9)
600 µL	Ultrapure water

Mix 3

3.3 mL	0.2 M Tricine/KOH, pH 9, 10 mM $MgCl_2$
200 µL	1000 u mL^{-1} G6PDH grade I (EC: 1.1.1.49)
400 µL	200 mM EDTA pH 8
200 µL	250 mM G6P
200 µL	10 mM PMS – light sensitive!!
1 mL	10 mM MTT – light sensitive !!

The amounts of chemicals for all mixes refer to one microplate (96-well).

Glucose-1-phosphate

Glucose-1-phosphate (G1P) was analyzed with 10 µL extract for the roots, 15 µL in case of the leaf material and, 10 µL were used for the calibration curve (0/0.4/1/2/4/10 µM F6P in 0.2 M Tricine/KOH, pH 9, 10 mM $MgCl_2$). After adding 30 µL of mix 1 the samples were homogenized. After 20 min of incubation at RT, 10 µL of 0.25 M HCl was added and samples were mixed again. After incubation for another 5 min at RT, 10 µL of 0.1 M Tricine/KOH, pH 9 containing 0.25 M NaOH was added.

Then, 10 µL of mix 2 was added and samples incubated for 20 min (RT). In the next step 20 µL of 0.5 M NaOH was added, the microplate was sealed and samples were subsequently incubated for 10 min at 98.5 °C in a dry bath. After cooling down, samples were centrifuged (1 min, 400 rpm, RT) and 20 µL of 0.1 M Tricine/KOH, pH 9 containing 0.5 M HCl was added and mixed. Finally, 52 µL of mix 3 was added and the samples were immediately measured at 570 nm (37 °C, kinetics 1 read every 30 s). When preparing mix 2 PMS and MTT were added last, because of their light sensitivity.

Mix 1

800 µL	0.2 M Tricine/KOH, pH 9, 10 mM, $MgCl_2$
200 µL	100 u mL^{-1} G6PDH grade II (EC: 1.1.1.49)
200 µL	2.5 mM NADP
1.8 mL	Ultrapure water

Mix 2

200 µL	100 u mL^{-1} G6PDH grade II (EC: 1.1.1.49)
200 µL	20 u mL^{-1} PGM (EC: 5.4.2.2)
200 µL	50 µM glucose 1,6 bis-phosphate
400 µL	Ultra pure water

Mix 3

3.3 mL	0.2 M Tricine/KOH, pH 9, 10 mM $MgCl_2$
200 µL	1000 u mL^{-1} G6PDH grade I (EC: 1.1.1.49)
400 µL	200 mM EDTA pH 8
200 µL	250 mM G6P
200 µL	10 mM PMS – light sensitive !!
1 mL	10 mM MTT – light sensitive !!

The amounts of chemicals for all mixes refer to one microplate (96-well).

To calculate the concentration of a hexose phosphate in nmol $well^{-1}$ the mean velocity (Mean V_{max}) of each sample and standard was calculated (Safas M96 software or Tec5 software, BioTek). Based on the regression equation of the hexose-phosphates standards, the amount of the hexose-phosphate in µmol g^{-1} FW was calculated, considering the total extraction volume, the amount of volume which was used for the single analysis as well as the amount of FW material for each sample.

Hexose-phosphate (HexP in nmol $well^{-1}$) = (ΔOD ± slope) / intercept

$$\text{HexP (µmol g}^{-1}\text{ FW)} = \text{HexP}_{\text{nmol well}^{-1}} * \frac{VolE}{VolA} * \frac{1}{FW}$$

where
$HexP_{nmol\ well\text{-}1}$ = Hexose-phosphate (nmol $well^{-1}$)
Vol_E = total extraction volume (µL)
Vol_A =used volume of extract for the assay (µL)
FW = Fresh weight (or DW) of sample (mg)

1.12.3 Organic acids

Citrate

The determination of citrate is based on the method of Tompkins and Toffaleti (1982) and was modified. Due to the risk of precipitation, citrate was always measured immediately after the extraction and the determination of chlorophyll; the ethanolic extract can be re-heated up at 37 °C to improve the measurement if nessccessary. For the analysis the extract (15 µL shoot, 20 µL root) was mixed with 90 µL assay mix and the absorbance was read at 340 nm for approximately 5 min, after a stable OD was reached. Then, 14 u ml^{-1} citrate lyase (EC: 2.3.3.8) solved in 0.1 M Tricine/KOH pH 8, was added and the measurement resumed until a final plateau was reached (Figure 1-6).

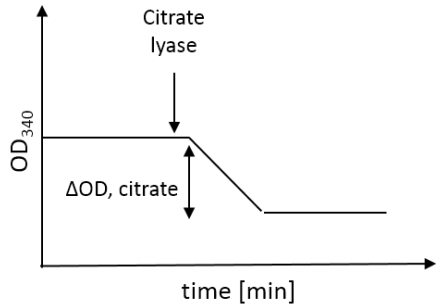

Figure 1-6: Scheme of citrate determination.
Citrate lyase is added after initial OD is stable.

Assay mix

6.25 mL	1 M Tricine/KOH, pH 8
6.25 µL	200 mM $ZnSO_4$
37.5 µL	66 mM NADH
18.8 µL	1000 u mL^{-1} malate dehydrogenase (EC: 1.1.1.37)
6.2 mL	Ultrapure water

The amounts of chemicals for all mixes refer to one microplate (96-well).

For the calculation, the ΔOD of every sample, based on the difference of the initial baseline and the final base line of the measurement was determined. The concentration of citrate in µmol g^{-1} FW or DW was calculated considering the ΔOD, the extinction coefficient (ε) 6.22 mM^{-1} cm^{-1} for NADPH and the length (l) of the optical path of 2.85 cm L^{-1}, the total extraction volume, the specific amount of extract which was used for the analysis as well as the amount of plant material which was used.

$$\text{Citrate } (\mu\text{mol g}^{-1}\text{ FW}) = \Delta\text{OD} \,/\, 6.22 \,/\, 2.85 * \frac{VolE}{VolA} * \frac{1}{FW} * 1000$$

where ΔOD difference between initial and final base line of the measurement
6.22 = extinction coefficient (ε) for NADPH (mM^{-1} cm^{-1})
2.85 = length (l) of the optical path (cm L^{-1})
Vol_E = total extraction volume (µL)
Vol_A =used volume of extract for the assay (µL)
FW = Fresh weight (or DW) of sample (mg)

Malate and fumarate

The determination of malate and fumarate was performed in a combined stopped assay (shoot 15 µL, root 7 µL). For SDs (0/31.25/62.5/125/250/500/1000 µM malate or fumarate in 0.2 M Tricine/KOH, pH 9) 20 µL each were used. After adding 80 µL of assay mix to samples and SDs, samples were mixed and immediately read at 540 nm until OD was stabilized. Then, 5 µL of 1000 u ml^{-1} malate dehydrogenase (EC: 1.1.1.37) was added and samples were read until the first cycling process of malate was finished. After stabilization of the OD, 5 µL of 100 u ml^{-1} of fumarase (EC: 4.2.1.2) was added and absorbance was read again until the cycling process was finished (Figure 1-7).

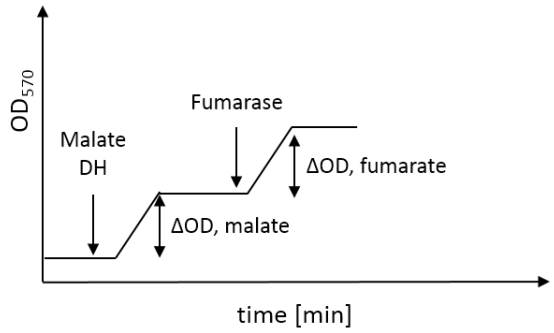

Figure 1-7: Scheme of malate and fumarate determination. Enzymes were successively added after every cycling step. After the entire measurement ΔODs for all samples were calculated. Malate DH, malate dehydrogenase.

Assay mix

5 mL	0.2 M Tricine/KOH, pH 9
1 mL	30 mM NAD
500 µL	10% Triton X-100
500 µL	2.5 mM PES – light sensitive !!
1 mL	100 mM MTT – light sensitive !!

The amounts of chemicals for all mixes refer to one microplate (96-well).

The calculation was done, defining ΔOD from the readings of the cycling process of each sample for each organic acid first. Using the equation from the calibration curve the amount of each metabolite was determined in nmol $well^{-1}$. The concentration of malate or fumarate in µmol g^{-1} FW was calculated considering the amount of each metabolite per well, the total extraction volume, the used volume of extract as well as the amount of weight plant material.

Malate/fumarate (nmol $well^{-1}$) (M_{well}) = (ΔOD ± slope) / intercept

$$\text{Malate/fumarate } (\mu\text{mol g}^{-1}\text{ FW}) = \text{M}_{\text{well}} * \frac{VolE}{VolA} * \frac{1}{FW}$$

where M_{well} = Metabolite in (nmol $well^{-1}$)
Vol_E = total extraction volume (µL)
Vol_A =used volume of extract for the assay (µL)
FW = Fresh weight of sample (mg)

1.12.4 Nitrate

Nitrate (NO_3-) concentrations in roots were determined with 5 µL and with 10 µL in case of shoots according Cross *et al.* (2006) with modifications. Samples were diluted with 0.1 M KOH buffer, pH 7.5 (dilution root 1:10, dilution shoot 1:5). Standards were prepared with 10 µL (0/0.25/0.5/0.75/1/1.5/2 mM mL^{-1} sodium nitrate in 96 % EtOH). For the analysis, 95 µL of the assay mix containing nitrate reductase (NR; EC: 1.7.1.2) were added to the samples. Blanks were prepared with the assay mix *without* NR to determine the nitrite amount in the samples. In case of the assay mix for the blanks, NR was replaced with 0.1 M KOH, pH 7.5. Afterwards, all samples were homogenized and incubated for 30 min at RT in the dark. Then, 15 µL of 0.25 mM PMS were added, samples were mixed again and incubated for another 20 min at RT. Subsequently, 60 µL of 1 % sulfanilamide (w/v) in 3 M phosphoric acid and 60 µL of 0.02 % (w/v) N(1-Naphtyl)ethylemdiamine dihydrochloride (NNEDA) in 3 M phosphoric acid were pipetted and samples were mixed. After 10 min of incubation in the dark (RT), samples were measured immediately at 540 nm.

Assay mix

8.4 mL	Ultrapure water
1 mL	1 M potassium phosphate buffer, pH 7.5
50 µL	50 mM NADPH
100 µL	5 u ml^{-1} NR or 0.1 M potassium buffer, pH 7.5
1.5 mL	PMS
6 mL	1 % sulfanilamide (w/v) in 3 M phosphoric acid
6 mL	0.02 % (w/v) NNEDA in 3 M phosphoric acid

The amounts of chemicals for all mixes refer to one microplate (96-well).

Using the equation from the calibration curve, the amount of nitrate was determined in nmol $well^{-1}$. The concentration of nitrate in µmol g^{-1} FW or DW was calculated considering the amount of nitrate in nmol $well^{-1}$, the total extraction volume, the used volume of extract and the dilution factor as well as the amount of plant material.

Nitrate (nmol $well^{-1}$) (NO_{3well}) = (OD ± slope) / intercept

$$\text{Nitrate } (\mu\text{mol g}^{-1}\text{ FW}) = (\text{NO}_{3\text{-well}} * \frac{VolE}{VolA} * \frac{1}{FW}) * Fdil$$

where
$NO_{3\text{-well}}$ = Nitrate (nmol $well^{-1}$)
Vol_E = total extraction volume (µL)
Vol_A =used volume of extract for the assay (µL)
FW = Fresh weight of sample (mg)
F_{dil} = Dilution factor

1.12.5 Amino acids

Total amino acid content

The AA_t was determined by a fluorescamine reaction. Here, fluorescamine react with primary amines and lysine chains at RT and AA_{tl} can be detected in picomole range. For the analysis, 3 µL of ethanolic extract for all samples and SDs (0/0.032/0.063/ 0.125/0.25/0.5/1 mM ml^{-1} glutamate sodium salt in 70 % EtOH (v/v) 0.1 M HEPES/KOH, pH 7) were added with 15 µL 0.1 M sodium borate buffer, pH 8, 100 µL of ultrapure water and finally 90 µL 0.1 % fluorescamine (w/v) in acetonitrile. Due to its light sensitivity fluorescamine was added in the last pipetting step, and the fluorescence was measured after incubation for 5 min at RT in the dark, at 405 nm for the excitation and at 485 nm for the emission. The glutamate SD was always prepared fresh.

Assay mix

1.5 mL	0.1 M sodium borate buffer, pH 8
10 mL	Ultrapure water
10 mL	0.1 % fluorescamine (w/v) in acetonitrile

The amounts of chemicals for all mixes refer to one microplate (96-well).

Using the equation from the calibration curve, the amount of AA_t was determined in nmol $well^{-1}$. The concentration in µmol g^{-1} FW or DW was calculated considering the amount of AA_t in nmol $well^{-1}$, the total extraction volume, the used volume of extract and the amount of plant material.

Calculation of the AA_t (nmol $well^{-1}$) $(AA_t) = (OD \pm slope) / intercept$

$$\mathrm{AA_t}\ (\mu\mathrm{mol\ g^{-1}\ FW}) = \mathrm{AA_{twell}} * \frac{VolE}{VolA} * \frac{1}{FW}$$

where AA_{twell} = Total amino acid content per well (nmol $well^{-1}$)
Vol_E = total extraction volume (µL)
Vol_A =used volume of extract for the assay (µL)
FW = Fresh weight of sample (mg)

Proline

Proline was analyzed using the ninhydrine reaction (Gibon *et al.* 2000). At low pH, ninhydrine almost specifically reacts with proline, yielding a red chromogene. But ornithine and lysine to a lesser extent, also yields in a red chromogen under these conditions. The sensitivity of this method is about 1 nmol and the linearity of the measurement range is 1 - 200 nmol.

For the analysis, 80 µL of the ethanolic extract or standard (0/32.25/62.5/125/250/500/1000 µM ml^{-1} proline in 70 % EtOH) was added with 100 µL of a 1 % ninhydrine solution (w/v) in 60 % (v/v) acetic acid and ethanol 20% (v/v). Samples and SDs floated for 20 min at 95°C in water bath and were sub-

sequently cooled down and centrifuged for 2 min at 4000 rpm. For the determination in the microplate reader, 80 µL of the sample was transferred into a microplate and absorbance was measured immediately at 520 nm to prevent the degradation of the red, light sensitive chromogene.

The concentration in nmol well^{-1} was calculated using the regression equation of the proline standards.

Proline (nmol well^{-1}) (Pro_{well}) = (OD ± slope) / intercept

$$\text{Proline } (\mu\text{mol g}^{-1}\text{ FW}) = \text{Pro}_{\text{well}} * \frac{VolE}{VolA} * \frac{1}{FW}$$

where Pro_{well} = Proline (nmol well^{-1})
Vol_E = total extraction volume (µL)
Vol_A =used volume of extract for the assay (µL)
FW = Fresh weight of sample (mg)

Glutamate

The determination of glutamate was done using 7 µL ethanolic extract for the roots and 20 µL for the leaves. Standards were measured with 10 µL of standard solution (0/32.25/62.5/125/250/500/1000 µM ml^{-1} glutamic acid in 0.1 M Tricine/KOH, pH 8.5). For the analysis, 185 µL of assay mix was added to all samples and subsequently homogenized. Samples were measured immediately at 570 nm (37 °C, kinetic 1 read every 40 s) until OD stabilized, then, 5 µL of 500 u ml^{-1} glutamate dehydrogenase (EC: 1.4.1.3) solved in 0.1 M Tricine/KOH, pH 8.5 was added and reading was continued until the end of the substrate cycling.

Assay mix

13.3 mL	Ultrapure water
2 mL	1 M Tricine/KOH, pH 8.5
1 mL	30 Mm NAD
200 µL	50 mM ADP
500 µL	10% Triton X-100
500 µL	2.5 mM PES – light sensitive !!
1 mL	100 mM MTT – light sensitive !!

The amounts of chemicals for all mixes refer to one microplate (96-well).

The calculation for glutamate in the samples was done, determining the ΔOD from the kinetics' of the cycling process of each SD and samples first. Using the equation from the calibration curve the amount of glutamate was determined in nmol well^{-1}. The concentration in µmol g^{-1} FW was calculated considering the amount of glutamate per well, the total extraction volume, the used volume of extract as well as the amount of weight plant material.

Glutamate (nmol well^{-1}) (glu_{well}) = (ΔOD ± slope) / intercept

$$\text{Glutamate } (\mu\text{mol g}^{-1}\text{ FW}) = \text{glu}_{\text{well}} * \frac{VolE}{VolA} * \frac{1}{FW}$$

where glu_{well} = Glutamate (nmol well^{-1})
Vol_E = total extraction volume (µL)
Vol_A =used volume of extract for the assay (µL)
FW = Fresh weight of sample (mg)

1.12.6 Soluble sugars

Glucose, Fructose, Sucrose

The determination of the hexoses glucose and fructose as well as sucrose is based on the method of Stitt *et al.* (1989). The determination of all sugars in the shoot was done with 40 µL of ethanolic extract. For the root glucose and fructose were determined in one measurement with 40 µL ethanolic extract. Due to the high sugar content in the taproots, the ethanolic extract for the sucrose determination was diluted 1:100 and then 30 µL of this dilution was taken for the analysis.

For the analysis, the extract was added with 160 µL of assays mix. Samples were shaken and subsequently measured at 340 nm (37 °C, kinetics 1 read every 30 s). Once the OD was stabilized the enzymes for the sugar determination were added successively (Figure 1-8) Firstly 5 µL of 180 u ml^{-1} hexokinase (HK, EC: 2.7.1.1) for determination of glucose, secondly 5 µL of 210 u ml^{-1} phosphoglucose isomerase (PGI, EC: 5.3.1.9) for the determination of fructose and finally 5 µL ≥ 300 u ml^{-1} invertase grade VII (INV, EC: 3.2.1.26) for the determination of sucrose in form of glucose equivalents. All enzymes were solved in 0.1 M HEPES/KOH, pH 7 containing 3 mM $MgCl_2$ and added when each cycling process was finished, observable when the OD was stabilized.

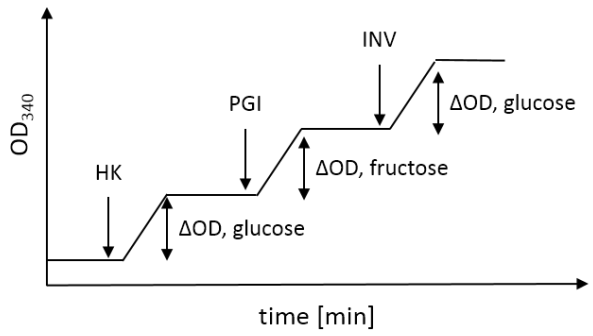

Figure 1-8: Scheme of sugar determination.
Enzymes were successively added after every cycling step. After the entire measurement ΔODs for all samples were calculated. HK, hexokinase; PGI, phosphogluco isomerase; INV, invertase.

Firstly 5 µL of 180 u ml^{-1} hexokinase (HK, EC: 2.7.1.1) for determination of glucose, secondly 5 µL of 210 u mL^{-1} phosphoglucose isomerase (PGI, EC: 5.3.1.9) for the determination of fructose and finally 5 µL ≥ 300 u mL^{-1} invertase grade VII (INV, EC: 3.2.1.26) for the determination of sucrose in form of

glucose equivalents. All enzymes were solved in 0.1 M HEPES/KOH, pH 7 containing 3 mM $MgCl_2$ and added when each cycling process was finished, observable when the OD was stabilized.

Assay mix

15.5 mL	0.1 M HEPES/KOH, pH 7 with 3 mM $MgCl_2$
480 µL	60 mg mL^{-1} ATP
480 µL	36 mg mL^{-1} NADP
80 µL	3500 u mL^{-1} G6PDH grade II (EC: 1.1.1.49)*

*Remove ammonium sulfate supernatant after centrifugation (2 min, 13400 rpm).
The amounts of chemicals for all mixes refer to one microplate (96-well).

Sugar concentrations were calculated, determining the ΔOD from the kinetics' of the cycling processes of each sample. The concentration of glucose, fructose and sucrose in form of glucose equivalents in µmol g^{-1} FW or DW was calculated considering the ΔOD, ε with 6.22 mM^{-1} cm^{-1} for NADPH and the length (l) of the optical path of 2.85 cm L^{-1}, the total extraction volume, the specific amount of extract which was used for the analysis and the dilution factor if necessary as well as the amount of plant material which was used. In case of sucrose the final result was divided by 2 because sucrose was determined as glucose equivalent as mentioned above.

$$\text{Sugar } (\mu\text{mol g}^{-1}\text{ FW}) = \Delta\text{OD} / 6.22 / 2.85 * \frac{\boldsymbol{VolE}}{\boldsymbol{VolA}} * \frac{\mathbf{1}}{\boldsymbol{FW}} * \mathbf{1000}$$

where
- ΔOD difference between initial and final base line of each measurement
- 6.22 = ε for NADPH (mM^{-1} cm^{-1})
- 2.85 = length (l) of the optical path (cm L^{-1})
- Vol_E = total extraction volume (µL)
- Vol_A =used volume of extract for the assay (µL)
- FW = Fresh weight (or DW) of sample (mg)

1.12.7 Starch and total protein

The pellet from the initial ethanolic (see 1.12) was re-suspended in 400 µL 0.1 M NaOH and subsequently heated (95°C, 30 min). After cooling down to RT, the samples were thoroughly homogenized and centrifuged (14.000 rpm, 5 min) before further analysis of the total protein content and for the starch determination in form of glucose equivalents.

Starch - Hydrolysis and digestion

In the first step, pellet and supernatant from the previous extraction were thoroughly re-suspended and hydrolyzed with 80 µL 0.5 M HCl + acetate/0.1 M NaOH buffer, pH 4.9 (neutralization step). In the second step, 35 µL of the thoroughly mixed aliquots were transferred into a new microplate

together with 65 µL of the degradation mix. For the preparation of the starch degradation mix, amyloglucosidase and α-amylase were centrifuged together (13.400 rpm, 2 min). After discarding the supernatant, the pellet was solved in 12.5 ml of 50 mM acetate buffer pH 4.9. Samples were then finally digested for 10-16 h at 37°C. After digestion, the plate was centrifuged (4000 rpm, 10 min, RT).

Determination of glucose equivalents

For the glucose determination, supernatant (20 µL shoot, taproot) was pipetted into a new microplate. After adding 160 µL of the glucose determination mix, samples were read as described in 1.12.6 Soluble sugars. Calculation was done as decribed 1.12.6.

Starch hydrolysis

8 mL	0.5 M HCl + acetate/0.1 M NaOH buffer, pH 4.9

Starch degradation mix

250 µL	Amyloglucosidase (EC: 3.2.1.3)
3 µL	α-amylase (EC: 3.2.1.1)
12.5 mL	50 mM acetate buffer pH 4.9

Glucose determination mix

15.5 mL	0.1M HEPES/KOH pH 7 + 3 mM $MgCl_2$
480 µL	60mg mL^{-1} ATP
480 µL	36 mg mL^{-1} NADP
80 µL	50 mM acetate buffer pH 4.9
80 µL	3500 u mL^{-1} G6PDH grade II (EC: 1.1.1.49)*

*Remove ammonium sulfate supernatant after centrifugation (2 min, 13400 rpm).
The amounts of chemicals for all mixes refer to one microplate (96-well).

Total protein content

After centrifugation of the extract aliquots (3 µL shoot, taproot) or 3 µL of a BSA (bovine serum albumin) standard (0.0875/0.175/0.35/0.70/1.4 mg/ml in 0.1 NaOH) were pipetted into a new plate. For blanks, 3 µL 0.1 M NaOH was used. After adding of 180 µL Bradford solution (Sigma Aldrich, ready to use) the plate was briefly shaken and measured at 595 nm after 5 min incubation in the dark.

BSA stock

100 mg	Bovine serum albumin (BSA)
10 mL	Ultrapure water

For the calculation of total protein content, the calibration curve for BSA in µg $well^{-1}$ from the blank corrected BSA SDs was used. The total protein content (mg g^{-1} FW or DW) was calculated as followed

$$\text{Total protein (mg g}^{-1}\text{ FW)} = \text{conc}_{\text{well}} * \frac{VolE}{Vol} * \frac{1}{FW}$$

where $\text{conc}_{\text{well}}$ = Protein concentration in µg well^{-1} from the blank corrected BSA SDs
Vol_E = total extraction volume (µL), 400 µL NaOH
Vol_A =used volume of extract for the assay (µL)
FW = Fresh weight (or DW) of sample (mg)

1.13 ^{1}H-NMR ANALYSIS

Proton nuclear magnet resonance analysis (^{1}H-NMR) of polar extracts of beet root and leaf samples was performed to provide an overview of some major determinants of the water stress resistance. Polar metabolites were extracted with an ethanol–water series (adapted from Moing *et al.* 2004) using a pipetting robot (Hamilton, Bonaduz, Switzerland). Briefly, for each sample, two subsamples (20 mg DW each) were extracted successively with twice 300 µL 80% ethanol–water (v/v), 300 µL 50% ethanol–water (v/v) and 300 µL water at 80°C for 15 min. The four supernatants of each sub-sample were pooled, dried under vacuum and lyophilized. The dried extracts were titrated with KOH to apparent pH 6.00 in 100 mM potassium phosphate deuterated buffer solution containing 3 mM EDTA (to chelate paramagnetic cations and improve spectrum resolution, especially in the citrate region), and lyophilized again. The dried titrated extracts were stored in the dark under vacuum at RT, before ^{1}H-NMR analysis was completed within one week. ^{1}H-NMR spectra were recorded on each dried titrated extract solubilized in 0.5 mL deuterium oxide (D_2O) added with sodium salt of (trimethylsilyl)propionic-2,2,3,3-d4 acid (TSP) at a final concentration of 0.01% (mg/mL) for chemical shift calibration. The mixture was centrifuged at 17,700 g for 5 min at RT; the supernatant was then transferred into a 5 mm NMR tube (Wilmad 507-PP7, Vineland, NJ, USA). NMR spectra were acquired at 500.162 MHz at 300 K on an Avance III spectrometer (Bruker Biospin, Wissembourg, FR) using a 5 mm ATMA broadband inverse probe flushed with nitrogen gas and an electronic reference for quantification (Digital ERETIC, Bruker TopSpin 3.0). Sixty-four scans of 32 K data points were acquired with a 90° pulse angle, a spectral width of 6,000 Hz, acquisition time of 2.73 s and recycle delay of 20 s. An automation procedure (automatic sample loading, 90 s temperature equilibration time, automatic tuning and matching and automatic shimming with Topshim) requiring about 35 min per sample was used for data acquisition. Preliminary data processing was carried out with TOPSPIN 3.0 software (Bruker Biospin, Karlsruhe, Germany). Each Free Induction Decay (FID) was Fourier transformed (0.3 Hz line broadening), manually phased and baseline corrected. The resulting spectra were aligned by setting the TSP signal to zero ppm. The assignments of metabolites in the NMR spectra were made by comparing the proton chemical shifts with literature (Fan 1996) and databases values (MeRy-B 2011, HMDB, BMRB), by comparison with spectra of authentic compounds recorded under the same buffer

solution conditions and by spiking the samples. Metabolite concentrations in the NMR tube were calculated using the Analytical Profiler mode of AMIX software (version 3.9.10, Bruker) for calculation of resonance areas, followed by data export to Excel software (Microsoft, Redmond, USA). For absolute quantification, three calibration curves (glucose and fructose: 1.25 to 50 mM, glutamate and glutamine: 0 to 15 mM) were prepared and analysed analyzed under the same conditions. The glucose calibration was used for the quantification of all compounds, as a function of the number of protons of selected resonances except fructose, glutamate and glutamine that were quantified using their own calibration curve. Then metabolite concentrations in each sample were calculated from concentrations in the NMR tube and sample dry weight. The concentration of each organic or amino acid was expressed as g of the acid form per weight unit. The concentration of NMR unknown compounds (named using the mid value of the chemical shift and the multiplicity of the corresponding resonance group: unknown D1.84 for a doublet at 1.84 ppm) was calculated hypothesizing that the observed resonance corresponded to one proton and using an arbitrary molecular weight of 100 Da. 1H–1H COSY (2D-homonuclear Correlation Spectroscopy), 1H–13C HSQC (2D-heteronuclear Correlation Spectroscopy) and 1D 13C experiments were carried out to verify the identity of known compounds and to check if unknown signals really correspond to different compounds.

1.14 INFRARED THERMOGRAPHY

Infrared thermography (IRT) was done in cooperation with the department of Phytomedicine (PD Dr. Anne Mahlein). For this, a sterling-cooled infrared scanning camera (VARIOSCAN 3021 ST, JENOPTIK, Jena, Germany) with a spectral sensitivity from 8 to 12 µm and a geometric resolution of 1.5 m radians (240 x 360 pixels focal plane array, 30° x 20° field of view lens, minimum focus distance 0.2 m) was used. The thermal resolution is 0.03 K with an accuracy of absolute temperature measurement less than ± 2K. Digital thermal images were analyzed using the software package IRBIS plus V 2.2 (Infratec, Dresden, Germany). Thermographic imaging took place every other day before the harvest between 7:30 am and 9:00 am, and sugar beet plants were previously acclimatized in the laboratory for 30 minutes. The environmental conditions during the measurements were 23 ± 2°C and between 50% and 65% RH. In order to correct for slight fluctuations of the surrounding temperature, absolute temperature values were always normalized to room temperature. For correlation analysis (n=4 per treatment and day), the mean leaf temperature was determined for the leaf that was subsequently destructively sampled for metabolite analysis.

1.15 REFERENCES

Barrs H, Weatherley P (1962) A re-examination of the relative turgidity technique for estimating water deficits in leaves. *Australian Journal of Biological Sciences*. http://www.publish.csiro.au/?paper=BI9620413.

Bhargava S, Sawant K (2013) Drought stress adaptation: metabolic adjustment and regulation of gene expression (R Tuberosa, Ed.). *Plant Breeding* 132, 21–32. doi:10.1111/pbr.12004.

Bloch D, Hoffmann CM, Märländer B (2006a) Solute accumulation as a cause for quality losses in sugar beet submitted to continuous and temporary drought stress. *Journal of Agronomy and Crop Science* 192, 17–24. doi:10.1111/j.1439-037X.2006.00185.x.

Bloch D, Hoffmann C, Märländer B (2006b) Impact of water supply on photosynthesis, water use and carbon isotope discrimination of sugar beet genotypes. *European Journal of Agronomy* 24, 218–225. doi:10.1016/j.eja.2005.08.004.

Brown KF, Biscoe P V (1985) Fibrous root growth and water use of sugar beet. *The Journal of Agricultural Science* 105, 679–691. doi:10.1017/S0021859600059591.

Crisp PA, Ganguly D, Eichten SR, Borevitz JO, Pogson BJ (2016) Reconsidering plant memory: Intersections between stress recovery, RNA turnover, and epigenetics. *Science Advances* 2, 1–14. doi:10.1126/sciadv.1501340.

Cross JM, von Korff M, Altmann T, Bartzetko L, Sulpice R, Gibon Y, Palacios N, Stitt M (2006) Variation of enzyme activities and metabolite levels in 24 Arabidopsis accessions growing in carbon-limited conditions. *Plant Physiology* 142, 1574–1588. doi:10.1104/pp.106.086629.

Draycott AP (2006) "Sugar Beet." (AP Draycott, Ed.). (Blackwell Publishing Ltd: Oxford) http://eu.wiley.com/WileyCDA/WileyTitle/productCd-140511911X.html.

Ehlers W, Goss M (2016) "Water dynamics in plant production." (Centre for Agriculture and Biosciences International) http://www.cabi.org/bookshop/book/9781780643816.

Enz M, Dachler C (1997) "Compendium of growth stage identification keys for mono- and dicotyledonous plants – extended BBCH scale." (BBA, BSA, IGZ, IVA, AgrEvo, BASF, Bayer, Novartis)

Flexas J, Barón M, Bota J, Ducruet JM, Gallé A, Galmés J, Jiménez M, Pou A, Ribas-Carbó M, Sajnani C, Tomàs M, Medrano H (2009) Photosynthesis limitations during water stress acclimation and recovery in the drought-adapted Vitis hybrid Richter-110 (V. berlandieri×V. rupestris). *Journal of Experimental Botany* 60, 2361–2377. doi:10.1093/jxb/erp069.

Galmes J, Hipolito M, Flexas J (2007) Photosynthetic limitations in response to water stress and recovery in Mediterranean plants with different growth forms. *The New Phytologist* 175, 81–93. doi:10.1111/j.1469-8137.2007.02087.x.

Gibon Y, Sulpice R, Larher F (2000) Proline accumulation in canola leaf discs subjected to osmotic stress is related to the loss of chlorophylls and to the decrease of mitochondrial activity. *Physiologia Plantarum* 110, 469–476. doi:10.1111/j.1399-3054.2000.1100407.x.

Gibon Y, Vigeolas H, Tiessen A, Geigenberger P, Stitt M (2002) Sensitive and high throughput metabolite assays for inorganic pyrophosphate, ADPGlc, nucleotide phosphates, and glycolytic intermediates based on a novel enzymic cycling system. *The Plant Journal : For cell and molecular biology* 30, 221–235. http://www.ncbi.nlm.nih.gov/pubmed/12000458.

Großkinsky DK, Svensgaard J, Christensen S, Roitsch T (2015) Plant phenomics and the need for physiological phenotyping across scales to narrow the genotype-to-phenotype knowledge gap. *Journal of Experimental Botany* 66, 5429–5440. doi:10.1093/jxb/erv345.

Hanson AD, Hitz WD (1982) Metabolic response of mesophytes to plant water deficits. *Annual Review of Plant Physiology* 33, 163–203. doi:10.1146/annurev.pp.33.060182.001115.

Hodges DM, DeLong JM, Forney CF, Prange RK (1999) Improving the thiobarbituric acid-reactive-substances assay for estimating lipid peroxidation in plant tissues containing anthocyanin and other interfering compounds. *Planta* 207, 604–611. doi:10.1007/s004250050524.

Hoffmann CM (2010) Sucrose accumulation in sugar beet under drought stress. *Journal of Agronomy and Crop Science* 196, 243–252. doi:10.1111/j.1439-037X.2009.00415.x.

Hoffmann CM (2014) Adaptive responses of Beta vulgaris L. and Cichorium intybus L. root and leaf forms to drought stress. *Journal of Agronomy and Crop Science* 200, 108–118. doi:10.1111/jac.12051.

Kadereit G, Borsch T, Weising K, Freitag H (2003) Phylogeny of Amaranthaceae and Chenopodiaceae and the evolution of C4 photosynthesis. *International Journal of Plant Sciences* 164, 959–986. doi:10.1086/378649.

Karnovsky MJA (1965) A formaldehyde-glutaraldehyde fixative of high osmollality for use in electron microscopy. *Journal of Cell Biology* 27, 137.

Knörzer K-H (1991) Geschichte der Rübe (Beta vulgaris L.) mit Beiträgen durch Großrestfunde vom Niederrhein. InHajnalova E (ed) "Paleoethnobotany Archaeol. 8th Symp. Int. Work Gr. Palaeoethnobotany," 159–164

Lawlor DW, Milford GFJ (1975) The control of water and carbon dioxide flux in water-stressed sugar beet. *Journal of Experimental Botany* 26, 657–665.

Lichtenthaler HK (1987) Chlorophylls and carotenoids: Pigments of photosynthetic biomembranes. *Plant Cell Membranes* 148, 350–382. doi:https://doi.org/10.1016/0076-6879(87)48036-1.

Loel J, Hoffmann CM (2014) Relevance of osmotic and frost protecting compounds for the winter hardiness of autumn sown sugar beet. *Journal of Agronomy and Crop Science* doi: 10.11, 1–11. doi:10.1111/jac.12083.

Loel J, Kenter C, Märländer B, Hoffmann CM (2014) Assessment of breeding progress in sugar beet by testing old and new varieties under greenhouse and field conditions. *European Journal of Agronomy* 52, 146–156. doi:10.1016/j.eja.2013.09.016.

Marschner H, Kylin A, Kuiper PJC (1981) Differences in salt tolerance of three sugar beet genotypes. *Physiologia Plantarum* 51, 234–238. doi:10.1111/j.1399-3054.1981.tb02704.x.

McKersie BD, Leshem YY (1994) "Stress and stress coping in cultivated plants." (Springer Netherlands: Dordrecht) doi:10.1007/978-94-017-3093-8.

Metzner R, van Dusschoten D, Bühler J, Schurr U, Jahnke S (2014) Belowground plant development measured with magnetic resonance imaging (MRI): exploiting the potential for non-invasive trait quantification using sugar beet as a proxy. *Frontiers in Plant Science* 5, 469. doi:10.3389/fpls.2014.00469.

Moing A, Maucourt M, Renaud C (2004) Quantitative metabolic profiling by 1-dimensional ^{1}H-NMR analyses: application to plant genetics and functional genomics. *Functional Plant Biology* 31, 889–902. doi:10.1071/FP04066.

Monti A, Brugnoli E, Scartazza A, Amaducci MT (2006) The effect of transient and continuous drought on yield, photosynthesis and carbon isotope discrimination in sugar beet (Beta vulgaris L.). *Journal of Experimental Botany* 57, 1253–1262. doi:10.1093/jxb/erj091.

Ober ES, Bloa M Le, Clark CJA, Royal A, Jaggard KW, Pidgeon JD (2005) Evaluation of physiological traits as indirect selection criteria for drought tolerance in sugar beet. *Field Crops Research* 91, 231–249. doi:10.1016/j.fcr.2004.07.012.

Ober E, Rajabi A (2010) Abiotic Stress in Sugar Beet. *Sugar Tech* 12, 294–298. doi:10.1007/s12355-010-0035-3.

Pariyar S, Eichert T, Goldbach HE, Hunsche M, Burkhardt J (2013) The exclusion of ambient aerosols changes the water relations of sunflower (Helianthus annuus) and bean (Vicia faba) plants. *Environmental and Experimental Botany* 88, 43–52. doi:10.1016/j.envexpbot.2011.12.031.

Pidgeon JD, Werker a. R, Jaggard KW, Richter GM, Lister DH, Jones PD (2001) Climatic impact on the productivity of sugar beet in Europe, 1961–1995. *Agricultural and Forest Meteorology* 109, 27–37. doi:10.1016/S0168-1923(01)00254-4.

van der Poel PW, Schwieck H, Schwartz T (1998) “Sugar Technology - Beet and Cane Sugar Manufacture.” (Bartens: Berlin)

Rogers A, Gibon Y (2009) Plant Metabolic Networks. “Plant Metab. Networks.” (Ed J Schwender)

Romano A, Sorgonà A, Lupini A, Araniti F, Stevanato P, Cacco G, Abenavoli MR (2012) Morpho-physiological responses of sugar beet (Beta vulgaris L.) genotypes to drought stress. *Acta Physiologiae Plantarum* 35, 853–865. doi:10.1007/s11738-012-1129-1.

Scholten OE, Lange W (2000) Breeding for resistance to rhizomania in sugar beet: A review. *Euphytica* 112, 219–231. doi:10.1023/A:1003988003165.

Soule M (1967) Phenetics of natural populations I. Phenetic relationships of insular populations of the side-blotched lizard. *Evolution* 21, 584. doi:10.2307/2406618.

Souza RP, Machado EC, Silva JAB, Lagoa AMMA, Silveira JAG (2004) Photosynthetic gas exchange, chlorophyll fluorescence and some associated metabolic changes in cowpea (Vigna unguiculata) during water stress and recovery. *Environmental and Experimental Botany* 51, 45–56. doi:10.1016/S0098-8472(03)00059-5.

Štajner D, Mimica-Dukić N, Gasić O (1995) Adaptability to drought in sugar beet cultivars. *Biologia Plantarum* 37, 107–112. doi:10.1007/BF02913005.

Stevanato P, Trebbi D, Panella L, Richardson K, Broccanello C, Pakish L, Fenwick AL, Saccomani M (2015) Identification and validation of a SNP marker linked to the gene HsBvm-1 for nematode resistance in sugar beet. *Plant Molecular Biology Reporter* 33, 474–479. doi:10.1007/s11105-014-0763-8.

Stitt M, McC Lilley R, Gerhardt R, Heldet HW (1989) Metabolite levels in specific cells and subcellular compartments of plants leaves in liomembranes,. “Methods Enzymol.” (Eds S Fleischer, B Fleischer) pp. 518–552. (Academic Press, Inc.: San Diego)

Sukumaran NP, Weiser CJ (1972) Freezing injury in potato leaves. *Plant Physiology* 50, 564–567.

Thomas S, Kuska MT, Bohnenkamp D, Brugger A, Alisaac E, Wahabzada M, Behmann J, Mahlein A-K (2017) Benefits of hyperspectral imaging for plant disease detection and plant protection: a technical perspective. *Journal of Plant Diseases and Protection*. doi:10.1007/s41348-017-0124-6.

Tompkins D, Toffaletti J (1982) Enzymic Determination of Citratein Serum and Urine, with use of the Worthington " Ultrafree " Device. 28, 2031–2033.

Weiland J, Koch G (2004) Sugarbeet leaf spot disease (Cercospora beticola Sacc.). *Molecular Plant Pathology* 5, 157–166. doi:10.1111/j.1364-3703.2004.00218.x.

Windt A, Märländer B (1994) Wurzelwachstum von Zuckerrüben unter besonderer Berücksichtigung des Wasserhaushaltes. *Zuckerindustrie* 119, 659–663.

Wirtschaftliche Vereinigung Zucker e.V. - WZV, VdZ V der Z e. V- (2016) Wirtschaftliche Vereinigung Zucker. http://www.zuckerverbaende.de/.

2 OSMOTIC ADJUSTMENT UNDER DROUGHT AND REWATERING

Osmotic adjustment of young sugar beets (*Beta vulgaris*) under progressive drought stress and subsequent rewatering assessed by metabolite analysis and infrared thermography

Rita Wedeking[A,C], Anne-Katrin Mahlein[B], Ulrike Steiner[B], Erich-Christian Oerke[B], Heiner E. Goldbach[A] and Monika A. Wimmer[A,D]

[A]Department of Plant Nutrition, Institute of Crop Science and Resource Conservation (INRES), University of Bonn, Bonn, Karlrobert-Kreiten-Str. 13, 53 115 Bonn, Germany.
[B]Department of Phytomedicine, Institute of Crop Science and Resource Conservation (INRES), University of Bonn, Meckenheimer Allee 166a, 53 115 Bonn, Germany.
[C]Environmental Safety/Metabolism, Bayer CropScience AG, Alfred-Nobel-Str. 50, 40789 Monheim, Germany.
[D]Corresponding author. Email: m.wimmer@uni-bonn.de

Functional Plant Biology, http://dx.doi.org/10.1071/FP16112

2.1 ABSTRACT

The main objective of this work was to provide the chronology of physiological and metabolic alterations occurring under drought and demonstrate how these relate to a phenotypic approach (infrared thermal imaging, IRT). This should provide tools to tailor phenotyping approaches for drought tolerance and underlying metabolic alterations. In the present study, destructive analysis of growth and cell morphology, water status, osmotic adjustment, metabolic changes and membrane damage were combined with non-destructive determination of leaf temperature using infrared thermography (IRT) in 6-week-old sugar beets subjected to progressive drought stress and subsequent rewatering. Different methods were suitable for the characterization of the dynamic development of distinct stress phases: although IRT allowed detection of initial impairment of transpiration within 1 day of drought stress, destructive methods allowed us to distinguish a phase of metabolic adjustment including redirection of carbon flow into protective mechanisms and a subsequent phase of membrane destabilization and cellular damage. Only the combination of invasive and non-invasive methods allowed for the differentiation of the complete sequence of physiological changes induced by drought stress. This could be especially beneficial for the selection of phenotypes that are adapted to early drought. During rewatering, sugar beet shoots rapidly re-established water relations, but membrane damage and partial stomatal closure persisted longer, which could have an impact on subsequent stress events. During the onset of secondary growth, taproots required more time to recover the water status and to readjust primary metabolites than shoots.

2.2 INTRODUCTION

Sugar beet (*Beta vulgaris* L. spp. *vulgaris*) is the main sugar producing crop in temperate climates, providing almost 90% of sugar for the European Union, with an annual sugar production of 14.9 million tons in 2015–16 (Wirtschaftliche Vereinigung Zucker 2016). It is considered as a highly drought- and salt tolerant crop, based on the ability of mature sugar beets to compensate temporal drought by complete leaf abscission, and to recover quickly after precipitation. However, high sugar yield and good technical quality of the taproot require sufficient precipitation, especially during the period of secondary root growth, and drought stress is the major environmental factor responsible for yield and quality losses in sugar beet production (Hoffmann2010). Wilting is often observed under environmental conditions with high evaporative demand, because sugar beets have a limited ability to regulate transpiration (Hanson and Hitz 1982). Similar to other plant species, sugar beets accumulate osmolytes such as sodium (Na^+), potassium (K^+) (Hoffmann 2010), proline (Gzik 1996) and a-amino compounds like amino acids and glycine betaine under drought stress (Mäck and Hoffmann 2006).

However, high concentrations of these osmolytes significantly reduce the technical quality, and thus impede the sugar production process (Van der Poel *et al.* 1998). In order to identify potential breeding traits for drought tolerant sugar beets, physiological and metabolic reactions (Shaw et al. 2002; Ober et al. 2005), genetic resources (Dohm *et al.* 2009) or genotypic variations of sugar beet cultivars under limited water supply (Ober and Luterbacher 2002) have been investigated. Studies considered drought effects during germination and seedling growth (Pestsova *et al*. 2008; Wu *et al.* 2014), or long-term drought stresses extending throughout the stage of taproot development, whereas the responses of young sugar beets to transient drought have rarely been considered (Hoffmann 2014). However, crucial physiological changes like the onset of secondary taproot growth occur during the youth stage between BBCH 14–18. Thereafter, sucrose storage begins, indicating a switch in the sink–source relationship of the plant (Trebbi and McGrath 2009), which is essential for sucrose accumulation and final sugar yield. Short drought events could negatively affect this early critical stage of development reduce the final yield (Chołuj *et al*. 2008), and thus economic gain. In Central Europe, contrasting with many arid environments of lower latitudes, drought events are often not terminal, but can occur at any stage throughout plant development. They are often interrupted by episodic precipitation periods that range from single, usually heavy rainfall events, to several days or weeks. For this region, climate change models predict an increase in extreme weather events and altered seasonal and regional precipitation patterns, more specifically a decrease of summer precipitation and concomitant increase of transient drought events early in the growing season (IPCC 2007). Crop yield in areas with such intermittent drought stress is highly dependent upon the capacity of the crop to recover after rehydration (Chaves *et al*. 2009), which includes mechanisms to re-establish shoot and root growth and osmotic homeostasis, to repair tissues damaged by oxidative stress, and to readjust metabolism. Incomplete or slow recovery may change the plant's response to a subsequent drought spell, a phenomenon that we observed in experiments with sugar beets subjected to repeated drought cycles with only short recovery periods (M. A. Wimmer, unpubl. data). In addition, incomplete recovery of osmotic adaptations of sugar beet roots after a long-term drought stress with subsequent rewatering were observed in a field experiment and were considered critical for the technical sugar quality (Chołuj *et al*. 2008). Until recently, little was known about the dynamics of metabolic and physiological processes that occur during this recovery phase in sugar beet (Bloch 2006; Sicher *et al.* 2012). Breeding programs for drought-prone environments require early and non-invasive stress detection to facilitate the characterisation of cultivars in phenotyping facilities and field trials. Rapid stress detection is required as well for a precise and sustainable irrigation management. A large number of non-invasive sensor techniques have been developed for stress detection in high-throughput phenotyping facilities (Fiorani *et al.* 2012). Infrared thermography (IRT) can be used to assess the plant water status (Jones *et al.* 2009; Zarco-Tejada *et al*. 2012; Gago *et al.* 2015), salt

stress responses (Munns et al. 2010) or manifestation of plant pathogen infections at early stages (Oerke *et al*. 2006; Mahlein *et a*l. 2012a). A gap still exists between the external phenotype and corresponding physiological and metabolic processes, which, however, represent the 'internal phenotype' and integrate environmental signals into cellular responses (Großkinsky *et al*. 2015). Hence, the aim for the present study was to combine non-destructive and destructive methodologies as a step towards establishing a link between non-invasive imaging and the dynamics of physiological and metabolic processes. With this methodological approach, the study addressed two purposes: (i) to determine the dynamics of the physiological and metabolic responses to progressive drought stress in Beta vulgaris plants during early phases of secondary taproot growth, and (ii) to investigate the dynamics of recovery of different physiological processes after rewatering.

2.3 MATERIALS AND METHODS

2.3.1 Plant growth conditions

Seeds of Beta vulgaris L. cultivar Pauletta (KWS Saat AG, Einbeck, Germany) were grown in a mixture of sand and potting soil (v/v, 1: 1) until the first leaf pair was fully developed, and transferred into 2 L pots filled with a substrate mix (3 : 2 : 1 peat, loam, perlite; Gepac, Type VM). Plants were grown under controlled conditions at 24°C day/18°C night temperature, 60/75% RH and 16 h light (>250 mmol m^{-2} s^{-1}: SON-T Agro, 400W, Philips)/8h darkness. Plants were arranged in a randomised block design with four biological replicates for each harvest day and treatment. Water and nutrients (1.4‰ Hakaphos blue, Compo Expert) were supplied three times a day for 3 min, each, using a time controlled, automated irrigation system. This resulted in a water content of 65–69% (w/w, based on substrate FW) during pre-treatment growth, corresponding to substrate pF (log_{10} of the absolute value of the soil matrix potential, unitless) values between 1.8 and 2.3 (Table 1-2). Every second day, a subset of 15 pots was weighed to confirm that neither water logging nor water deficit occurred. During the experiment, plants were kept free of pests and diseases by integrated plant protection. Preliminary experiments ensured that drought stress and rewatering treatments were repeatable.

2.3.2 Treatments and sampling

Treatments started when plants reached BBCH 16–17 (Enz and Dachler 1997). Plants were then either watered as before (control), subjected to 17 days of progressive drought, or drought stressed for 9 days followed by gradual rewatering for 11 days. Because the water volume supplied during each irrigation event was not adjusted to plant growth during the experiment, the average substrate water content (WC_{sub}) of control pots decreased within the treatment period. Nevertheless, an average of 65 ± 5% (w/w; based on substrate FW) was maintained throughout the experiment (Figure 2-1),

which corresponds to a substrate suction of pF = 2.3 and can be considered as optimum water supply.

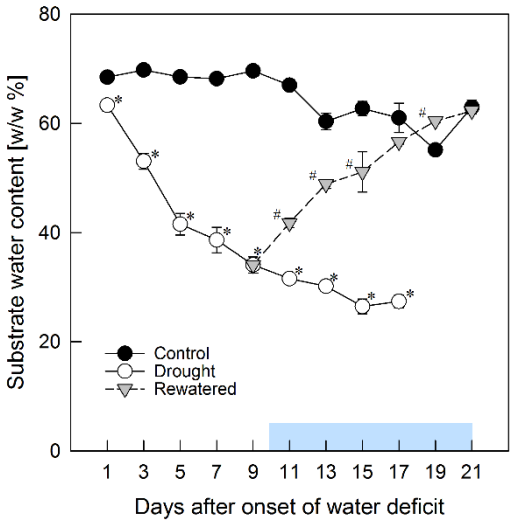

Figure 2-1: Gravimetric water content of GEPAC Anzuchterde. Gravimetric water content (w/w, based on substrate FW) of the soil substrate mix under regular water supply (control, closed circles), progressive drought stress (open circles) and rewatering (triangles). The horizontal bar represents the recovery period. Values are means ± SE, n=4. For each harvest day, significant differences to the control plants (α=0.05) are indicated by asterisks (drought treatment) and rhombs (rewatering).

During the drought period, the WC_{sub} decreased quickly to 42 ± 4% (w/w) within 5 days, and then more slowly to a minimum of 27 ± 2% (w/w %; Figure 2-1). This means that the substrate reached a soil moisture suction of pF = 4.2 after 5 days, and plants did not have access to soil water during the remaining drought treatment. After 17 days of drought, plants had reached a level of desiccation that did not allow further sampling. The WC_{sub} of the rewatered plants increased linearly and reached control levels after 7 days (Figure 2-1). Plants were harvested every other day. We chose 4 h after the onset of the light period as harvest time to avoid uncontrolled side effects caused by the circadian rhythm of the water status and metabolite concentrations. All plants were photographed by a RGB camera (Panasonic, Lumix DMC-FZ18), measured with a Stirling-cooled infrared scanning camera, and then sampled destructively. The root part 1.5 cm below the crown and the youngest fully expanded leaf pair (YEL) were harvested for taproot and leaf analysis respectively. One leaf of the YEL was used for metabolite analysis. The other leaf was divided into two halves, and one half was used for the determination of the osmotic potential (OP). From the other half, six leaf discs (diameter 9 mm) were punched out from the intercostal areas, and used for the determination of relative water content (RWC) and electrolyte leakage (EL). Plant material for metabolite analysis was immediately frozen in liquid nitrogen, ground under liquid nitrogen (leaf) or lyophilised (root), and stored at -80°C until further analysis. Material for physiological measurements was frozen at -20°C (OP) or directly processed (RWC, EL).

2.3.3 Biomass, relative water content and electrolyte leakage

FW of shoots and roots were determined immediately after harvest and DW after drying at 70°C until reaching a constant weight. Leaf discs were briefly rinsed, incubated in 30 mL of ultrapure water at room temperature (22 ± 2°C) for 4h, and initial conductivity (EL1) was determined in the incubation medium. Discs were then frozen at -20°C for 36h, thawed, equilibrated at room temperature, and final conductivity (EL2) was measured. Electrolyte leakage (EL) was determined:

$$\mathrm{EL}\ (\%) = \left(\frac{\mathrm{EL1}}{\mathrm{EL2}}\right) \times 100$$

The RWC was calculated:

$$\mathrm{RWC}\ (\%) = \left(\frac{\mathrm{FW} - \mathrm{DW}}{\mathrm{TW} - \mathrm{DW}}\right) \times\ 100$$

where TW is the leaf disc turgid weight after rehydration for 4h.

2.3.4 Metabolite extraction and analysis

For metabolite analysis, 20 mg (leaf) or 10 mg (root) of powdered material was sequentially extracted with 250 mL and 150 mL of 80% ethanol (v/v) in 10 mM HEPES KOH pH7, followed by 250 mL of 50% ethanol (v/v) in 10 mM HEPES KOH pH7 at 80°C for 20 min. The three supernatants were pooled and constantly kept on ice. Samples were analysed using a microplate reader (Power Wave XS2, Bio-Tek).

Sucrose, glucose and fructose were determined based on work by Stitt *et al.* (1989) with modifications. For the analysis,160 mL of assay mix consisting of 0.1 M HEPES/KOH pH7,3 mM $MgCl_2$, 60 mg mL^{-1} ATP, 36 mg mL^{-1} NADP and 3500 units mL^{-1} glucose-6-phosphate dehydrogenase grade II (EC 1.1.1.49) were added to 40 mL of ethanolic extract, and absorbance was measured at 340 nm (37°C). Once optical density (OD) was stabilised, 180 units mL^{-1} hexokinase (EC 2.7.1.1), 210 units mL^{-1} phosphoglucose isomerase (EC 5.3.1.9) and 300 units mL^{-1} invertase grade VII (EC 3.2.1.26) were added successively for glucose, fructose and sucrose determination, respectively. Sugar concentrations were calculated from the difference in optical density (ΔOD) before and after addition of the respective enzyme, based on the conversion of the involved cofactor $NADP^+$ to NADPH, and using an extinction coefficient of 6.22 mM^{-1} cm^{-1} for NADPH. Sucrose concentration was calculated by dividing the glucose equivalents by two. Although all extracts were permanently kept on ice to prevent hexose formation from uncontrolled invertase activity, the possibility of such postharvest processes should be kept in mind.

Proline was analysed using the ninhydrin reaction based on the method by Gibon *et al.* (2000). Briefly, 100 mL of a 1% (w/v) ninhydrin solution in 60% (v/v) acetic acid and 20% (v/v) ethanol were added

to 80 mL of extract, heated at 95°C for 20 min, cooled and centrifuged for 2 min at 3300g. Absorbance (l = 520 nm) of the supernatant was measured immediately. For glutamate determination, 185 mL of assay mix containing 1 M Tricine/KOH pH8.5, 30 mM NAD^+, 50 mM ADP, 10% Triton X-100, 2.5 mM PES (phenazine ethosulfate) and 100 mM MTT (thiazol blue tetrazolium bromide) were added to an adequate volume of extract. After stabilisation of the OD at 570 nm (37C), 500 units mL^{-1} of glutamate dehydrogenase (EC 1.4.1.3) dissolved in 0.1 M Tricine/KOH pH8.5 were added.

Malate was measured by adding 80 mL of assay mix (0.2 M Tricine/KOH pH9, 30 mM NAD^+, 10% Triton X-100, 2.5 mM PES and 100 mM MTT) to an adequate volume of extract. After stabilisation of the OD at 540 nm, 1000 units mL^{-1} of malate dehydrogenase (EC 1.1.1.37) were added. Both malate and glutamate concentrations were calculated from ΔOD of standard solutions (0 to 1 mM glutamate and malate respectively) before and after addition of the respective enzyme.

2.3.5 Osmotic potential, osmotic adjustment and metabolite contribution

Frozen leaf or root material was thawed and cell sap was extracted using a manual press. Aliquots of 100 mL were centrifuged at 9600g for 5 min (leaves) or 10 min (roots) to remove debris. The osmolality (in osmol kg^{-1}) was determined using a cryoscopic osmometer (Osmomat 030, Gonotec GmbH), and the OP (in MPa) was obtained by multiplying the osmolality with -2.479 (conversion factor at 25°C; Pariyar *et al.* 2013). Osmotic adjustment (OA) was defined as the difference in OP (ΔOP) between control and stressed plants. DW-based metabolite concentrations ($conc_{metab\ DW}$) were transformed into tissue water-based concentrations ($conc_{metab\ H2O}$):

$$conc_{metab\ H2O} = \frac{conc_{Metab\ DW} \times (1 - WC_{leaf})}{\mathrm{WC}_{leaf}}$$

where WC_{leaf} represents the leaf water content. The contribution to the OP was then calculated:

$$Contribution_{\ metab}(\%) = \frac{\mathrm{conc}_{\ metab\ H2O} \times 100}{\mathrm{OP}}$$

The contribution to OA was calculated accordingly by using the difference in water-based concentrations between control and stressed plants, and ΔOP respectively.

2.3.6 Determination of sodium, potassium and magnesium

Ions were determined in oven-dried, ground material after digestion with HNO_3 and filtration (MN 640 m, Macherey Nagel) by flame emission spectrometry for Na^+ and K^+ (ELEX 6361 Spectrometer, Eppendorf) and atom absorption spectrometry for Mg^{2+} (AAS 1100 B, Perkin Elmer).

2.3.7 IR-Thermography

The IRT camera Varioscan 3021 ST (Jenoptik) had a spectral sensitivity from 8 to 12 mm and a geometric resolution of 1.5 m radians (240 x 360 pixels focal plane array, 30° x 20 field of view lens, minimum focus distance 0.2 m). The thermal resolution was 0.03 K with accuracy of absolute temperature measurement less than ± 2 K. Thermal images were taken at a distance of 100 cm between the camera and the plant material, and analysed using the software IRBIS plus ver. 2.2 (Infratec). Before thermographic imaging, plants were adapted to laboratory conditions for 30 min (which sufficed to avoid side effects by the handling). The environmental conditions during measurements were 23 ± 2°C, 50-65% RH and light conditions were similar to the greenhouse (>250 mmol m^{-2} s^{-1}). In order to correct for differences in the ambient temperature, absolute temperature values were normalised to room temperature. The mean leaf temperature was determined from polygons of leaves (n = 4, per treatment and day) selected for subsequent destructive sampling.

2.3.8 Microscopy

Sugar beet leaf tissue (3-5 mm x 3-5 mm) was sampled and prepared for histological analysis according to Karnovsky (1965) and as described in Mahlein *et al.* (2012b). Toluidine blue stained samples were microscopically examined with a Leitz DMR 6000B photomicroscope.

2.3.9 Statistical analysis

The experiment was conducted in a completely randomized design. Statistical analyses were performed with SPSS 22.0 (SPSS Inc.). Significant differences between treatments were analyzed using a non-parametric test for independent scores. Thus, a one-factorial ANOVA according to Kruskal-Wallis (α=0.05) with the stepwise step-down procedure, was performed. Regression coefficients (r) were calculated with SigmaPlot 12.0 (Systat Software Inc.).

2.4 RESULTS

2.4.1 Growth and development

In the control, root and shoot growth was exponential throughout the experiment (Figure 2-2), and plant developed from BBCH 16-17 on day 1 to BBCH 19 on day 21 (Figure 2-3). Growth was strongly inhibited in drought stressed plants, starting 5-7 days (shoots) and 11-13 days (roots), respectively, after cutting off the irrigation (Figure 2-2). Wilting of older leaves became visible after 5 days and severely affected all fully expanded leaves after 9 days (Figure 2-3). Youngest leaves, however, remained green and turgescent until day 11. Towards the end of the drought treatment (13–17 days),

older leaves became chlorotic and were completely dry. During rewatering, growth of roots and shoots resumed after 5–7 days (Figure 2-2). Younger leaves regained turgescence within 1 day, and wilting of the older leaves disappeared within 7 days (Figure 2-3).

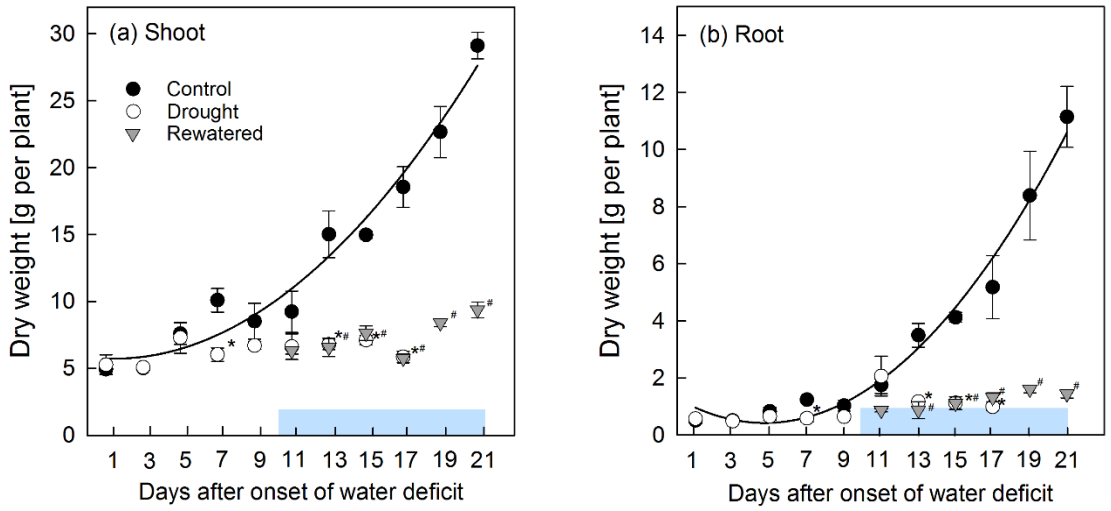

Figure 2-2: Dry weight (DW) of young sugar beet shoots and taproots.
Dry weight (DW) of (a) young sugar beet shoots and (b) taproots under regular water supply (control, closed circles), progressive drought stress (open circles) and rewatering (triangles). The horizontal bar represents the recovery period. Values are means ± s.e. *n* = 4, the regression lines visualise exponential growth of control plants. For each harvest day, significant differences to the control plants (a = 0.05) are indicated: *, *P* < 0.05 (drought treatment) and #, *P* < 0.05 (rewatering).

2.4.2 Leaf temperature

Control plants maintained relatively constant leaf temperatures (excluding the oldest, senescing leaves) throughout the experiment, whereas leaf temperature of drought stressed plants continuously increased and reached ambient temperatures at the end of the stress period (Figure 2-4), when plants were visually completely desiccated (Figure 2-3). To monitor changes in leaf temperature over time, temperature differences (ΔT) between the average temperature of the YEL and the air temperature were used (Figure 2-5). For control plants, ΔT ranged between 2.9 and 1.4 K throughout the experiment, but it decreased from 3.0 to -0.3 K during the drought stress treatment. The difference to controls was significant (P ≤ 0.024) as soon as 5 days after water withholding (Figure 2-5). The main drop of ΔT occurred within the first 3 days of drought with an average rate of 0.50 K day^{-1}, and continued at average rates of 0.18 K/d until day 7 and 0.06 K day^{-1} until day 17 respectively. Under rewatering, ΔT started to increase after a lag period of 2 days, and reached control values after 12 days.

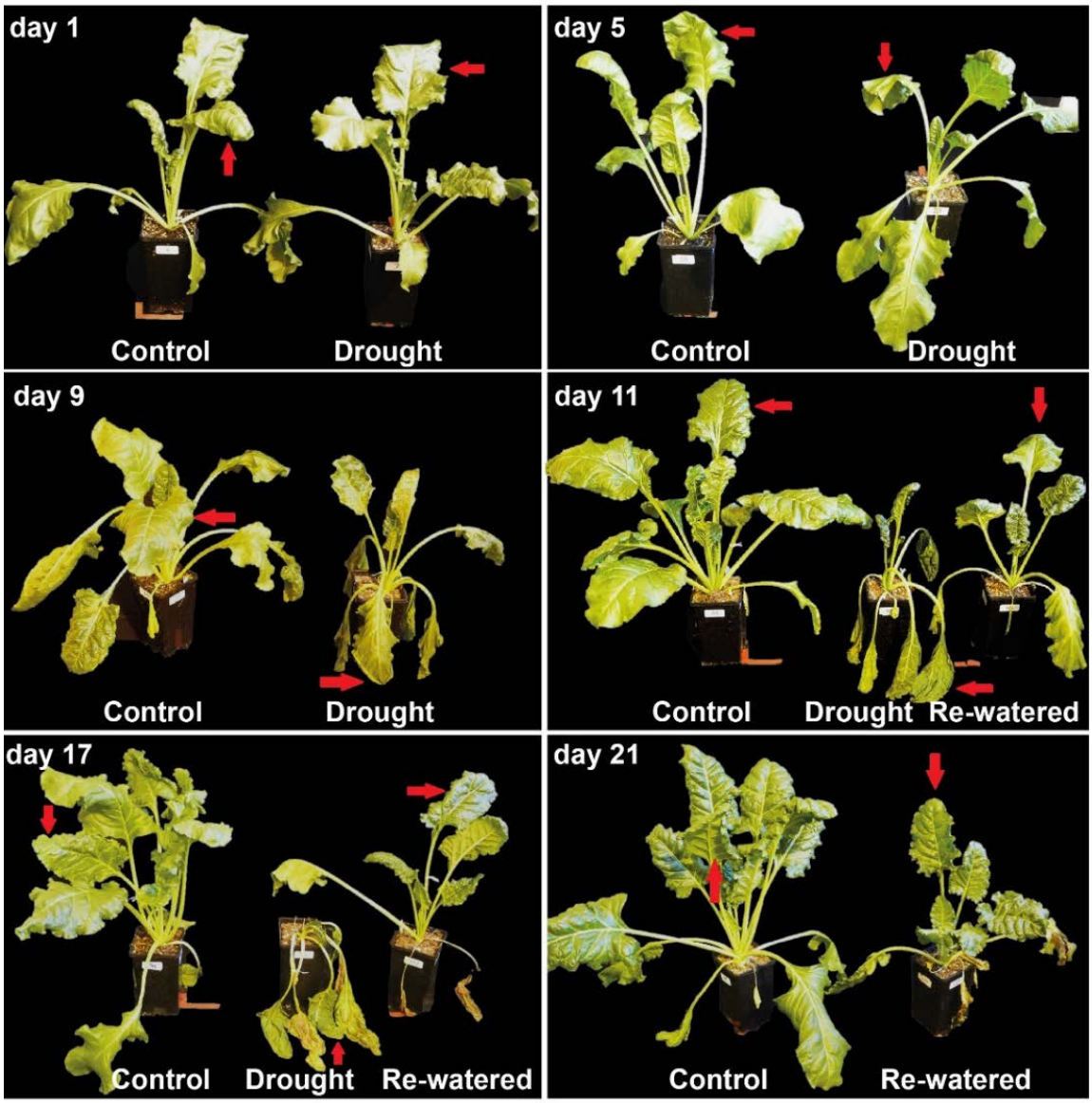

Figure 2-3: RGB images of sugar beet plants during the experimental period.
RGB images of young sugar beet plants under regular water supply (control), drought stress and during rewatering on day 1, 5, 9, 11, 17 and 21 of treatments. The arrow indicates the measured leaf.

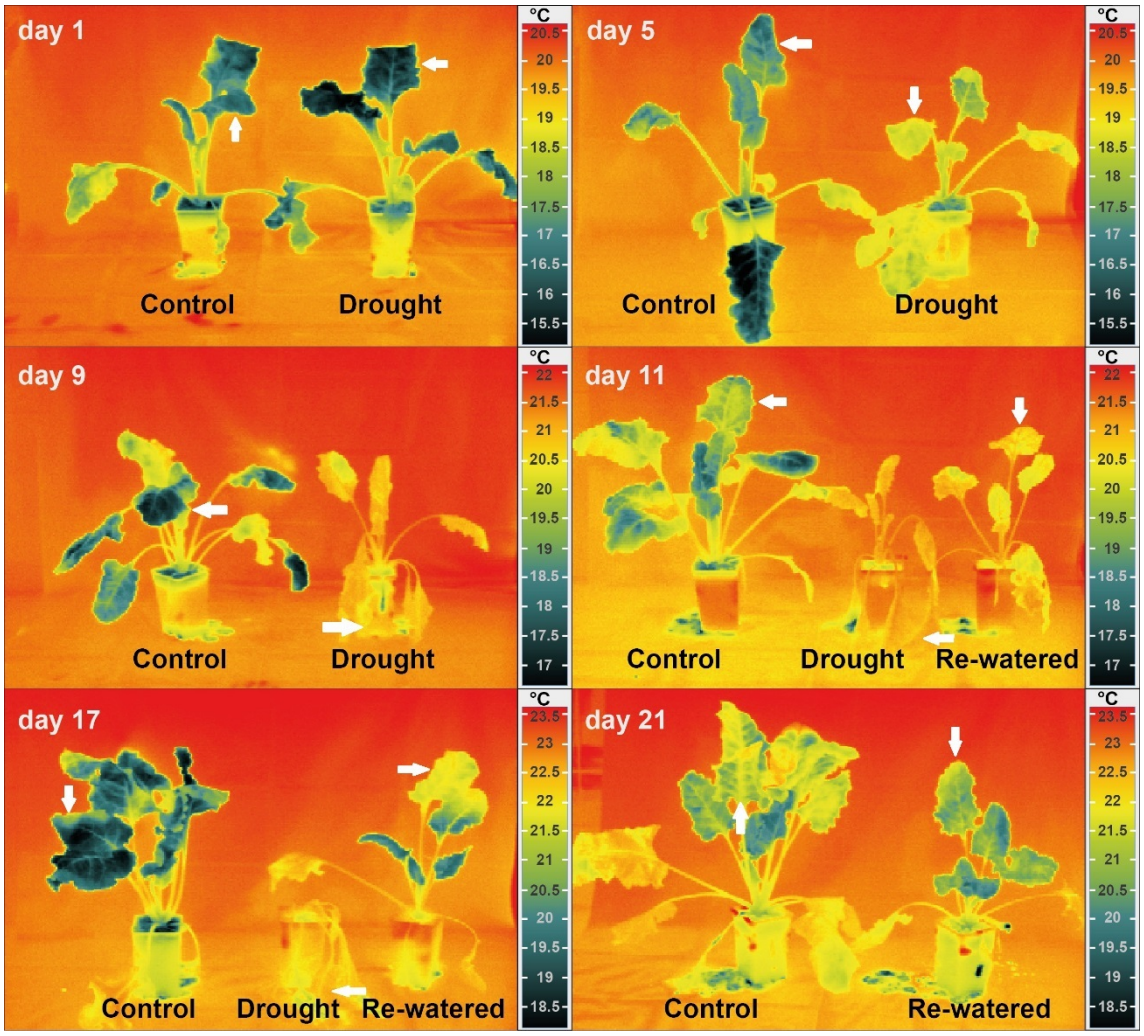

Figure 2-4: Infrared thermal images.
Infrared thermal images of the young sugar beet plants under regular water supply (control), under drought stress and during rewatering 1, 5, 9, 11, 17 and 21 days of treatment. The arrow indicates the measured leaf.

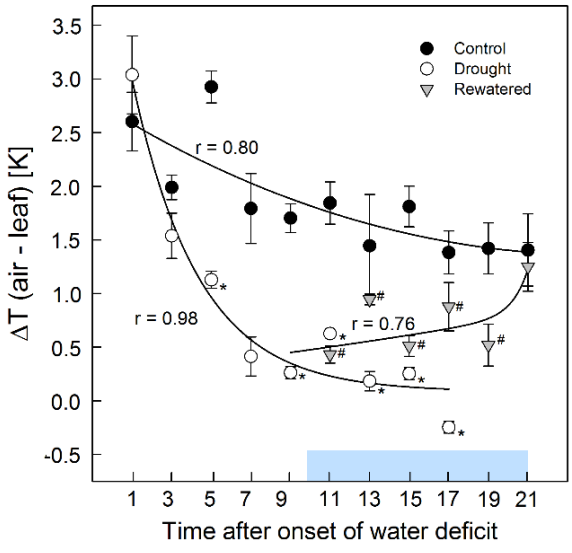

Figure 2-5: Mean temperature difference between the sampled leaf and the ambient temperature.
Mean temperature difference between the sampled leaf and the ambient temperature (ΔT) under regular water supply (control, closed circles), progressive drought stress (open circles) and rewatering (triangles). The horizontal bar represents the recovery period. Values are means ± s.e., *n*=4. For each harvest day, significant differences to the control plants (α=0.05) are indicated: *, $P < 0.05$ (drought treatment) and #, $P < 0.05$ (rewatering).

2.4.3 Plant water status and membrane stability

Under control conditions, RWC of the shoot (RWC_S) and OP of the shoot (OP_S) and root (OP_R) were stable with average values of 86 ± 1%, -1.0 ± 0.2 MPa, and –1.4 ± 0.1 MPa respectively (Figure 2-6). All three parameters responded to drought conditions with comparable temporal dynamics. They did not change during the first 3 days of water withholding, then slowly decreased until day 7 or 9, and significantly dropped thereafter Figure 2-6). The slopes of the corresponding curves significantly changed between days 7 to 11. The RWC_S reached 42 ± 4% after 11 days and maintained this level until the end of the experiment, whereas the final OP after 17 days was -3.5 ± 0.5 MPa in shoots and -4.1 ± 0.3 MPa in roots. The response curves were mirrored by the drought response of EL_S, with a moderate but significant increase from day 3 to 9, and a much steeper increase from day 9 to 17, indicating severe membrane damage during this stress phase (Figure 2-6). Overall highly significant linear correlations were observed between RWC_S and EL_S (r = 0.89) as well as OP_S and RWC_S (r = 0.88, Figure 2-7). Shoots and roots responded differently to rewatering. Whereas the drought-induced decrease in RWC_S and OP_S was stopped immediately, and the increase in EL_S between days 9 and 11 was reduced by 53%, OP_R continued to decrease for another 2 days before it started to recover (Figure 2-6). Relative water content and OP remained below control levels for at least 6–8 days, whereas EL_S did not fully return to control values until the end of the recovery period.

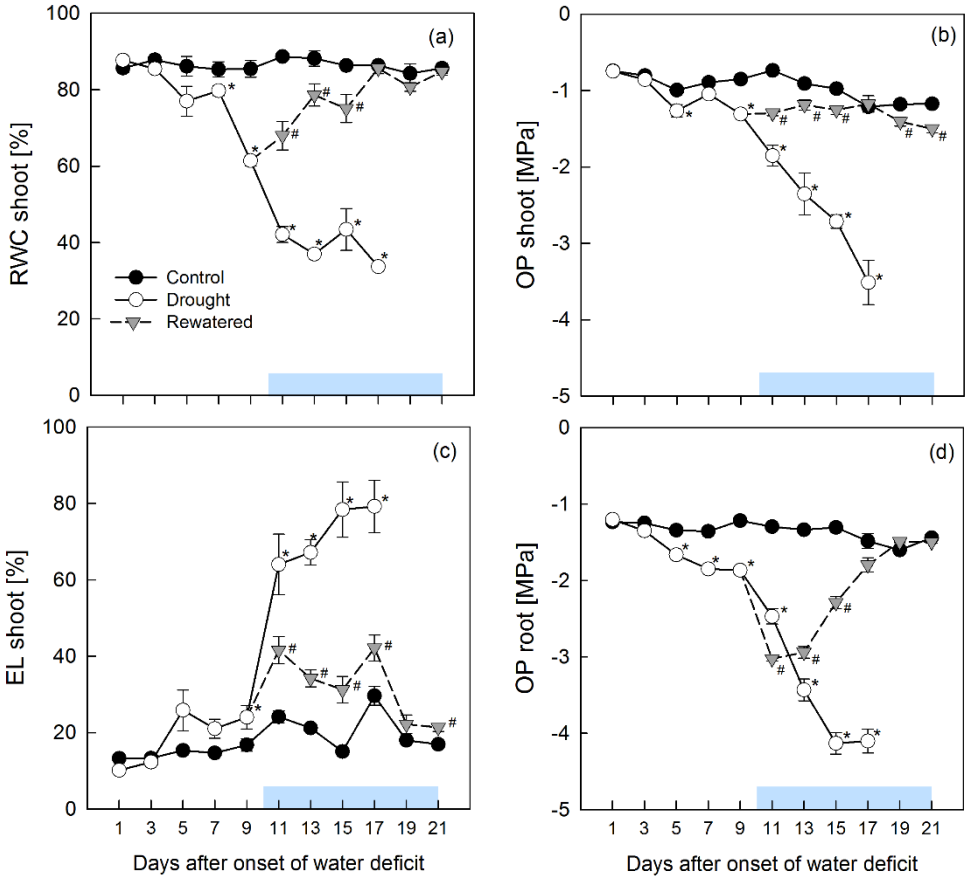

Figure 2-6: RWC, OP and EL of the shoot and OP of the taproot.

Caption 2-6 continued:

(a) Relative water content (RWC), (b) osmotic potential (OP), (c) electrolyte leakage (EL) of the young sugar beet shoot and (d) osmotic potential of the young taproot under regular water supply (control, closed circles), progressive drought stress (open circles) and rewatering (triangles). The horizontal bar represents the recovery period. Values are means ± s.e., *n*=4. For each harvest day, significant differences to the control plants (α=0.05) are indicated: *, *P* < 0.05 (drought treatment) and #, *P* < 0.05 (rewatering).

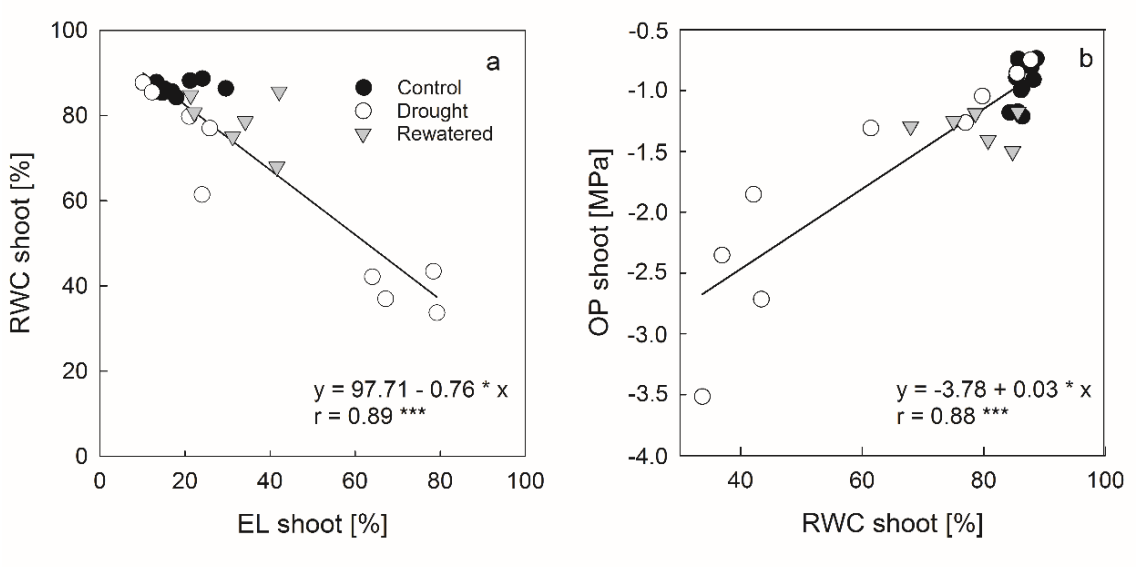

Figure 2-7: Correlation analysis of the relative water content, electrolyte leakage and osmotic potential.
Correlation between electrolyte leakage (EL) and relative water content (RWC) (A) and between RWC and osmotic potential (OP) B) of sugar beet shoots under regular water supply (closed circles), drought stress (open circles) and re-watering (triangles). Values are means ±SE (n=4).

2.4.4 Relationship between leaf temperature and water status of leaves

To reveal the nature of the relationship between ΔT and leaf water status (RWC_S, OP_S) or membrane damage (EL_S), means of each parameter and treatment were correlated. In all cases highly significant ($P < 0.001$) exponential correlations were obtained (Figure 2-8).

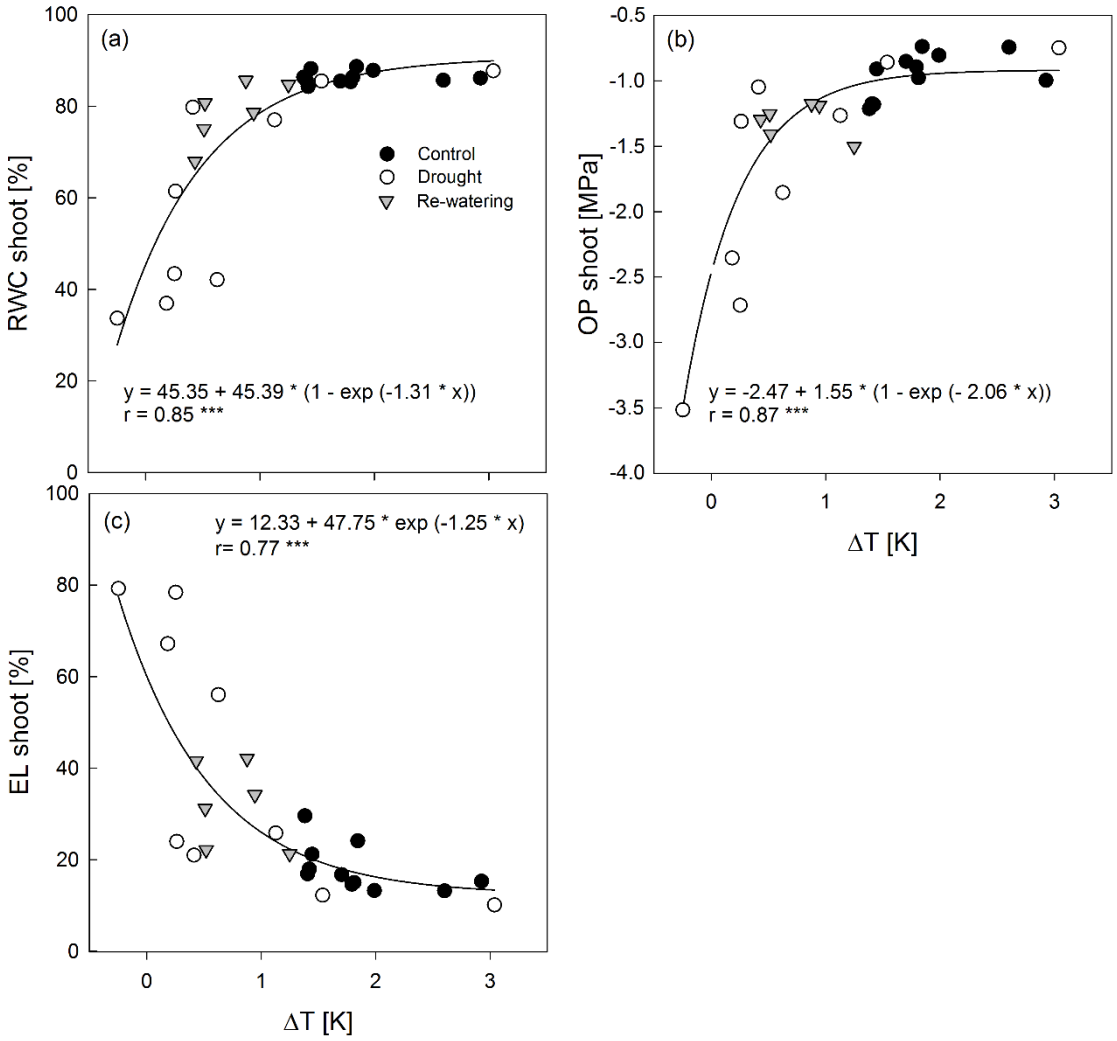

Figure 2-8: Correlation analysis of the mean temperature difference and RWC, OP and EL.
Correlation analysis between the mean temperature difference between the sampled leaf and the ambient temperature (ΔT) and (a) the relative water content (RWC), (b) the osmotic potential (OP) and (c) the electrolyte leakage (EL) of sugar beet shoots under regular water supply (control, closed circles), drought stress (open circles) and rewatering (triangles). Values are means, n=4.

2.4.5 Cellular structures under desiccation and rewatering

Morphological changes in sugar beet leaves under progressive drought stress and rewatering were analysed microscopically (Figure 2-9). Under control conditions, leaf palisade parenchyma and spongy mesophyll cells appeared turgescent and regular (Figure 2-9 a). The upper and lower epidermis and the waxy cuticle were smoothly attached. Some mesophyll cells showed crystalline structures

(Figure 2-9 b). Under drought conditions, wilting and loss of turgor led to sagged leaves after 7–9 days (Figure 2-9 d). The upper epidermis and the palisade parenchyma still appeared quite structured, but the spongy mesophyll and the lower epidermis were sunken and shrunk. Contracted vacuoles were observed as indicated by diffusely arranged chloroplasts. With increasing water deficit, wilting and morphological changes became more serious as the upper epidermis appeared sunken and shriveled at day 11 (Figure 2-9 e). Additionally, crystalline structures were more prominent compared with control leaves. On the last day of drought stress, the whole leaf was collapsed and intracellular structures were clearly ruptured due to shearing forces (Figure 2-9 f). Under rewatering, leaves recovered visually almost completely within one day (Figure 2-3, day 11), the upper and lower epidermis appeared smooth, and palisade parenchyma and spongy mesophyll cells almost regained their regular structure (Figure 2-9g). After 9 days of rewatering, leaves were fully rehydrated and intracellular structures appeared completely regular (Figure 2-9 h).

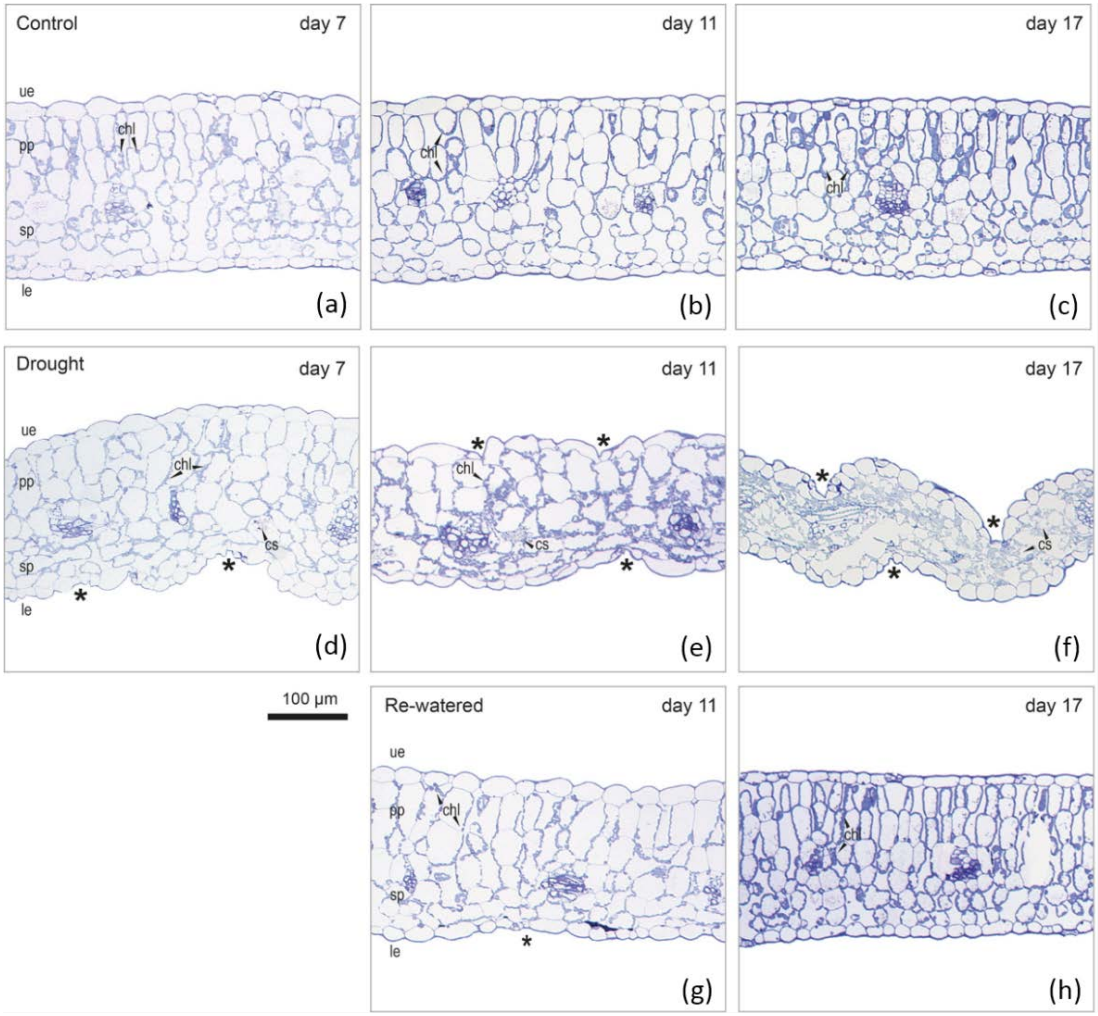

Figure 2-9: Thin-sections of young sugar beet leaves.
Thin-sections of young sugar beet leaves under regular water supply: (a-c): control, (d-f): drought stress, and (g, h): during rewatering at day 7, 11 and 17 of the experiment. Shrunken tissue is indicated: *. Abbreviations: cs, crystalline structures; chl, chloroplast; pp, palisade parenchyma; sp, spongy parenchyma; ue, upper epidermis; le, lower epidermis.

2.4.6 Metabolite changes

Under control conditions, mean leaf concentrations of proline, malate, hexoses and sucrose were 39.0 ± 7.6, 52.0 ± 24.3, 45.3 ± 30.3 and 12.8 ± 2.3 mmol g^{-1} DW respectively (Figure 2-10). Whereas levels of proline and sucrose remained constant, malate concentrations slowly increased over time, and hexose concentrations were subject to fluctuations and showed a strong peak from day 5–7 irrespective of the treatment. Under drought stress, none of the metabolite levels changed from day 1–3. Thereafter, proline levels increased slowly from day 3 to 9, and steeply from day 9 to 17, when proline concentration reached a maximum of 219 mmol g^{-1} DW (Figure 2-10). Hexoses and malate concentrations were lower than in control plants from day 11 to 13, followed by a significant increase in malate on days 15–17 (Figure 2-10). Sucrose concentrations increased from day 3 to 9 after water withholding, decreased from day 9–15, and then increased again during the last 2 days of drought (Figure 2-10).

Metabolite levels of control plants differed between roots and shoots, with mean root concentrations of 0.7 ± 0.2 mmol g^{-1} DW proline, 7.8 ± 1.3 mmol g^{-1} DW malate, 20.3 ± 4.3 mmol g^{-1} DW hexoses and 1.5 ± 0.2 mmol g^{-1} DW sucrose (Figure 2-10). Due to the sucrose sink capacity of the taproot, concentrations of root sucrose were in the millimolar range compared with the micromolar concentrations of the shoot. A steady increase in sucrose was observed for control plants, whereas proline, malate and hexoses remained fairly stable (Figure 2-10). Under drought conditions, concentrations of proline, malate and hexoses were not altered from day 1 to 3, increased slowly from day 3 to 9, followed by a sudden steep increase (Figure 2-10). Different from leaves, root sucrose levels remained lower than controls until day 9, followed by a short but significant increase on day 11, and a continuous decrease thereafter (Figure 2-10).

Rewatering resulted in a transient increase in shoot hexoses and sucrose concentrations, exceeding those of control plants. Concentrations returned to control levels after 7 (hexoses) and 9 (sucrose) days respectively (Figure 2-10). The drought-induced increase in leaf proline was stopped after 2 days of rewatering and proline decreased to control levels within 7 days (Figure 2-10). Malate concentrations returned to control levels immediately after rewatering (Figure 2-10), but a strong malate peak was observed 9 days into the rewatering period. Drought-induced increases in metabolite levels of roots were reversed upon rewatering after a lag period of 2, 4–6, and 5–7 days for malate, proline, and hexoses, respectively (Figure 2-10). Although malate and hexoses returned to control levels, proline concentrations remained higher than controls until the end of the rewatering period.

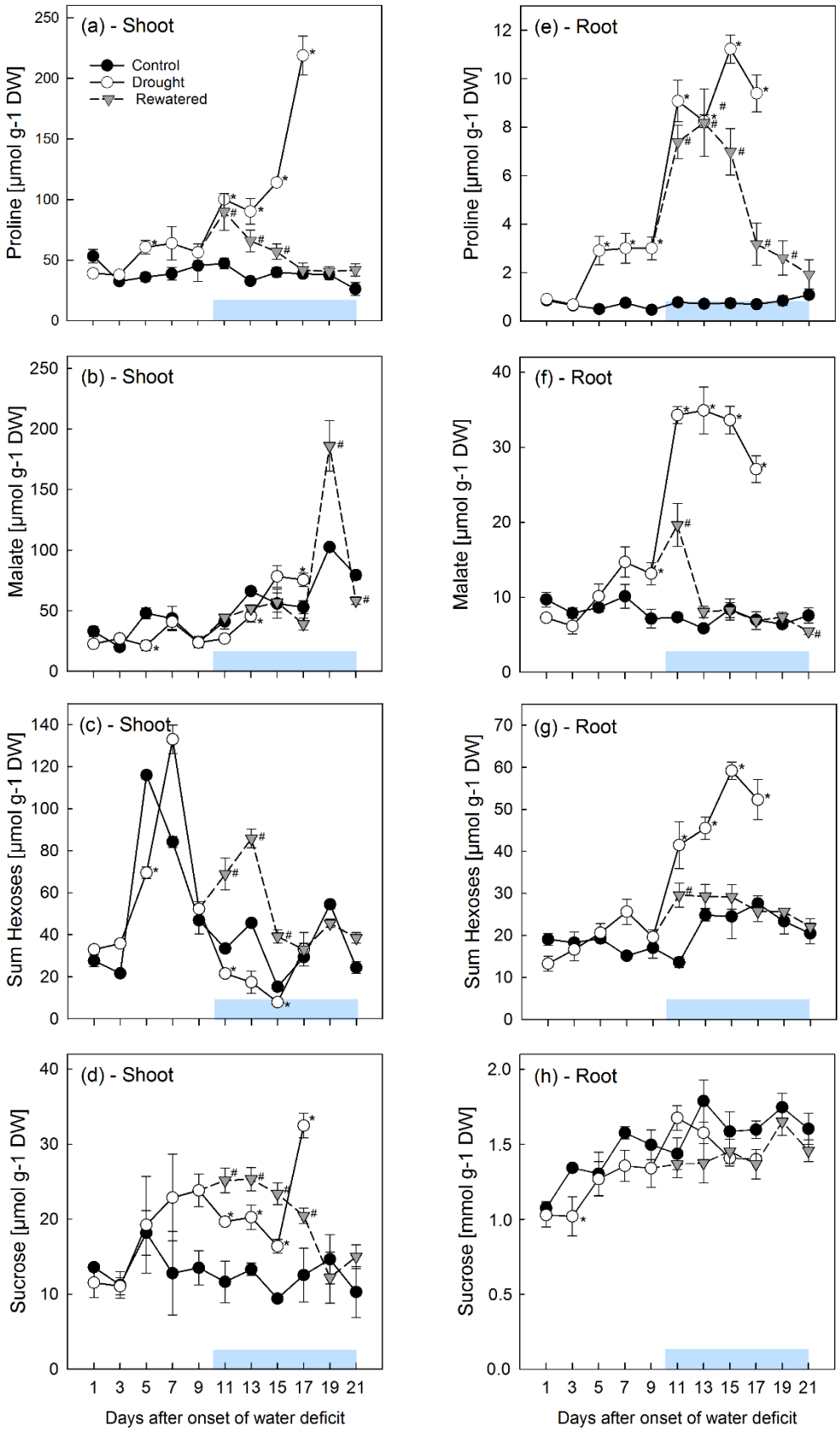

Figure 2-10: **Concentrations of osmotically active compounds in young sugar beet shoots and taproots.**
Concentrations of osmotically active compounds in (a-d) young sugar beet shoots and (e-h) young taproots under regular water supply (control, closed circles), drought stress (open circles) and rewatering (triangles). The horizontal bar represents the recovery period. Values are means ± s.e., n=4. For each harvest day, significant differences to the control plants (α=0.05) are indicated: *, $P < 0.05$ (drought treatment) and #, $P < 0.05$ (rewatering).

2.4.7 Inorganic cation concentrations in taproots

In control plants, root Na^+, K^+ and Mg^{2+} concentrations decreased throughout the experimental period (Figure 2-11). Under drought stress, this decrease was slowed down (Na^+), or stopped (K^+, Mg^{2+}) during the last 6 days of drought, and final K^+ and Mg^{2+} concentrations were significantly higher than in controls. Upon rewatering, cation concentrations returned to control levels within 2 days (Na^+), 6 days (K^+) and 8 days (Mg^{2+}), respectively.

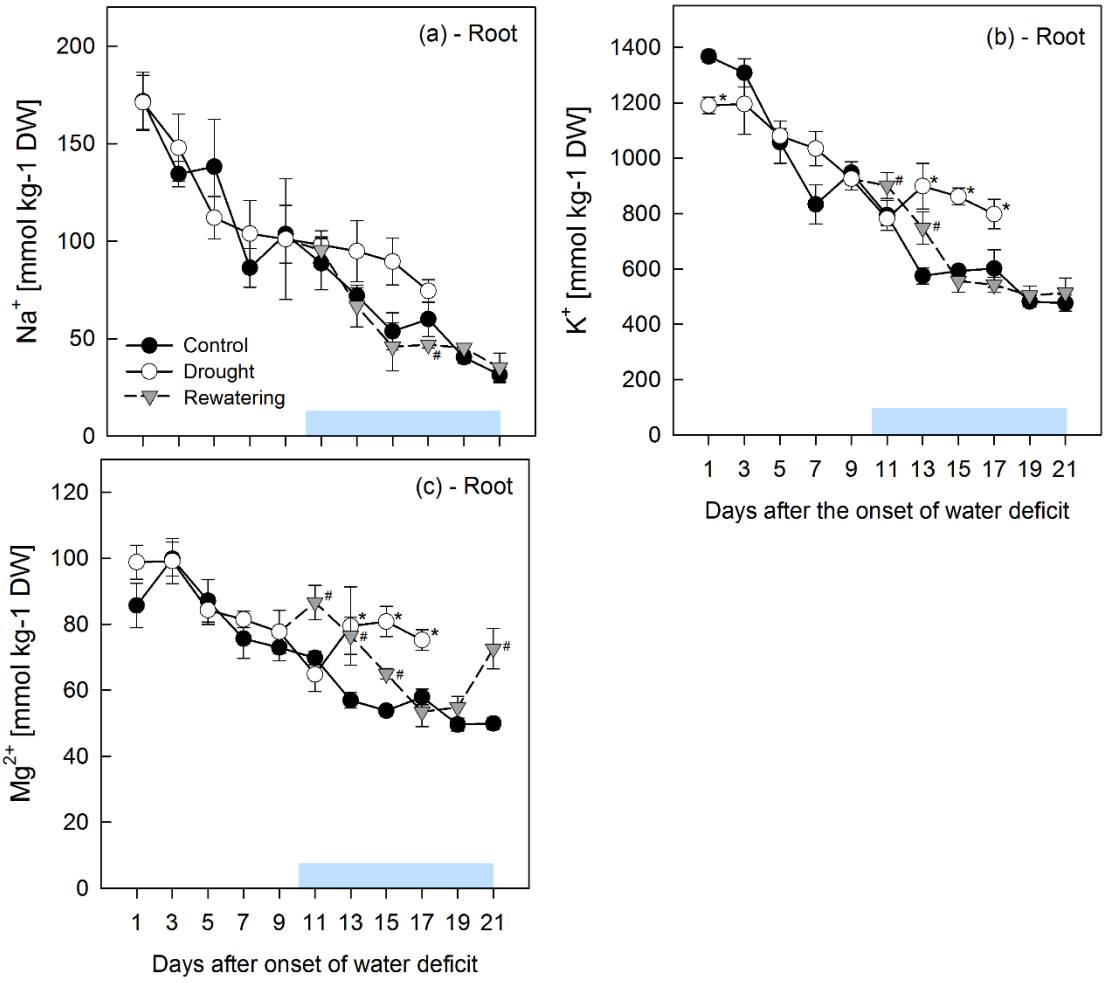

Figure 2-11: Inorganic cation concentrations in taproots.
Concentrations of (a) sodium (Na^+), (b) potassium (K^+), and (c) magnesium (Mg^{2+}) in young sugar beet roots under regular water supply (control, closed circles), drought stress (open circles) and rewatering (triangles). The horizontal bar represents the recovery period. Values are means ± SE, n=4. For each harvest day, significant differences to the control plants (α=0.05) are indicated by asterisks (drought treatment) and rhombs (rewatering).

2.4.8 Contribution of metabolites and inorganic cations to osmotic adjustment

The overall mean relative contribution of metabolites and ions to OP between days 1 and 17 of the experiment was different for shoots and roots, but was not significantly affected by the drought stress treatment (Table 2-1). In shoots, the OP was generated predominantly by inorganic ions (control: 68 ± 2%; stress: 77 ± 4%) and only slightly by metabolites (control: 6.0 ± 0.7%; stress:

5.7 ± 0.7%), whereas in roots the contribution was higher for metabolites (control: 23 ± 2; stress: 20 ± 4%) compared with ions (control: 15 ± 1; stress 16 ± 2%). Under drought stress, osmotic adjustment (OA) resulted in a significant reduction in OP from day 5 onwards (Figure 2-6). In order to estimate which ions and metabolites were mostly responsible for this OA, we calculated the relative contribution of each ion/metabolite to the ΔOP. In shoots, between 74% (P II) and 91% (P III) of OA were explained by the increase in ion concentrations, and K^+ alone accounted for up to 49% of OA, followed by Na^+ (23%) and Mg^{2+} (19%) (Table 2-2). Among the metabolites, only proline contributed 3.8% during day 9–17 of the stress treatment, whereas the other metabolites remained below 1.5%. In roots, the contribution of metabolites to OA increased over time and reached 25% during day 9–17, but root ion contribution decreased with stress intensity from 25 to 17% (Table 2-2). Potassium was again the main ionic contributor in roots, but while proline was the main metabolite contributing to OA in shoots, sucrose played by far the dominant role in roots, explaining up to 23% of OA. All other metabolites (including proline) contributed less than 1% to OA throughout the treatment period. Overall, up to 98% (shoots) and 43% (roots) of the OA could be explained by the analysed ions and metabolites.

Table 2-1: Contribution of ions and metabolites to the osmotic potential of sugar beet leaves and taproots.
The shown values represent means of all days (1-17) of either control or drought stressed plants.

Shoot	**Ions/ Metabolite**	**Mean**	**SE**	**Roots**	**Ions/ Metabolite**	**Mean**	**SE**
Control	K^+	39.2	1.4	Control	K^*	12.9	0.8
	Na^+	14.4	0.6		Na^*	1.4	0.1
	Mg^{2+}	15.2	0.9		Mg^{2*}	1.1	0.0
	Ions total	*68.3*	*1.8*		*Ions total*	*15.4*	
	Proline	1.0	0.1		Proline	0.2	0.1
	Glutamate	2.4	0.3		Glutamate	0.4	0.0
	Malate	1.1	0.2		Malate	0.1	0.0
	Glucose	0.6	0.1		Glucose	0.1	0.0
	Fructose	0.6	0.1		Fructose	0.2	0.0
	Sucrose	0.3	0.0		Sucrose	22.4	2.1
	Metabolites total	*6.0*	*0.7*		*Metabolites total*	*23.3*	*2.11.0*
Stress	Na^+	17.6	1.1	Stress	Na^*	1.5	0.2
	K^+	43.7	1.7		K^+	3.7	2.0
	Mg^{2+}	15.6	1.7		Mg^{2*}	1.1	0.1
	Ions total	76.9	3.9		Ions total	16.1	1.9
	Proline	1.9	0.4		Proline	0.1	0.0
	Glutamate	1.6	0.1		Glutamate	0.4	0.1
	Malate	0.9	0.2		Malate	0.3	0.1
	Glucose	0.4	0.1		Glucose	0.2	0.1
	Fructose	0.5	0.1		Fructose	0.2	0.0
	Sucrose	0.4	0.0		Sucrose	19.2	3.8
	Metabolites total	*5.7*	*0.7*		*Metabolites total*	*20.4*	*4.1*

Table 2-2: Relative contribution of inorganic ions and metabolites to OA of shoots and taproots.
Since the first significant reduction in OP was detected on day 5 of the drought stress, contributions were calculated for days 3-9 (P II: early protective metabolic adaptation) and day 9-17 (P III: intensified metabolic responses and cell damage), but not for day 1-3 (P I: initial phase characterized by stomatal closure). For an explanation of the phases, see also discussion. Values are means of the respective days ± s.e.

Organ	**Shoot**		**Root**	
Phase	P II	P III	P II	P III
Days	3-9	9-17	3-9	9-17
Cation (%)				
K^+	42.1 ± 22.3	49.3 ± 5.4	20.1 ± 5.0	14.4 ± 2.7
Na^+	22.6 ± 10.1	22.8 ± 2.5	3.1 ± 1.4	1.7 ± 0.4
Mg^{2+}	9.3 ± 3.1	19.4 ± 3.9	1.9 ± 0.6	1.2 ± 0.2
Total	73.9	91.4	25.1	17.3
Metabolite (%)				
Proline	1.4 ± 0.9	3.8 ± 0.8	0.1 ± 0.01	<0.1
Glutamate	<0.1	1.0 ± 0.5	0.5 ± 0.1	0.4 ± 0.1
Malate	<0.1	1.1 ± 0.5	0.2 ± 0.04	0.8 ± 0.2
Sum Hexoses	0.2 ± 1.7	0.3 ± 0.2	0.4 ± 0.1	0.9 ± 0.2
Sucrose	0.6 ± 0.2	0.7 ± 0.1	4.4 ± 1.5	23.3 ± 7.1
Total	2.3	6.9	5.7	25.2
Others	23.8	1.6	69.2	57.5

2.5 DISCUSSION

2.5.1 Dynamic sequence of drought stress responses in young sugar beets

Three phases of drought response were distinguished on the basis of plant and soil water status (RWC, OP, ΔT, WC_{sub}), membrane damage (EL, Table 2-3) and metabolites (proline, glutamate, malate, sum of hexoses, sucrose, (Table 2-2). During an initial phase from day 1–3 (P I), only an increase in leaf temperature was detected as primary physiological adaptation reaction. Leaf temperature is a proxy for transpiration, and has been shown to allow estimation of stomatal conductance (Costa et al. 2013). The first signs of wilting became visible and parameters of plant water status and metabolites changed significantly, but with a slow rate, from day 3 to 9 (P II). During the third phase (days 9–17: P III), physiological changes intensified at a significantly higher rate and were accompanied by severe cell damage.

During P I and P II, no significant tissue damage was observed, although there was an initial water loss from the cells when water availability decreased as indicated by the onset of tissue shrinkage. P I and P II were clearly distinct because the cooling effect of leaf transpiration was reduced rapidly and predominantly during P I (day 1–3), whereas metabolic adjustment only started in P II (day 3–9). Drought induces a complex system of biochemical and molecular reactions enabling plants to initiate adaptive responses, before visual symptoms such as wilting occur, and before plant growth is inhibited (Tuteja 2009). Metabolic changes in abiotic stress response can be considered to be differentiated

into three levels (i) the immediate response to environmental alternations, (ii) the transient adaptation to stress conditions and (iii) the new equilibrium established under extended stress conditions (Obata and Fernie 2012).

Table 2-3: The dynamics of drought stress responses of young sugar beets.
The dynamics of drought stress responses of young sugar beets characterized by the parameters substrate water content (WC_{sub}, w/w, based on substrate FW), relative water content (RWC), osmotic potential (OP), electrolyte leakage (EL) and temperature difference (ΔT). Phase I (P I) is the initial stress phase characterized by stomatal closure; Phase II (P II) is the early protective metabolic adaptation; Phase III (P III) is the intensified metabolic responses and cell damage. Values are means of the respective days ± s.e. For each parameter, values followed by the same letter do not differ significantly (α=0.05)

Phase			**P I**	**P II**	**P III**
Days			1-3	3-9	9-17
	Parameter	**Unit**			
Substrate	WC_{sub}	%	58 ± 4b	42 ± 4b	30 ± 1a
Shoot	RWC	%	87 ± 1b	76 ± 4b	44 ± 4a
	OP	MPa	-0.8 ± 0.1b	-1.1 ± 0.1b	-2.3 ± 0.1a
	EL	%	11 ± 1a	21 ± 3a	61 ± 9b
	ΔT	K	2.3 ± 0.5a	0.8 ± 0.1ab	0.2 ± 0.1a
Root	OP	MPa	-1.3 ± 0.1b	-1.7 ± 0.1b	-3.2 ± 0.1a

In the present study, stomatal closure and cessation of transpiration were among the earliest reactions in young drought stressed sugar beets, preceded adaptive responses of metabolism and can be therefore referred to as a direct reaction to the environmental change. The rapid changes in ΔT are in line with the limited ability of sugar beets to regulate transpiration under high evaporative demand (Hanson and Hitz 1982). Rapid stomatal closure indicates a shift to a water-saving strategy of the plants, but it also reduces CO_2 assimilation, and might lead to severely reduced yield (Cruz de Carvalho 2008). This is especially detrimental in cases of moderate and intermittent drought spells early in the growing season, where rapid stomatal closure might represent an undesirable trait in targeted environments, especially if they are combined with a slow recovery of CO_2 assimilation upon rewatering.

During metabolic adjustment in P II, the drought stressed plants tried to establish a new steady-state to cope with the changed water availability as reflected by the enhanced levels of e.g. sucrose, malate and proline. The comparison with the rewatered plants indicates that these changes can be interpreted as adaptive processes, since the increased metabolic and physiological parameters decreased to control levels under rewatering. This phase would correspond to the transient adaptation to stress conditions described by Obata and Fernie (2012). The significant changes of leaf sucrose, malate or proline also point to alterations of carbon metabolism, probably directing the carbon flow into pathways relevant for protective responses (Watkinson *et al.* 2003). In drought-stressed grape-

vines, photosynthesis was maintained or repaired during the initial stress period (Cramer *et al*. 2013), which resulted in an increased availability of carbon for the production of protective and osmotically active metabolites such as proline, organic acids, or sugars, as soon as growth was inhibited (Hummel *et al.* 2010). This is consistent with the present results, where leaf proline and sucrose started to accumulate after 5–7 days, exactly when shoot growth was significantly reduced.

The most remarkable feature of P III (day 9–17) was the occurrence of significant membrane damage, indicated by increased EL_S, which coincided with a drop in RWC_S and OP_S, first cell collapse and distortion of chloroplasts in palisade and spongy parenchyma. Drought is known to ultimately lead to cellular damage by an overproduction of reactive oxygen species (ROS), caused by an over reduction of the photosynthetic electron transport chain and increased Mehler reactions in response to a limitation of CO_2 fixation, and increased photorespiration (Cruz de Carvalho 2008). Even though neither ROS nor malondialdehyde – a degradation product of lipid peroxidation (Heath and Packer 1968) – were determined in the present experiment, previous own experiments showed a significant correlation (R^2 = 0.697, sig. at $P < 0.05$) between EL and malondialdehyde concentration (data not shown), indicating that EL can be used as a proxy for cellular damage in sugar beet. The observed strong increase of cellular damage during P III fits well with a model proposed by Cruz de Carvalho (2008), and indicates that ROS production is initially counterbalanced by antioxidative responses (P II), followed by cellular damage once ROS production exceeds the detoxification capacity of the antioxidant system (P III).

There is increasing evidence that plants can sense the degree of stress and activate distinct response programs for mild and severe stresses (Watkinson et al. 2003). The common classification of drought stress into ‘low’, ‘moderate’ and ‘severe’ is frequently based on soil water capacity (Hoffmann 2010) or soil water potential (Hummel et al. 2010), but usually lacks information about the physiological status of the plant, and thus the stress level perceived by the individual plant. It therefore remains difficult to compare the stress response of plants from different experiments. Our results indicate that cellular damage seems to be the critical factor causing the transition from P II (representing ‘moderate stress’) to P III (representing ‘severe stress’) in sugar beets during taproot development. Since cellular damage can be easily assessed e.g. by EL, further studies should determine whether critical values of EL, or rather critical increases in EL could be used to objectively distinguish between moderate and severe stress in different plant species.

During the final 2 days of drought stress, an abrupt increase in shoot sucrose and proline concentrations may indicate another shift in metabolism, possibly related to the beginning of senescence triggered by ROS accumulation under severe drought stress (Munné-Bosch and Alegre 2004). Correlations between sugar accumulation and leaf senescence are common, and sugar signalling is likely

involved in the senescence response to drought stress (Wingler and Roitsch 2008). Despite the sucrose accumulation during this late stress phase in shoots, the contribution to OA was only minor (<1%, Table 2-1), which supports the idea that sucrose may function as a signalling molecule or membrane stabiliser rather than as an osmoprotectant in sugar beet shoots (Bogeat-Triboulot *et al.* 2007). A significant proline accumulation was consistently observed in sugar beets under water deficit (Gzik 1996; Monreal *et al.* 2007) and can be seen as another indicator of senescence resulting from protein degradation (Hajheidari *et al.* 2005), as well as a protective mechanism contributing to membrane stabilisation (Mansour 1998).

2.5.2 Osmotic adjustment in young sugar beet taproots

Sugar beet taproots seemed to intensify pathways related to protective compounds during P III, as indicated by the abrupt changes in OP and metabolites between days 9 and 11. Taproots are storage organs characterised by a high accumulation of sucrose up to 19% of the root FW at harvest (Trebbi and McGrath 2009). The present experiment was conducted when taproots had just started to become a sink for sucrose, indicated by the slow but constant sucrose increase in control roots. The high sucrose concentration enables sugar beets to establish a much lower OP in roots compared with shoots, which might partly be responsible for the ability to compensate temporary water deficits. Together with K^+, sucrose was one of the main contributors to OA in roots. However, root sucrose concentrations did not sufficiently increase under drought to completely account for the strong drought-induced decrease in OPR. Other compatible solutes also increased during P III, but their concentrations were low compared with shoots, and their capacity to contribute to OA was limited, as also indicated by the plateaus observed for proline and malate from days 11 to 15 when OPR still continued to decrease. Despite the fact that these metabolites did not significantly contribute to OA in taproots, their stress-induced increase still indicates other important roles, e.g. protective functions against reactive oxygen species and thus membrane damage. Since the contribution of cations to root OA also decreased over time, further studies are needed to identify other compounds contributing 58–69% of root OA during drought stress. Metabolites previously reported to increase in taproots under drought are glycine betaine and glutamine (Mäck and Hoffmann 2006), which were not determined in this study, but may play a major role in OA of sugar beet roots.

2.5.3 Dynamics of the recovery process after transient drought stress

Even though it is commonly observed that field-grown sugar beets have a high capacity to recover from temporary drought periods, very little is known about the underlying metabolic responses and to what extent such recovery is complete (Choluj *et al*. 2008). In the present study, rewatering was initiated when membrane leakage of the leaves started to intensify and cellular damage was confirmed by histological analysis. Wilting of young leaves and shrinkage of leaf tissues disappeared

within 1 day of rewatering, but water status and metabolic changes for osmoregulation required more time to return to control levels. Shoot and root growth resumed only after RWC and OP values of both organs had nearly reached control levels, indicating that a sufficient cell turgor has to be established before cell elongation resumes.

During the first 6 days of rewatering, leaf hexoses and sucrose concentrations increased beyond control levels, indicating that photosynthetic activity was immediately, at least partly, resumed. However, growth was still inhibited and therefore sink capacity of shoots and roots was low, probably resulting in the observed accumulation of soluble sugars in source tissues. Sugars returned to control levels approximately at the same time as growth resumed, which indicates that accumulated sugars served as energy and C source to facilitate the onset of growth after a transient drought period. Continuously decreasing shoot proline concentrations indicate proline turnover, and possibly the use of proline as an alternative energy source during this initial recovery phase (Leprince *et al.* 2015).

We noted that ΔT required at least 9 days of rewatering before it returned to control levels and adapted to the increasing water availability, even though cellular structures appeared fully functional and RWC_S returned to control levels after 7–8 days. This is in accordance with reports of persistently reduced photosynthetic CO_2 assimilation following transient water stress (Chaves *et al*. 2009). The physiological limitations for photosynthetic recovery after drought are not fully understood, but the slow recovery of cellular membranes as indicated by EL_S, supports the idea that photosynthetic electron transport in chloroplasts may have been impaired for a longer period of time due to membrane damage (Sofo *et al.* 2004). Sustained (partial) stomatal closure, which was observed for different species (Boyer 1976; Bogeat-Triboulot *et al*. 2007; Gallé *et al.* 2007) and lasted up to several weeks after rewatering (Galmés *et al.* 2007), might be an alternative explanation for the observed slow recovery of leaf transpiration. Actually, stomatal limitations were most important in delaying photosynthesis recovery of *Vitis vinifera* after rewatering, where stomatal closure recovered more slowly than mesophyll conductance to CO2 (Flexas *et al*. 2012). It was hypothesised that sustained stomatal limitation might be a physiological adjustment to prevent further water loss in anticipation of future stress events (Gallé *et al.* 2007). Reduced CO_2 fixation and additional growth restriction due to sustained stomatal closure could be alleviated by induction of malic enzyme activities (Guo *et al*. 2009), providing an increased internal leaf CO_2 concentration (Doubnerová and Ryšlavá 2011). In the present study, the rapid reduction of malate concentrations in roots upon rewatering and the transient malate peak in shoots might be interpreted as malate export from roots to leaves, where it could serve as an additional source of CO_2.

The lag phase for the recovery of OPR, proline, and malate concentrations in roots indicates that the reversal of adaptive metabolic responses in roots occurs more slowly than in shoots. This makes

physiological sense, because under field conditions, the root environment is less exposed to rapidly changing environmental conditions, e.g. drought usually develops more slowly in the soil compared with the air. A slow reversal of metabolic responses would keep the root 'prepared' for a subsequent drought spell, which might be an energy saving mechanism under unfavourable conditions like repeated drought spells.

The sugar yield depends on the replacement of non-sucrose compounds by sucrose during taproot growth under balanced water and nutrient supply, and it was suggested that sucrose storage was likely constrained by elevated levels of osmolytes (Hoffmann 2010) or cations like K^+, Na^+ and Mg^{2+} (Saftner and Wyse 1980). This is consistent with the present results, where peaks of compatible solutes and increased concentrations of cations during P III, coincided with a continuous decrease in root sucrose concentration. Apart from reducing sucrose yield, high levels of osmolytes and ions additionally impair the technical quality of the root by diminishing sugar crystallization (Van der Poel *et al*. 1998). In a field study, 2 months of recovery were not sufficient after a 35 days drought stress to prevent accumulation of Na^+ and α-amino-N compounds (Chołuj *et al.* 2008). In the present study, however, osmolyte and cation concentrations of taproots returned to control levels within 8 days after rewatering, indicating that transient drought stresses during early sugar beet development are unlikely to result in negative effects on technical quality, unless the drought extends into the final stage of beet development.

Overall, the presented results indicate that the analysed cultivar Pauletta almost completely recovered during a rewatering period of 11 days after a transient drought spell of 9 days, which caused alterations in water relations as well as significant membrane damage. However, different parameters required different timespans for a full recovery to control levels, which might be relevant if plants face repeated drought spells with only short recovery times. This study also indicates that a single transient drought spell during the youth stage of sugar beet might affect the further plant development not just by a temporary inhibition of root and shoot growth during the stress, but also by reduced CO_2 assimilation lasting beyond the stress situation. Whether this may also affect final yield, or can be compensated during the remaining growth period, likely depends on the subsequent water availability. Further work is under way to establish whether (i) the dynamics of recovery are different if rewatering is started before severe cellular damage occurs (i.e. during P II), and (ii) genotypic differences in speed and completeness of recovery can be used as traits for breeding sugar beets with a high potential to compensate drought spells during early development.

2.5.4 Benefit of combining IRT and destructive analyses

The reliable detection of early stages of stress development is highly important in breeding programs, where a large number of cultivars need to be characterized under high-throughput condi-

tions. IRT allows non-invasive high-throughput monitoring of plants under limited water supply (Maes and Steppe 2012; Costa *et al.* 2013), implementable for field (Prashar and Jones 2014) and greenhouse conditions (Grant *et al*. 2006). Its suitability to detect very early drought responses was, however, not yet demonstrated. Similarly, invasive measurements have not been used successfully in combination with non-destructive approaches to detect initial stress responses, and even though they can be adapted to high-throughput conditions using robot based platforms (Gibon *et al.* 2004), they are still time consuming and do not allow continuous measurements. The present study has shown that IRT does indeed enable monitoring of the initial reduction in transpiration upon onset of drought stress, which is before significant changes can be detected using destructive measurements. Therefore, IRT might be a promising tool for rapid screening of initial stress responses of large numbers of genotypes and could accelerate large scale high-throughput phenotyping under controlled environments (Munns *et al.* 2010). However, IRT alone is not able to distinguish later stress phases, and thus fails to select genotypes differing in their response to more severe drought stresses. Care should be taken when transferring results from greenhouse studies to field conditions, since plant temperature in the field is influenced by various external factors such as plant architecture, soil temperature, and weather conditions (Prashar and Jones 2014). However, the use of IRT technology in the field is continuously improved (Zarco-Tejada *et al.* 2012; Lima *et al.* 2016), and may become a valuable tool for pre-symptomatic detection of drought stress and optimised irrigation management, e.g. in highly productive irrigated agricultural systems.

Non-destructive methods can assess genotypic differences of whole plant responses, e.g. early closure of stomata upon stress onset, or time required for recovery, but they provide limited information on the underlying metabolic processes or genetically tractable traits (Berger *et al.* 2010). Whether a slow recovery of transpiration is a genotypic trait, providing a sort of 'predictive protection' against future drought spells, or whether it is just a response to the extent of cellular damage of the photosystem, cannot be assessed by non-invasive measurements alone. By combining non-invasive and destructive measurements, the present study seems to indicate that slow recovery of transpiration is correlated with cellular damage (EL_S). This might open an opportunity to use non-invasive measurements of recovery by IRT to select promising genotypes, which are less affected by cellular damage during a preceding drought stress. Future experiments should be used to determine whether the recovery time of transpiration depends on the stress intensity for a larger set of genotypes, and whether sufficient variability exists between cultivars to be used in breeding programs and/or phenotyping facilities.

2.6 CONCLUSION

IRT was suitable to detect the initial drought-induced reduction in transpiration before significant changes were identified by invasive (metabolic or physiological) analyses. However, IRT alone was not able to distinguish more severe stress phases. During ongoing drought stress in young sugar beets, initial stomatal closure was followed by a phase of protective metabolic adaptation, and finally intensified metabolic responses coinciding with increasing cellular damage. Although most metabolic parameters returned to control levels within 10 days of rewatering, leaf transpiration and membrane damage recovered only slowly. This might have long-lasting effects on CO_2 assimilation during the remaining growth period and thus final yield, and/or keep plants prepared to cope better with subsequent drought events. For breeding purposes, speed and completeness of recovery could become a useful trait. Combining non-invasive (IRT) phenotyping methods with the analysis of selected metabolites can speed up the selection of better drought-adapted cultivars.

ACKNOWLEDGEMENTS

We are grateful to Yves Gibon and Duyên Prodhomme (INRA, Bordeaux) for the introduction to high throughput metabolite analysis and the fruitful discussions. To Yves Gibon for critical reading of the manuscript, to Britta Schulz (KWS Saat AG, Einbeck, Germany) for providing sugar beet seeds, to Manfred Trimborn (INRES, Plant Nutrition, University of Bonn) for his contribution regarding the irrigation management, and to Daniela Keller (Statistik and Beratung, Kuernach, Germany) for rewarding discussion about the statistical analysis. This study was financially supported by the German Federal Ministry of Education and Research (BMBF 0315529) and the European Union for regional development (EFRE z1011bc001a) and is part of CROPSENSe.net, the competence network for phenotyping research.

2.7 REFERENCES

Berger B, Parent B, Tester M (2010) High-throughput shoot imaging to study drought responses. *Journal of Experimental Botany* 61*, 3519-3528.* doi:10.1093/jxb/erq201

Bloch D (2006) Solute accumulation as a cause for quality losses in sugar beet submitted to continuous and temporary drought stress. *Journal of Agronomy and Crop Science* 24, 17-24. doi:10.1111/j.1439-037X.2006.00185.x

Bogeat-Triboulot M-B, Brosché M, Renaut J, Jouve J, Le Thiec D, Fayyaz P, Vinocur B, Witters E, Laukens K, Teichmann T, Altman A, Hausman JF, Polle A, Kangasjärvi J, Dreyer E (2007) Gradual soil water depletion results in reversible changes of gene expression, protein profiles, ecophysiology, and growth performance in *Populus euphratica*, a poplar growing in arid regions. *Plant Physiology* 143, 876-892. doi:10.1104/pp.106.088708

Boyer JS (1976) Photosynthesis at low water potentials. *Philosophical transactions of the Royal Society of London. Series B, Biological sciences* 273, 501-512. doi:10.1098/rstb.1976.0027

Chaves MM, Flexas J, Pinheiro C (2009) Photosynthesis under drought and salt stress: regulation mechanisms from whole plant to cell. *Annals of Botany* 103, 551-60. doi:10.1093/aob/mcn125

Choluj D, Karwowska R, Ciszewska A, Jasińska M (2008) Influence of long-term drought stress on osmolyte accumulation in sugar beet (*Beta vulgaris* L.) plants. *Acta Physiologiae Plantarum* 30, 679-687. doi:10.1007/s11738-008-0166-2

Costa JM, Grant OM, Chaves MM (2013) Thermography to explore plant-environment interactions. *Journal of Experimental Botany* 64, 3937-3949. doi:10.1093/jxb/ert029

Cramer GR, Van Sluyter SC, Hopper DW, Pascovici D, Keighley T, Haynes PA (2013) Proteomic analysis indicates massive changes in metabolism prior to the inhibition of growth and photosynthesis of grapevine (*Vitis vinifera* L.) in response to water deficit. *BMC Plant Biology* 13, 49-71. doi:10.1186/1471-2229-13-49

Cruz de Carvalho MH (2008) Drought stress and reactive species: production, scavenging and signaling. *Plant Signaling and Behavior* 3, 156-165. doi:10.4161/psb.3.3.5536

Dohm JC, Lange C, Reinhardt R, Himmelbauer H (2009) Haplotype divergence in *Beta vulgaris* and microsynteny with sequenced plant genomes. *Plant Journal* 57, 14–26. doi:10.1111/j.1365-313X.2008.03665.x

Doubernová V, Ryslavá H (2011) What can enzymes of C_4 photosynthesis do for C_3 plants under stress? *Plant Science* 180, 575-583. doi:10.1016/j.plantsci.2010.12.005

Enz M, Dachler C (1997) 'Compendium of growth stage identification keys for mono- and dicotyledonous plants - Extended BBCH scale'(2nd edn) (Allcomm Business Communication: Bezug, Germany)

Fiorani F, Rascher U, Jahnke S, Schurr U (2012) Imaging plants dynamics in heterogenic environments. *Current Opinion in Biotechnology* 23, 227-35. doi:10.1016/j.copbio.2011.12.010

Flexas J, Gallé A, Galmés J, Ribas-Carbo M, Medrano H (2012) "The response of photosynthesis to soil water status", in *Plant Responses to Drought Stress*, (Ed. R Aroca) pp. 129-144. (Springer: Berlin)

Gago J, Douthe C, Coopmann RE, Gallego PP, Ribas-Carbo M, Flexas J, *et. al.* (2015) UAVs challenge to assess water stress for sustainable agriculture. *Agricultural Water Management* 153, 9-19. doi:10.1016/j.agwat.2015.01.020

Gallé A, Haldimann P, Feller U (2007) Photosynthetic performance and water relations in young pubescent oak (*Quercus pubescens*) trees during drought stress and recovery. *New Phytologist* 174, 799-810. doi:10.1111/j.1469-8137.2007.02047.x

Galmés J, Medrano H, Flexas J (2007) Photosynthetic limitations in response to water stress and recovery in Mediterranean plants with different growth forms. *New Phytologist* 175, 81-93. doi:10.1111/j.1469-8137.2007.02087.x

Gibon Y, Sulpice R, Larher F (2000) Proline accumulation in canola leaf discs subjected to osmotic stress is related to the loss of chlorophylls and to the decrease of mitochondrial activity. *Physiologia Plantarum* 110, 469-476. doi:10.1111/j.1399-3054.2000.1100407.x

Gibon Y, Blaesing OE, Hannemann J, Carillo P, Höhne M, Hendriks JHM, Palacios N, Cross J, Selbig J, Stitt M (2004) A robot-based platform to measure multiple enzyme activities in *Arabidopsis* using a set of cycling assays: Comparison of changes of enzyme activities and transcript levels during diurnal cycles and in prolonged darkness. *Plant Cell* 16, 3304-3325. doi:10.1105/tpc.104.025973

Grant OM, Chaves MM, Jones HG (2006) Optimizing thermal imaging as a technique for detecting stomatal closure induced by drought stress under greenhouse conditions. *Physiologia Plantarum* 127, 507-518. doi:10.1111/j.1399-3054.2006.00686.x

Großkinsky DK, Svensgaard J, Christensen S, Roitsch T (2015) Plant phenomics and the need for physiological phenotyping across scales to narrow the genotype-to-phenotype knowledge gap. *Journal of Experimental Botany* 66*,* 5429-5440. doi:10.1093/jxb/erv345

Guo PG, Baum, M, Grando, S, Ceccarelli S, Bai GH, Li RH, von Korff M, Varshney RK, Graner A, Valkoun J (2009) Differentially expressed genes between drought-tolerant and drought-sensitive barley genotypes in response to drought stress during the reproductive stage. *Journal of Experimental Botany* 60, 3531-3544. doi:10.1093/jxb/erp194

Gzik, A (1996) Accumulation of proline and pattern of α-amino acids in sugar beet plants in response to osmotic, water and salt stress. *Environmental and Experimental Botany* 36, 29-38. doi:10.1016/0098-8472(95)00046-1

Hajheidari M, Abdollahian-Noghabi M, Askari H, Heidari M, Sadeghian, SY, Ober ES, Salekdeh GH (2005) Proteome analysis of sugar beet leaves under drought stress. *Proteomics* 5, 950-60. doi:10.1002/pmic.200401101

Hanson AD, Hitz WD (1982) Metabolic response of mesophytes to plant water deficits. *Annual Review of Plant Biology* 33, 163-203. doi:10.1146/annurev.pp.33.060182.001115

Heath RL, Packer L (1968) Photoperoxidation in isolated chloroplasts. I. Kinetics and stoichiometry of fatty acid peroxidation. *Archives of Biochemistry and Biophysics* 125, 189-198. doi:10.1016/0003-9861(68)90654-1

Hoffmann CM (2010) Sucrose accumulation in sugar beet under drought stress. *Journal of Agronomy and Crop Science* 196, 243-252.

Hoffmann CM (2014) Adaptive responses of *Beta vulgaris* L. and *Cichorium intybus* L. root and leaf forms to drought stress. *Journal of Agronomy and Crop Science* 200, 108-118. doi:10.1111/jac.12051

Hummel I, Pantin F, Sulpice R, Piques M, Rolland G, Dauzat M, *et al*. (2010) *Arabidopsis thaliana* plants acclimate to water deficit at low cost through changes of C usage; an integrated perspective using growth, metabolite, enzyme and gene expression analysis. *Plant Physiology* 154, 357-372. doi:10.1104/pp.110.157008

IPCC (2007) "Summary for Policymakers", in *Climate Change 2007: Impacts, Adaptation and Vulnerability. Contribution of Working Group II to the Fourth Assessment Report of the Intergovernmental Panel on Climate Change*, eds. ML Parry, OF Canziani, JP Palutikof, PJ van der Linden and CE Hanson, Cambridge, UK, Cambridge University Press, 7-22.

Jones HG, Serraj R, Loveys B (2009) Thermal infrared imaging of crop canopies for the remote diagnosis and quantification of plant responses to water stress in the field. *Functional Plant Biology* 36, 978-989. doi:10.1071/FP09123

Karnovsky MJA (1965) A formaldehyde-glutaraldehyde fixative of high osmolality for use in electron microscopy. *The Journal of Cell Biology* 27, 8A.

Leprince A, Magalhaes N, De Vos D, Bordenave M, Crilat E, Clément G, Meyer C, Munnik T, Savouré A (2015) Involvement of phosphatidylinositol 3-kinase in the regulation of proline catabolism in *Arabidopsis thaliana*. *Frontiers in Plant Science* 5, 1-13. doi:10.3389/fpls.2014.00772

Lima RSN, Garcia-Tejero I, Lopes TS, Costa JM, Vaz M, Duran-Zuazo VH, *Chaves M, Glenn DM, Campostrini E* (2016) Linking thermal imaging to physiological indicators in *Carica papaya* L. under different watering regimes. *Agricultural Water Management* 164, 148-157. doi:10.1016/j.agwat.2015.07.017

Mäck G, Hoffmann, CM (2006) Organ-specific adaptation to low precipitation in solute concentration of sugar beet (*Beta vulgaris* L.). *European Journal of Agronomy* 25, 270-279. doi:10.1016/j.eja.2006.06.004

Maes WH, Steppe K (2012) Estimating evapotranspiration and drought stress with ground-based thermal remote sensing in agriculture: a review. *Journal of Experimental Botany* 63, 4671-4712. doi:10.1093/jxb/ers165

Mahlein, A-K, Oerke, E-C, Steiner, U, Dehne H-W (2012*a*) Recent advances in sensing plant diseases for precision crop protection. *European Journal of Plant Pathology* 133, 197-209. doi:10.1007/s10658-011-9878-z

Mahlein A-K, Steiner U., Hillnhütter C, Dehne H-W, Oerke, E-C (2012*b*) Hyperspectral imaging for small-scale analysis of symptoms caused by different sugar beet diseases. *Plant Methods* 8, 3-16. doi:10.1186/1746-4811-8-3

Mansour MMF (1998) Protection of plasma membrane of onion epidermal cells by glycinebetaine and proline against NaCl stress. *Plant Physiology and Biochemistry* 36, 767-772. doi:10.1016/S0981-9428(98)80028-4

Monreal JA, Jiménez ET, Remesal E, Morillo-Velarde R, García-Mauriño S, Echevarría C (2007) Proline content of sugar beet storage roots: Response to water deficit and nitrogen fertilization at field conditions. *Environmental and Experimental Botany* 60, 257-267. doi:10.1016/j.envexpbot.2006.11.002

Munné-Bosch S, Alegre L (2004) Die and let live: leaf senescence contributes to plant survival under drought stress. *Functional Plant Biol*ogy 3, 203-216. doi:10.1071/FP03236

Munns R, James RA, Sirault XRR, Furbank RT, Jones HG (2010) New phenotyping methods for screening wheat and barley for beneficial responses to water deficit. *Journal of Experimental Botany* 61, 3499-3507. doi:10.1093/jxb/erq199

Obata T, Fernie A (2012) The use of metabolomics to dissect plant responses to abiotic stresses. *Cellular and Molecular Life Sciences* 59, 3225-3243. doi:10.1007/s00018-012-1091-5

Ober ES, Luterbacher MC (2002) Genotypic variation for drought tolerance in *Beta vulgaris*. *Annals of Botany* 89, 917-924. doi:10.1093/aob/mcf093

Ober ES, Bloa M, Le Clark, CJA, Royal A, Jaggard KW, Pidgeon JD (2005) Evaluation of physiological traits as indirect selection criteria for drought tolerance in sugar beet. *Field Crops Research* 91, 231-249. doi:10.1016/j.fcr.2004.07.012

Oerke EC, Steiner U, Dehne HW, Lindenthal M (2006) Thermal imaging of cucumber leaves affected by downy mildew and environmental conditions. *Journal of Experimental Botany* 57, 2121-2132. doi:10.1093/jxb/erj170

Pariyar S, Eichert T, Goldbach HE, Hunsche M, Burkhardt J (2013) The exclusion of ambient aerosols changes the water relations of sunflower (*Helianthus annuus*) and bean (*Vicia vaba*) plants. *Environmental and Experimental Botany* 88, 43-52. doi:10.1016/j.envexpbot.2011.12.031

Pestsova E, Meinhard J, Menze A, Fischer U, Windhövel A, Westhoff P (2008) Transcript profiles uncover temporal and stress-induced changes of metabolic pathways in germinating sugar beet seeds. *BMC Plant Biology* 8, 1-21. doi:10.1186/1471-2229-8-122

Prashar A, Jones H (2014) Infrared thermography as a high-throughput tool for field phenotyping. *Agronomy* 4, 397-417. doi:10.3390/agronomy4030397

Saftner RA, Wyse RE (1980) Alkali cation/sucrose co-transport in the root sink of sugar beet. *Plant Physiol*ogy 6, 884-889. doi:10.1104/pp.66.5.884

Shaw B, Thomas TH, Cooke DT (2002) Response of sugar beet (*Beta vulgaris* L.) to drought and nutrient deficiency stress. *Plant Growth Regu*lation 37, 77–83. doi:10.1023/A:1020381513976

Sicher RC, TimLin D, Bailey B (2012) Responses of growth and primary metabolism of water-stressed barley roots to rehydration. *Journal of Plant Physiology* 169, 686-695. doi:10.1016/j.jplph.2012. 01.002

Sofo A, Dichio B, Xiloyannis C, Masia A (2004) Effects of different irradiance levels on some antioxidant enzymes and on malondialdehyde content during rewatering in olive tree. *Plant Science* 166, 293-302. doi:10.1016/j.plantsci.2003.09.018

Stitt M, Lilley R, Gerhardt R, Heldt HW (1989) Metabolite levels in specific cells and subcellular compartments of plant leaves. *Methods in Enzymology* 174, 518-552. doi:10.1016/0076-6879(89)74035-0

Trebbi D, McGrath JM (2009) Functional differentiation of the sugar beet root system as indicator for developmental phase change. *Physiologia Plantarum* 135, 84-97. doi:10.1111/j.1399-3054.2008.01169.x

Tuteja N (2009) Cold, salinity, and drought stress. In 'Plant stress biology: from genomics to systems biology'. (Ed. H Hirt) pp. 137-159. (Wiley: Weinheim, Germany)

Van der Poel PW, Schwieck H, Schwartz T (1998) 'Sugar technology - beet and cane sugar manufacture'. (Bartens: Berlin)

Watkinson JI, Sioson AA, Vasquez-Robinet C, Shukla M., Kumar D, Ellis M, Heath LS, Ramakrishnan N, Chevone B, Watson LT, van Zyl L, Egertsdotter U, Sederoff RR, Grene R (2003) Photosynthetic acclimation is reflected in specific patterns of gene expression in drought-stressed loblolly pine. *Plant Physiol*ogy 133, 1702-1716. doi:10.1104/pp.103.026914

Wingler A, Roitsch T (2008) Metabolic regulation of leaf senescence: interactions of sugar signaling with biotic and abiotic stress responses. *Plant Biology* 10, 50-62. doi:10.1111/j.1438-8677.2008.00086.x

Wirtschaftliche Vereinigung Zucker (2016) Available at http://www.zuckerverbaende.de/zuckermarkt/zahlen-und-fakten/eu-zuckermarkt/ zuckererzeugung.html (Accessed 2016–10–11)

Wu G, Wang C, Su Y (2014) Assessment of drought tolerance in seedlings of sugar beet (*Beta vulgaris* L.) cultivars using inorganic and organic solutes accumulation criteria. *Journal of Soil Science and Plant Nutrition* 60, 565-57. doi:10.1080/00380768.2014.921579

Zarco-Tejada PJ, Gonzales-Dugo V, Berni JA (2012) Fluorescence, temperature and narrow-band indices acquired from a UAV platform for water stress detection using a micro-hyperspectral imager and a thermal camera. Remote Sensing of Environment 117, 322-337. doi:10.1016/j.rse.2011.10.007

3 METABOLOMIC PROFILING UNDER TEMPORARY DROUGHT

^{1}H-NMR metabolomic profiling reveals a distinct metabolic recovery response in shoots and roots of temporarily drought stressed sugar beets

Rita Wedeking[1,#a], Mickaël Maucourt[2,3], Catherine Deborde[2,3], Annick Moing[2,3], Yves Gibon[2], Heiner E. Goldbach[1], Monika A. Wimmer[1,#b,*]

[1]Department of Plant Nutrition, INRES, University of Bonn, Bonn, Germany
[2]UMR1332 Biologie du Fruit et Pathologie, INRA, Univ. Bordeaux, Centre INRA de Nouvelle Aquitaine – Bordeaux, Villenave d'Ornon, France
[3]Plateforme Métabolome du Centre de Génomique Fonctionnelle Bordeaux, MetaboHUB, PHENOME, Centre INRA de Nouvelle Aquitaine - Bordeaux, Villenave d'Ornon, France
[#a]Current address: Environmental Safety – Metabolism, Research & Development Crop Science, Bayer AG, Monheim am Rhein, Germany
[#b]Current address: Institute of Crop Science, Quality of Plant Products 340e, University of Hohenheim, Stuttgart, Germany

*Corresponding author
E-Mail: m.wimmer@uni-hohenheim.de

This chapter served as base for the eponymous publication submitted in January 2018. The final publication is available at https://doi.org/10.1371/journal.pone.0196102

3.1 ABSTRACT

Yield formation in regions with intermittent drought periods depends on the plant's ability to recover after cessation of the stress. The present work assessed differences in metabolic recovery of shoots and roots of drought-stressed sugar beets with high temporal resolution. Plants were subjected to drought for 13 days, and rewatered for 12 days. At one to two-day intervals, material was harvested for untargeted ^{1}H-NMR metabolomic profiling, targeted analyses of hexose-phosphates, starch, amino acids, nitrate and proteins, and physiological measurements including relative water content, osmotic potential, electrolyte leakage and malondialdehyde concentrations. Drought triggered changes in primary metabolism, especially increases in amino acids in both organs, but shoots and roots responded with different dynamics to rewatering. After a transient normalization of most metabolites within 8 days, a second accumulation of amino acids in shoots might indicate a stress imprint beneficial in upcoming drought events. Repair mechanisms seemed important during initial recovery, and occurred at the expense of growth for at least 12 days. These results indicate that organ specific metabolic recovery responses might be related to distinct functions and concomitant disparate stress levels in above- and belowground organs. With respect to metabolism, recovery was not simply a reversal of the stress responses.

3.2 INTRODUCTION

Yield stability under changing and variable water conditions is of strategic importance in securing food for a still growing world population (Cattivelli *et al.* 2008). Although the yearly amount of precipitation in Europe changed only marginally during the last 100 years, meteorologists observe a larger shift between the seasons, i.e. longer drought periods occur during spring and summer (EEA 2015). Hence, crops are under increasing strain to cope with changing environmental conditions still maintaining high productivities. In sugar beet production, climate change scenarios for the period 2021-2050 predict drought-related yield decreases of about 1 t sugar ha-1 in northern France, Belgium and west/central Poland (Jones *et al.* 2003). While the impact of progressive drought on the physiological and metabolic processes of plants is frequently described, studies of metabolic plant responses to rehydration are limited (e.g. Meyer *et al.* 2014; Morari *et al.* 2015; Lyon *et al.* 2016). Rapid recovery after drought spells is a desirable trait for crops, particularly since plants are usually exposed to repeated drought events throughout their life cycle, which may even progress in severity.

Recovery defines the time period after cessation of a stress until a new physiological and metabolic equilibrium is established, and is a crucial step in metabolism. In response to a stress, physiological

adaptations and modifications of the metabolism lead to the accumulation of metabolites, including protective compounds that may confer tolerance or resistance to drought stress (Bhargava and Sawant 2013). Once the stress is terminated, recovery processes set in, and the plant must strike a balance between the investment of resources into damage repair, maintained acclimation (priming for upcoming stress events), or into new growth/reproduction (resetting) (Crisp *et al.* 2016). While resetting maximizes growth and yield under favorable conditions, it carries the risk of major and possibly fatal damage if the stress recurs. Maintained acclimation, on the other hand, makes the plant "alert" for future stress events (stress imprint), but comes at the cost of reduced growth or development and reduced yield (Crisp *et al.* 2016). The latter authors argue that such a "stress imprint" is a rather rare event and that return to the initial (pre-stress) metabolic and physiological state is more common, but metabolic studies confirming this hypothesis are still scarce. It seems likely that intermediate forms of recovery (to some extent, but not to the pre-stress level) might be more common, since they would represent the most promising response strategy at least in regions where recurring stresses are usually erratic and not predictable. Indeed, in a recent study it was shown that drought stress and subsequent recovery in Medicago had distinct dynamics and were independently regulated (Lyon *et al.* 2016).

Under recovery the metabolic energy flows into preparation and adjustment for the reactivation of photosynthesis and respiration (Chaves *et al.* 2009), highly-synchronized and sensitive processes that are delicate to manage. For sugar beet, available studies of recovery processes after a drought spell are mainly restricted to describe changes of the biochemical composition and sucrose accumulation of the root (Bloch *et al.* 2006a; Hoffmann 2010), or handle the effect of transient and continuous drought on yield, photosynthesis and carbon discrimination (Monti *et al.* 2006). To maintain a high yield, it is of particular importance that shoots and roots recover quickly after drought to assure water and nutrient uptake and to continue sugar accumulation. A better understanding of the similarities and specificities of shoots and roots in metabolic adjustment and recovery after a transient drought is required, and is a major objective of the present study.

The current work aimed at the identification and characterization of major metabolites of the primary metabolism to uncover the metabolomic strategy of the transiently stressed sugar beets. The integrated use of metabolomic tools such as proton nuclear magnetic resonance spectroscopy (^{1}H NMR) and systems biology are powerful tools to gain a comprehensive overview of the involved pathways and the identification of crucial compounds of the metabolic response (Obata and Fernie 2012). Since plant metabolites are extremely diverse in their biological function as well as in their chemical structure, ^{1}H-NMR analysis is an excellent tool to study not only the composition of compounds of the plant metabolism, but also dynamic aspects as recently reviewed by Deborde *et al.* (2017).

3.3 MATERIALS AND METHODS

3.3.1 Plant growth conditions

Seeds of *Beta vulgaris* L. cultivar Pauletta (KWS Saat AG, Einbeck, Germany) were cultivated in a complete randomized block with four biological replicates for each harvest day and treatment as described in Wedeking *et al.* (2016). During the experiment plants were grown under controlled conditions at 24°C day/18°C night temperature, 75 ± 10% relative humidity and a photoperiod of 16 h light (> 250 µmol m^2 s^{-1}: SON-T Agro, 400W, Philips, Germany). Three times a day water and nutrients (1.4‰ Hakaphos blue, Compo Expert, Münster, Germany) were supplied for 3 minutes each using a time controlled, automated irrigation system, which resulted in a water content of 65-69% (w/w based on substrate fresh weight (FW)) during pretreatment growth, corresponding to substrate pH values between 1.8 and 2.3.

3.3.2 Treatments and sampling

Treatments were initiated at BBCH 14-15 (Enz and Dachler 1997). Plants were then either watered as before (control) for 25 days or subjected to intermitted drought, that means 13 days of progressive desiccation with subsequent rewatering for 12 days (recovery period). For control plants, a substrate suction of pF=2.3 was maintained, which corresponds to a substrate water content (WC_{sub}) of 65 ± 1% (w/w; based on substrate FW) and can be was considered as an optimum water supply (Wedeking *et al.* 2016). Under desiccation, WC_{sub} decreased slowly to 52 ± 4% (w/w) within 7 days, and then quickly further to 27 ± 1% (w/w; day 9). Finally, WC_{sub} reached 4 ± 1% (w/w) at day 13. Under rewatering, WC_{sub} resumed to 54 ± 1% (w/w) after 9 days. To confirm that neither water logging nor water deficit during the experimental period occurred, a subset of 15 pots was weighed every second day. Plants were kept free of pests and diseases by integrated plant protection. To avoid uncontrolled side effects triggered by circadian rhythm and metabolite concentrations plants were sampled 2 h after beginning of the photoperiod.

During the desiccation period, plant sampling was every second day. Under recovery, plants were harvested daily for the first 4 days (days 13-16) and every second or third day until the end of the experimental period. The youngest fully expanded leaf pair (YEL) and the root part 1.5 cm below the crown were sampled for leaf and taproot analysis, respectively. The first YEL was used for the metabolite analysis and the determination of malondialdehyde (MDA). The second leaf was halved. One half was used for the analysis of osmotic potential (OP) and from the other half, six leaf discs (diameter 9 mm) were punched out avoiding leaf veins, and used for the determination of relative water content (RWC) and electrolyte leakage (EL) (Figure 3-1). For the analysis, plant material was directly processed (RWC, EL), stored at -20°C (OP) or Plant material for the MDA determination and the

metabolite analysis was immediately frozen and ground under liquid nitrogen (leaf) or lyophilized (root), and stored at -80°C until further analysis. For ^{1}H-NMR analysis leaf material was also lyophilized and stored at -80°C until further analysis. Material for OP was frozen at -20°C or directly processed (RWC, EL).

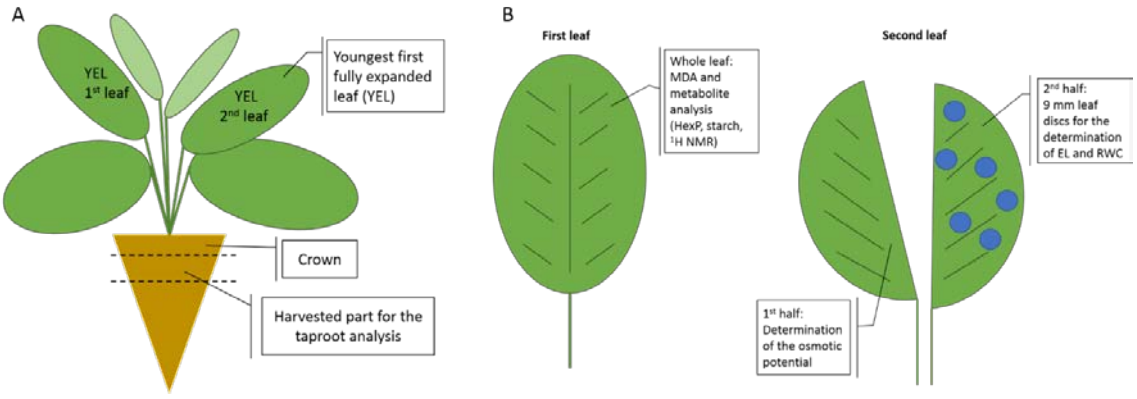

Figure 3-1: Harvest scheme of the young sugar beet plant and how the leaves were processed.
(A) Overview of the entire plant. The first leaf pair of the youngest fully expended leaves were sampled for physiological and metabolomic analysis as shown in (B).

3.3.3 Biomass, relative water content, electrolyte leakage and osmotic potential

Fresh weights (FW) of shoots and taproots were recorded directly after harvest and dry weights (DW) after drying at 70°C until constant weight was reached. The determination of EL, RWC and OP was determined previously described in Wedeking *et al.* (2016).

3.3.4 Malondialdehyde

The analysis of Malondialdehyde (MDA) in leaves was determined according based on the thiobarbituric acid assay of Hodges *et al.* (1999), with modifications. All solutions were prepared fresh before use and samples were determined in duplicate. For the extraction, 20 mg of frozen ground plant material were homogenized with 500 µL 0.1% trichloroacetic acid (TCA). After centrifugation (3,500 g, 15 min, RT) 150 µL of the supernatant was mixed either with 150 µL of reagent 1 (Reagent 1 (R1): 0.01% 2,6-di-tert-butyl-4-methylphenol in 20% (w/v) TCA), or reagent 2 (Reagent 2 (R2): R1 plus 0.65% 2-thiobarbituric acid). All samples were heated (at 95°C; for 30 min), cooled, and briefly centrifuged (<1 min, 3,500 g, RT) and immediately measured at 440, 532 and 600 nm using a microplate reader (Power Wave XS2, BioTek, USA). Malonaldehyde equivalents in nmol mL^{-1} were calculated according as follows

$$A = [(\text{Abs } 532_{R2} - \text{Abs } 600_{R2}) - (\text{Abs } 532_{R1} - \text{Abs } 600_{R1})]$$
$$B = [(\text{Abs } 440_{R2} - \text{Abs } 600_{R2}) \times 0.0571]$$
$$\text{MDA } [\text{nmol mL}^{-1}] = \frac{[(A-B)]}{41448} \times 10^{6}$$

where 0.0571 corresponds to the ratio of the molar absorbance of 1^{-10} mM sucrose at 532 nm and 440 nm (Hodges *et al.* 1999) and, 41448 refers to the molar extinction coefficient (ε) of MDA calculated for $d_{100\mu L} = 0.264$.

3.3.5 Proton NMR metabolomic profiling

Polar metabolites were extracted from beet root and leaf samples. Briefly, polar metabolites were extracted from 20 mg of ground lyophilised powder with an ethanol-water series at 80°C (adapted from Moing *et al*. 2004) using a pipetting robot (Hamilton, Bonaduz, Switzerland) with two technological replicates per sample. The supernatants were combined, dried under vacuum and lyophilised. Each lyophilised extract was solubilized in 500 µL of 100 mM deuterated potassium phosphate buffer solution pH 6.0, containing 3 mM ethylene diamine tetraacetic acid disodium salt (EDTA), adjusted with KOD solution to pH 6 when necessary, and lyophilised again. The lyophilised titrated extracts were stored in darkness under vacuum at room temperature, before ^{1}H-NMR analysis was completed within one week.

For ^{1}H-NMR analysis, 500 µL of D_2O with sodium trimethylsilyl [2,2,3,3-d4] propionate (TSP, 0.01% mg/mL final concentration for chemical shift calibration) were added to each lyophilised titrated extract. The mixture was centrifuged at 17,700 g for 5 min at room temperature. The supernatant was then transferred into a 5 mm NMR tube for acquisition. Quantitative ^{1}H-NMR spectra were recorded at 500.162 MHz and 300 K on a Avance III spectrometer (Bruker Biospin, Wissembourg, France) using a 5-mm ATMA broadband inverse probe, a 90° pulse angle and an electronic reference for quantification (Digital ERETIC, Bruker TopSpin 3.0). The assignments of metabolites in the NMR spectra were made by comparing the proton chemical shifts with literature (Fan 1996) or database values (MERy-B: Ferry-Ferry-Dumazet *et al.* 2011; Deborde and Jacob 2014; HMDB: Wishart *et al.* 2013; BMRB http://www.bmrb.wisc.edu), by comparison with spectra of authentic compounds and by spiking the samples. For assignment purposes, ^{1}H-1H COSY, ^{1}H-^{13}C HSQC and ^{13}C NMR spectra were acquired for selected samples. The identified metabolites are indicated in Table 1. For absolute quantification three calibration curves (glucose and fructose: 1.25 to 50 mM, glutamate and glutamine: 0 to 15 mM) were prepared and analysed under the same conditions. The glucose calibration was used for the quantification of all compounds, as a function of the number of protons of selected resonances except fructose, glutamate and glutamine that were quantified using their own calibration curve. The metabolite concentrations were calculated using AMIX (version 3.9.10, Bruker) and Excel (Microsoft, Redmond, WA, USA) software.

3.3.6 Hexose phosphates

The determination of the glycolytic intermediates glucose-6-phospahte (G6P) and fructose-6-phosphate (F6P) was based on Cross *et al*. (2006) with modifications. For the ethanolic extraction 20 mg and 10 mg of shoot and taproot was used. The powdered material was extracted as previously described in Wedeking *et al.* (2016). For the analysis of G6P, 75 µL of assay mix 1 consisting of 0.2 M tricine/KOH pH9 with 10 mM $MgCl_2$, 100 u mL^{-1} glucose-6-phosphate dehydrogenase grade II (G6PDH, E.C. 1.1.1.49), 2.5 mM NADP and ultrapure water were added to 5 µL of the ethanolic extract. After 20 min incubation at RT, 20 µL of 0.5 M sodium hydroxide (NaOH) was added and samples were incubated for 10 min at 98.5 °C in a dry bath. Then, 20 µL of 0.1 M Tricine/KOH pH 9 containing 0.5 M hydrogen chloride (HCl) were added to the cooled and briefly centrifuged (1 min, 1000 g, RT) samples. Finally, assay mix 2 consisting of 0.2 M Tricine/KOH pH 9 with 10 mM $MgCl_2$, 500 u mL^{-1} G6PDH grade I (EC: 1.1.1.49), 200 mM EDTA pH 8, 250 mM G6P, 10 mM phenazine methosulfate (PMS) and 10 mM thiazol blue tetrazolium bromide (MTT) were added, and samples were immediately measured at 570 nm (37 °C, kinetics: one read every 30 s) using a microplate reader (Safas M96, Monaco). For the analysis of F6P, 30 µL of assay mix 1 consisting of 0.2 M Tricine/KOH pH 9 with 10 mM MgCl2, 100 u mL^{-1} G6PDH grade II, 2.5 mM NADP and ultrapure water were added to 10 µL of the ethanolic extract and incubated for 20 min at RT. Subsequently, 10 µL 0.25 M HCl were added and samples were incubated for another 5 min at RT, before 10 µL of assay mix 2, consisting of 100 u mL^{-1} G6PDH grade II, 20 u mL^{-1} phosphoglucoisomerase (PGI, EC: 5.3.1.9) and ultrapure water were added. After incubation for 20 min at RT, 20 µL 0.5 M NaOH were added and samples were incubated for 10 min at 98.5 °C in a dry bath. Before 20 µL of 0.1 M Tricine/KOH pH 9 with 0.5 M HCl were added, samples were cooled and briefly centrifuged (1 min, 1000 g, RT). Finally, 52 µL of assay mix 3 consisting of 0.2 M Tricine/KOH pH 9 with, 10 mM $MgCl_2$, 1000 u mL^{-1} G6PDH grade I, 200 mM EDTA pH 8, 250 mM G6P, 10 mM PMS and 10 mM MTT were added and samples were immediately measured at 570 nm (37 °C, 1 read every 30 s) using a microplate reader. Both, G6P and F6P concentrations were calculated based on the regression equations of standard solutions (0 to 10 µM G6P and F6P respectively).

3.3.7 Starch

Starch was determined in form of glucose equivalents, using the pellet from the ethanolic extraction of the hexose phosphates. After resuspension in 400 µL 0.1 M NaOH, samples were heated at 95°C for 30 min, cooled, homogenized and centrifuged (1000 g, 5 min). Subsequently, samples were hydrolyzed by adding 0.5 M HCl with acetate/0.1 M NaOH buffer, pH 4.9. For the starch degradation, 35 µL of the thoroughly mixed sample were transferred into a new 96-well plate, adding 65 µL of a degradation mix consisting of 250 µL Amyloglucosidase (EC: 3.2.1.3), 3 µL α-amylase (EC: 3.2.1.1) and 50 mM acetate

buffer pH 4.9. Finally, samples were digested for 10-16 h at 37°C. Before the determination of the glucose as previously described (Wedeking et al. 2016), the plate was centrifuged (1000 g, 10 min, RT).

3.3.8 Nitrate

Root and shoot samples were diluted with 0.1 M potassium phosphate buffer, pH 7.5. Standards were prepared with 10 µL (0/0.25/0.5/0.75/1/1.5/2 mM mL^{-1} sodium nitrate in 96 % EtOH). For the analysis, 95 µL of the assay mix containing nitrate reductase (NR; EC: 1.7.1.2) were added to the samples. Blanks were prepared with the assay mix without NR to determine the nitrite amount in the samples. In case of the assay mix for the blanks, NR was replaced with 0.1 M potassium buffer, pH 7.5. Afterwards, all samples were homogenized and incubated for 30 min at RT in the dark. Then, 15 µL of 0.25 mM PMS were added, samples were mixed again and incubated for another 20 min at RT. Subsequently, 60 µL of 1 % sulfanilamide (w/v) in 3 M phosphoric acid and 60 µL of 0.02 % (w/v) N(1-Naphtyl)ethylemdiamine dihydrochloride (NNEDA) in 3 M phosphoric acid were pipetted and samples were mixed. After 10 min of incubation in the dark (RT), samples were measured immediately at 540 nm.

3.3.9 Total amino acid content

For the analysis, 3 µL of ethanolic extract for all samples and SDs (0/0.032/0.063/ 0.125/0.25/0.5/1 mM mL^{-1} glutamate sodium salt in 70 % EtOH (v/v) 0.1 M HEPES/KOH, pH 7) were added with 15 µL0.1 M sodium borate buffer, pH 8, 100 µL of ultrapure water and finally 90 µL 0.1 % fluorescamine (w/v) in acetonitrile. Due to its light sensitivity fluorescamine was added in the last pipetting step, and the fluorescence was measured after incubation for 5 min at RT in the dark, at 405 nm for the excitation and at 485 nm for the emission. The glutamate SD was always prepared fresh.

3.3.10 Statistical analysis

Statistical analyses were performed with SPSS 23.0 (SPSS Inc., New York, USA). Significant differences between the treatments were analyzed using a non-parametric test for independent scores. Hence, a one-factorial ANOVA according to Kruskal-Wallis (Duncan, α=0.05) with the stepwise step-down procedure, was performed. To explore the multidimensional data set, a correlation based principal component analysis (PCA) was performed. A Kaiser-Meyer-Olkin (KMO) value of >0.80 and a significant Bartlett test ($p<0.001$) for sphericity indicated that PCA after unit variance scaling was suitable. The analysis was done with a matrix of 84 samples for each plant part (2 treatments, 14 harvests, 3 biological replicates), 2 factors (treatment, day) and 27 or 26 variables for shoot and root, respectively. Rotated orthogonal components (Varimax rotation) with eigenvalues >1 were extracted and relative scores were determined. Values calculated for the heatmaps represent the change of each analysed metabolite relative to the control for the respective day.

3.4 RESULTS

3.4.1 Plants overcome drought-induced impairments of plant water status and membrane stability

During progressive drought, the soil water content (SWC) decreased slowly within the first 7 d and then faster until d 13 (Figure 3-2) Under these conditions shoot dry weight (DW) was not significantly reduced compared to controls (Figure 3-2), which developed slowly from BBCH 16-17 (6-7 leaves, d 1) to BBCH 17-19 (7-9 leaves, d 25), but plants subjected to drought had a significantly higher root DW at the end the drought period (Figure 3-2).

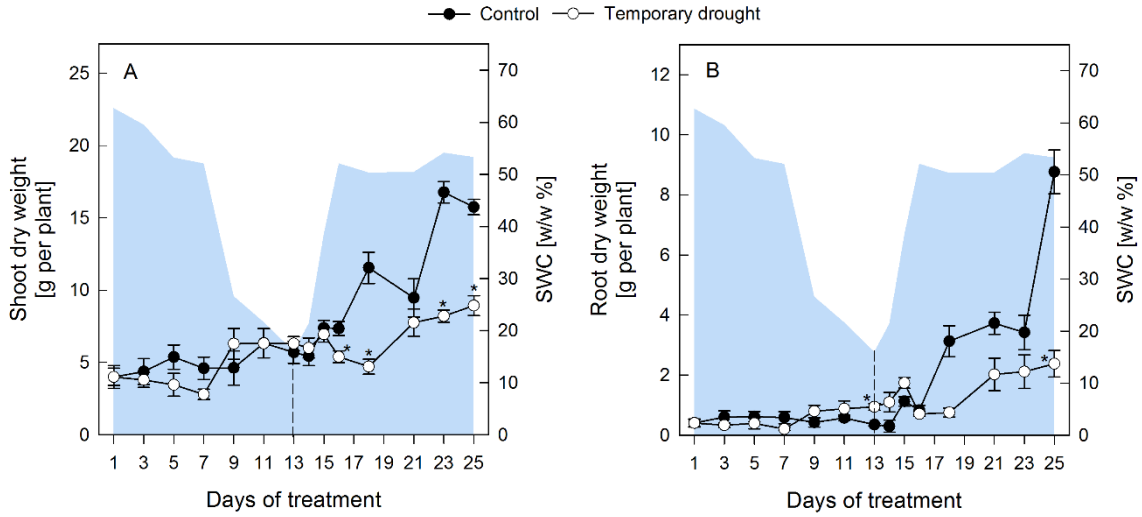

Figure 3-2: Change of biomass of sugar beet shoots and roots.
Plant dry weight of sugar beets shoots (A), roots (B) of control (closed circles) and rewatered (open circles) plants. Plants were rewatered after 13 d as indicated by the dashed line. The area plot represents the gravimetric soil water content based on substrate (SWC w/w %). All values are means ± s.e. (n=4). Significant differences to the control plants (Duncan, α=0.5) are indicated by *P < 0.05.

The RWC (Figure 3-3 A) dropped significantly after d 7 and reached a minimum value of 37 ± 2 % on d 11 of drought, while the largest decrease in OP (Figure 3-3 B) was observed between d 9 and 13 of drought with final values of 1.56 ± 0.2 MPa. Leakage (Figure 3-3 C) and MDA (Figure 3-3 D), both indicators of membrane damage due to lipid peroxidation, were measured and first signs of membrane damage in the shoot were observed after 7-9 d of desiccation.

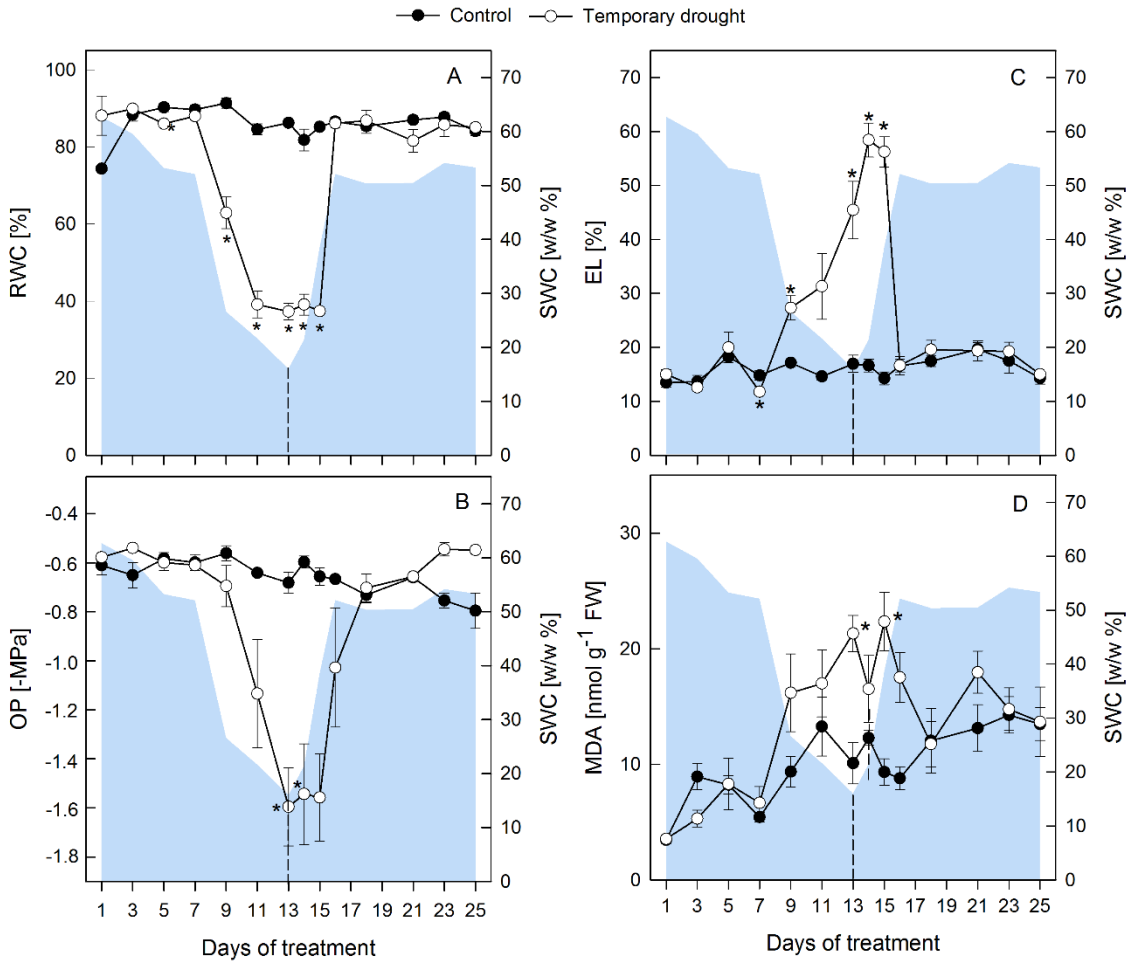

Figure 3-3: Parameters of plant water status and membrane damage.
Relative water content (RWC, A) osmotic potential (OP, B), electrolyte leakage (EL, C) and malondialdehyde (MDA) concentrations (D) of the shoot under regular water supply (closed circles) and temporary drought (open circles). The area plot represents the gravimetric soil water content based on substrate (SWC w/w %). Plants were rewatered after 13 d as indicated by the dashed line. All values are means ± s.e. (n=4). Significant differences to the control plants (xx, α=0.5) are indicated by *P < 0.05.

After the onset of rewatering, younger leaves of stressed plants regained turgor within 2 d, but oldest leaves did not fully recover until the end of the experiment (Figure 3-4). A lag period of 5 d was observed before stressed plants started regrowth, but they maintained a low relative growth rate of only 26% (shoots) and 31% (roots) of the control growth rates between d 14 and 25 (Figure 3-1 A). Both, RWC and OP showed a lag-phase of 2 d after the onset of rewatering, before they started to recover, and then reached control levels within 1 d (RWC) and 2 d (OP), respectively (Figure 3-3 A, B). MDA returned to control levels within 4-6 d. However, EL continued to increase for 1-2 d into the rewatering period, but then recovered more quickly compared to MDA and reached control levels within 3 d (Figure 3-3 C, D).

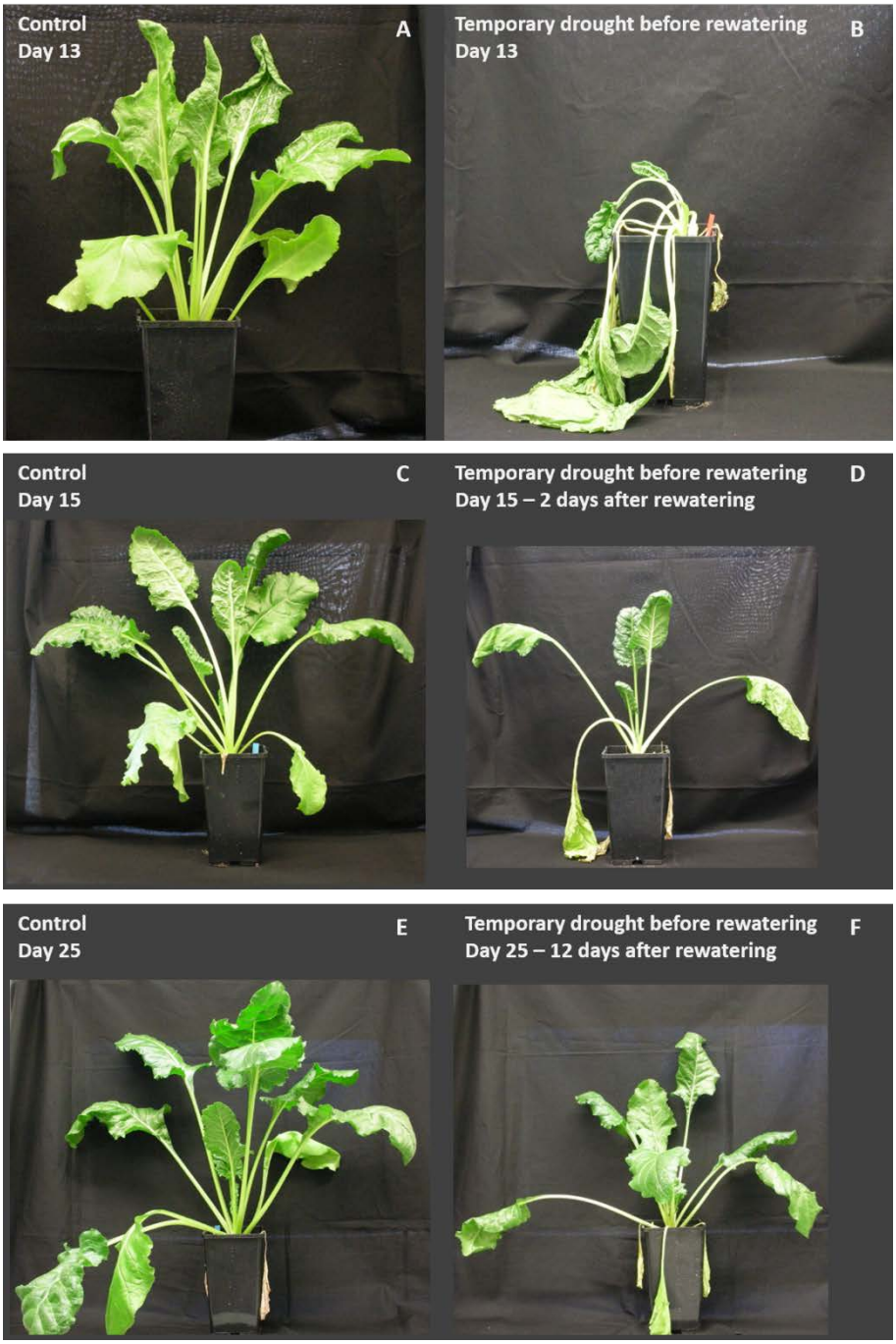

Figure 3-4: RGB Images of temporarily drought-stressed sugar beets.
Young *Beta vulgaris* plants under regular water supply (control) at day 13 (A), 15 (C) and 25 (E) with the respective drought stressed (B) and rewatered plants (D, F).

3.4.2 Temporary drought leads to changes in primary metabolism

Overall, 30 metabolites were identified by ^{1}H-NMR, including five carbohydrates, 17 amino acids (AA), five organic acids, two quaternary ammonium compounds and one alkaloid (Table 3-1, Figure 3-5 for representative spectra). For the comparison of drought induced changes (1-13 d) and the differences between shoots and roots (13-25 d) under rewatering, metabolic maps were created showing the log2-

fold change between well-watered and drought-stressed/rewatered plants for each harvest day (Figure 3-6).

Table 3-1: Chemical shifts used for identification and quantification of metabolites in ^{1}H-NMR spectra.
Chemical shifts of sugar beet roots and leaves polar extracts (in D_2O), expressed as relative values to the TSP resonance at 0 ppm. s: singlet, d: doublet, dd: doublet of doublets, t: triplet, m: multiplet.

Compound	Group	Multiplicity	δ^1H (ppm) D_2O pH 6	Shoot (S) Root (R)	Identification status[a]
Soluble sugars					
Fructose	α(C3H+C5H)+βC5H	m	4.12	S	2
α-Glucose	C1H	d	5.22	SR	1
β-Glucose	C1H	d	4.65	SR	1
β-Glucose	C2H	t	3.25	SR	1
Raffinose	Galactosyl-C1H	d	5.00	SR	1
Sucrose	Glucopyranosyl-C1H	d	5.42	SR	1
UDP-glucose-like	C1H ribose	m	5.98	R	3
Organic acids					
Citric acid	$C2H_2$+$C4H_2$	dd	2.58	SR	1
Formic acid	C1H	s	8.46	S	2
Fumaric acid	C2H+C3H	s	6.52	R	2
Malic acid	C2H	dd	4.30	SR	1
Amino acids and other amino compounds					
Alanine	$C3H_3$	d	1.48	SR	1
Arginine	$C7H_2$	m	1.63	S	1
Asparagine	½ ($C3H_2$)	m	2.88	SR	1
Aspartic acid	½ ($C3H_2$)	½ dd	2.82	SR	1
GABA	$C2H_2$	t	2.30	R	1
Glutamic acid	$C3H_2$	m	2.36	SR	1
Glutamine	$C4H_2$	m	2.46	SR	1
Isoleucine	$C6H_3$	s	1.02	SR	1
Phenylalanine	C5H+C6H	m	7.41	SR	1
Proline	$C4H_2$	m	2.33	SR	2
Pyroglutamic acid	C2H	dd	4.17	SR	1
Serine	$C2H_2$	m	3.97	SR	1
Tryptophan	C7H	d	7.55	SR	1
Tyrosine	$C3H_2$	d	6.91	SR	1
	$C2H_2$	d	7.19	S	1
Valine	$C4H_3$	d	1.04	SR	1
	$C5H_3$	d	1.00	SR	1
Choline	N-$C3H_3$+N-$C4H_3$+N-$C5H_3$	s	3.20	R	1
Glycine betaine	N-$C3H_3$+N-$C4H_3$+N-$C5H_3$	s	3.27	SR	1
	$C2H_2$	s	3.83	SR	1
Trigonelline	C2H	s	9.17	S	2
Other compounds					
Xanthine_like	C2H	s	8.46	R	3
UnknownS8.29		s	8.29	S	4
UnknownS5.35		s	5.35	R	4
UnknownS5.25		s	5.25	S	4
UnknownS2.75		s	2.75	R	4
UnknownD1.84		d	1.84	S	4

[a] Identification level according to MSI (Sumner *et al.* 2007): 1, Identified compounds (checked with standard); 2, Putatively annotated compounds; 3, Putatively characterized compound classes; 4, Unknown.

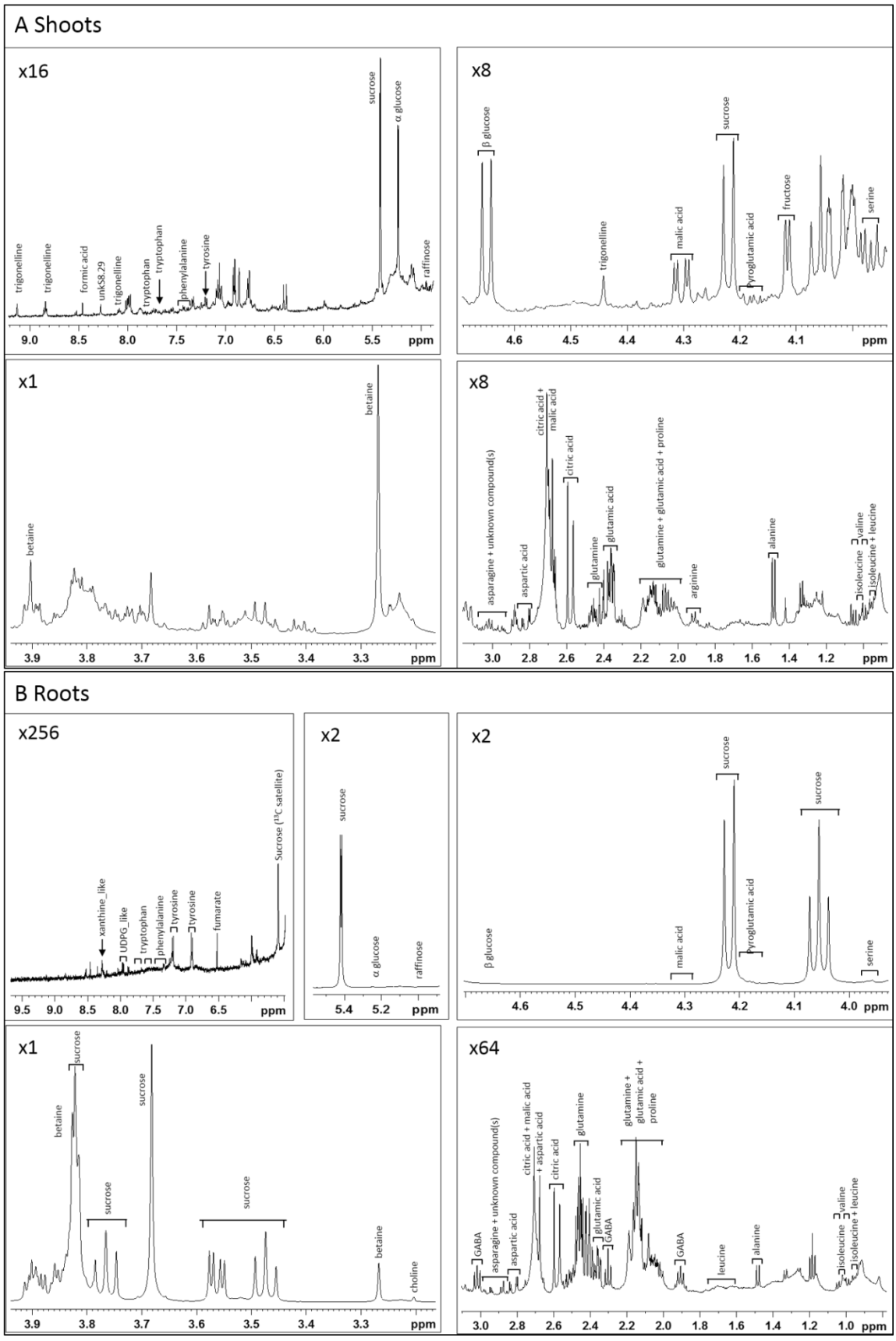

Figure 3-5: Representative ^{1}H-NMR spectra of sugar beet shoots and roots.

Two representative ^{1}H-NMR spectra in different magnifications of polar extracts of shoots (A) and roots (B) of well-watered *Beta vulgaris* plants at day 15 of the experimental period. Numbers in the left upper corner correspond to the magnification of the selected section. Resonances are annotated according to Table 3-1.

Temporary drought caused a change of several metabolites including sugars, organic acids, compatible solutes and especially AA in both organs (Figure 3-6 A). In leaves, opposite effects were observed for sucrose and starch, where sucrose levels increased, while starch concentrations decreased towards the end of the desiccation period (Figure 3-6 A; Figure 3-7). The quantifiable intermediates of the TCA cycle (citrate, malate, fumarate) were only marginally affected during drought, with the exception of a reduction of fumarate levels in roots (Figure 3-6 A). Drought induced metabolic reprogramming resulted in an increase of total amino acids (AAt), as well as decreases in nitrate and protein (Figure 3-8). The most significant increase was observed for branched chain amino acids (BCAA: leucine, isoleucine, valine), alanine derived from pyruvate, and aromatic amino acids (AAA: tryptophan, phenylalanine, tyrosine) derived from phosphoenolpyruvate, with the maximum change observed for phenylalanine (>200 fold in shoots, >70 fold in roots). Especially in shoots, drought-induced increases in glutamine, pyroglutamate, arginine, and proline were associated with a decrease of their precursor glutamate (Figure 3-6 A). Correspondingly, an increase of asparagine in shoots was accompanied by a decrease of its precursor aspartate. The quaternary ammonium compound glycine betaine (GB) and proline also accumulated towards the end of the stress in shoots, but only marginally in roots, where the GB increase was nevertheless associated with a decline of its precursor choline (Figure 3-6 A). Overall, the metabolic pathway map indicates that under drought stress, glycolysis and TCA cycle were rather downregulated, while levels of AA were significantly enhanced.

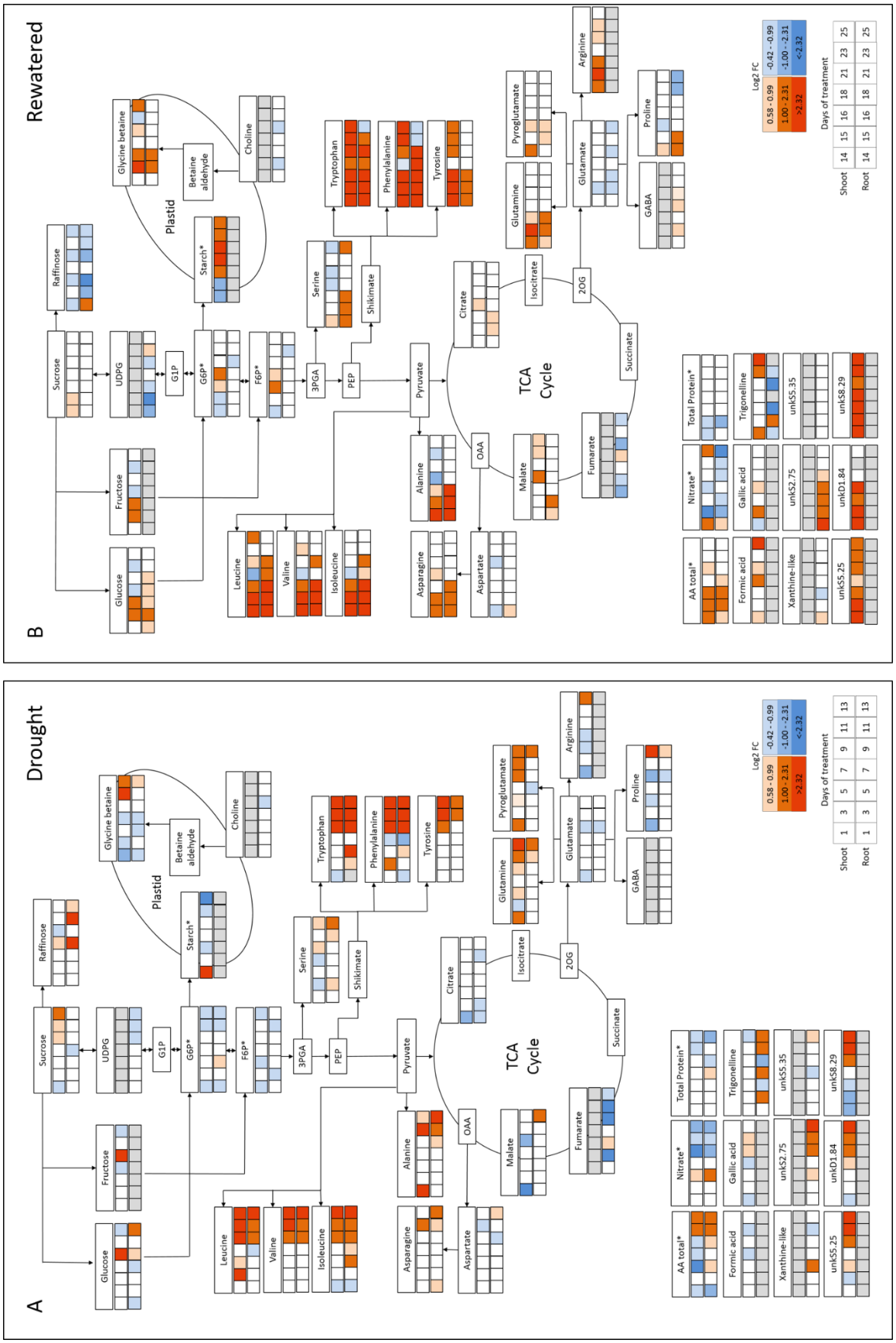

Figure 3-6: Metabolic map of drought stresses and rewatered sugar beets.

Caption Figure 3-6

Differences in the ^{1}H-NMR metabolomic profile during 13 days of progressive drought and rewatering. (A) Drought treatment, day 1-13, (B) Rewatering day 14-25. The first row indicates the metabolic alterations in the shoot, the second row indicate the changes in the root. Red and blue colors indicate the log_2-transformated abundance (log2 Fold change, log_2FC) of each metabolite relative to the controls. Grey boxes indicate that the respective metabolite was not identified (shoot only: Fructose, starch, formic acid, gallic acid, unkS5.25, unkD1.84. Root only: UDPG-like sugar, choline, GABA, xanthine-like metabolite, unkS2.75, unkS5.35.). Asterisks (*) indicates that metabolites were determined by robotized enzyme assays (G6P, F6P, starch, total amino acids (AA total), nitrate, total protein).

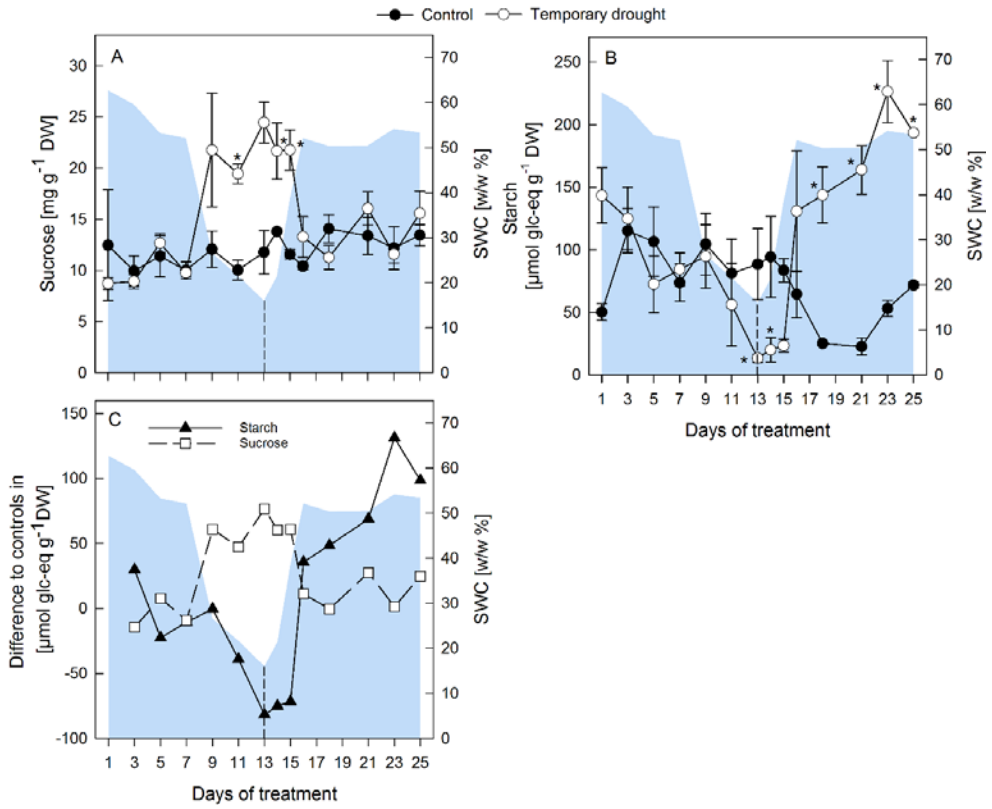

Figure 3-7: Changes in sucrose and starch concentrations.

Changes of sucrose (A) and starch (B) under control conditions (closed circles) and temporary drought (open circles). C: Difference to the control of starch (filled triangles) and sucrose (open squares) concentrations under temporary drought. All values are means ± s.e. (n=4). Significant differences to the control plants (Duncan, α=0.5) are indicated by *P < 0.05

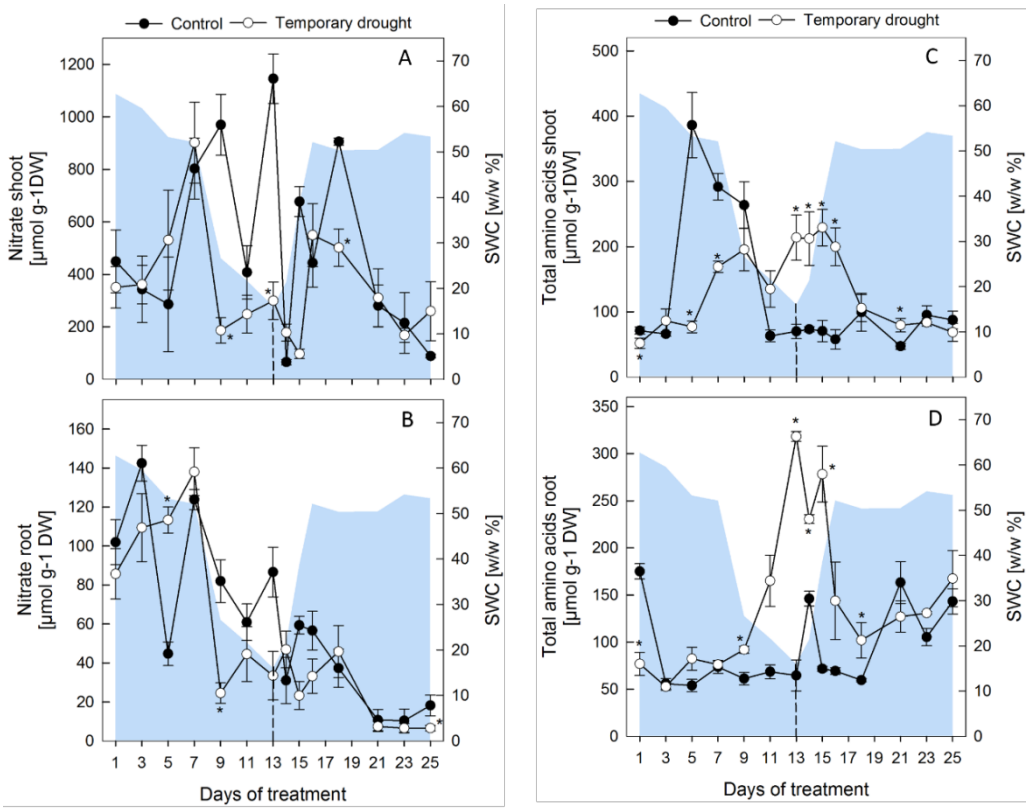

Figure 3-8: Targeted analysis of nitrate, totoal amino acid content and total protein content.

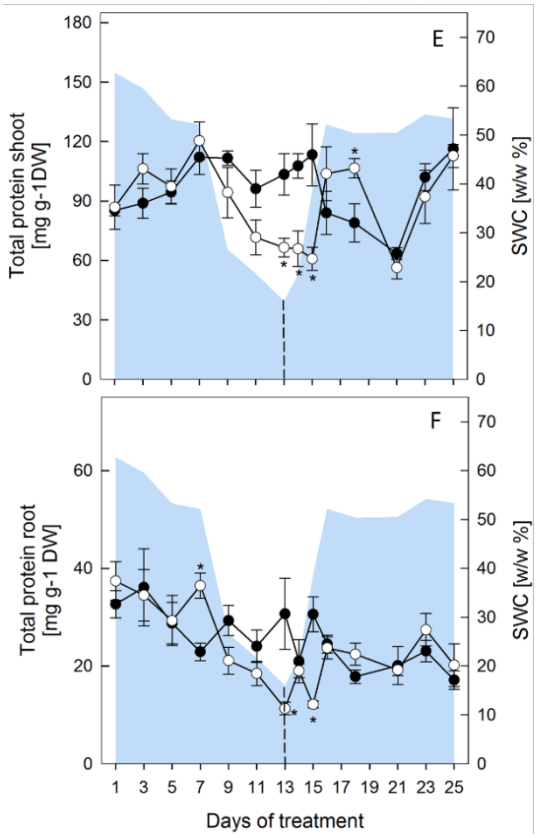

Figure 3-8 continued

Changes of nitrate (A, shoot; B, root), total amino acid content (C, shoot; D, root) and total protein (E, shoot, F, root) under control conditions (closed circles) and temporary drought (open circles). All values are means ± s.e. (n=4). Significant differences to the control plants (Duncan, α=0.5) are indicated by*P < 0.05.

3.4.3 Different dynamics in shoots and roots during the recovery process

The majority of the increased metabolites under drought approached or returned to control level between d 15-18 (2-5 d after rewatering, DAR), with the notable exception of starch, which increased throughout the recovery period and reached significantly higher values at the end of the experiment compared to controls (Figure 3-6). Some distinct differences were observed between shoots and roots (Figure 3-6 B). In shoots, glucose (and similarly fructose) quickly dropped below controls at the beginning of rewatering, but then showed a second transient peak, from d 15-16, while in roots, glucose only slowly returned to control levels (d 23).

Citrate and malate increased slightly during rewatering in shoots and roots, while fumarate (only detectable in roots) remained lower than control levels throughout the recovery. In shoots, rewatering mostly reversed the drought induced increases of AA within 5 d of rewatering (d 18), while accumulated AA decreased more slowly, but constantly, in roots and reached control levels at d 23. Notably the AAAs, and less pronounced leucine, valine and GB, showed a second strong increase towards the final days of the rewatering in shoots, but not in roots.

A major difference between roots and shoots was the response of serine, which was more strongly induced by drought in roots, where it only slowly returned to control levels during rewatering, and also showed a strong second increase towards the end of the rewatering period, similar to the dynamics observed for AAAs in shoots. Summarized, the observed dynamics in the metabolite abun-

dance indicate distinct alterations in the metabolic activity of the involved pathways under drought and recovery, and between shoots and roots.

In order to search for metabolites that were the most important indicators for stress and recovery, and to assess whether and how the drought induced changes were reversed under rewatering, a principal component analysis (PCA) was performed for each plant part using a matrix containing the data of 27 (shoots) and 26 (roots) quantified metabolites in 84 samples for each shoots and roots (Figure 3-9). The PCA allowed to visualize the separation of the different time points, and to identify the metabolites involved in the dynamic response.

For the shoot PCA (Figure 3-9 A, B), the first two principal components (PCs) explained 53.6% of total variability, with 40.0% for the first principal component (PC1) and 13.6% for the second principal component (PC2). In the scores plot (Figure 3-9 A), PC1 separated a large group containing control, mildly stressed (<d 9) and late rewatered (>d 15) samples on the negative side from a group containing samples taken at later stages of drought and early rewatering (d 9 15, positive side), indicating that PC1 seems related to drought stress intensity. PC2 tended to separate younger (~d 1-15, negative side), from older plants (~d 16-25, positive side), suggesting that PC2 seems related to shoot development. However, this separation was less clear than for PC1, in line with a more gradual change in metabolism throughout development. The trajectories (Figure 3-9 A) visualize the differences in metabolic patterns over time between control and drought stressed/rewatered plants.

Comparison of the scores plot (Figure 3-9 A) and loadings plot (Figure 3-9 B) showed that the samples taken at later stages of drought and early rewatering tended to have higher contents in a range of AA including tyrosine, tryptophan, phenylalanine, pyroglutamate, leucine, isoleucine, valine and glutamine. Along PC2, the younger plants seemed characterized by higher contents of trigonelline, and the older ones by higher contents of citrate.

For the root PCA (Figure 3-9 C, D), the first two PCs explained 68.3% of total variability (PC1 50.6%, PC2 17.7%). In the scores plot (Figure 3-9 C), PC1 separated one large group containing control plants, mildly stressed (<d 11) and plants of late rewatering (>d 16) on the negative side, from a smaller group characterized by samples taken at later stages of progressive drought and early rewatering (d 11-16) on the positive side, which indicates that PC1 also seems related to stress intensity. PC2 tended to progressively separate samples at early stages on its negative side from samples at late stages of development on its positive side. Comparison of the scores plot (Figure 3-9 C) and loadings plot (Figure 3-9 D) showed that the samples taken at later stages of drought and early rewatering tended to have higher contents in a range of amino acids similarly to leaves and also sucrose and GB. Roots at the later stages had higher contents in aspartate, glutamate and raffinose.

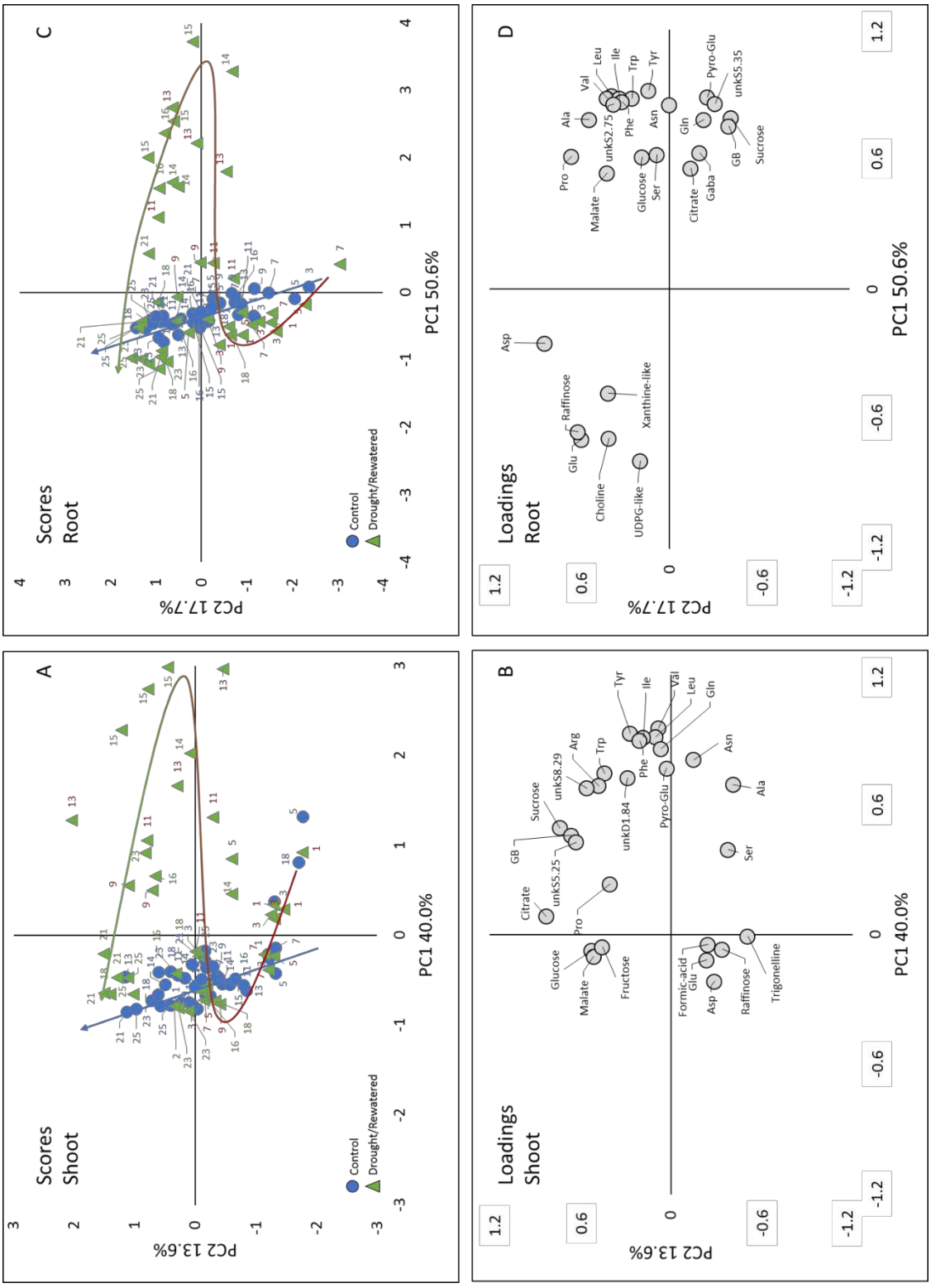

Figure 3-9: PCA scores and loadings of drought-stressed sugar beets.
Result of the principal component analysis (PCA) of the ^{1}H-NMR profiles. Scores plot of the shoot (A) and root (C), loadings plot of shoot (B) and root (D); samples size n=3. The PC1 x PC2 plots represent 53.6% and 68.3% of total variance for shoots and roots, respectively. In the scores plot circles represent control plants and triangles represents temporary stressed plants. Trajectories in the scores plot represent the temporal development of metabolic response during the treatments (blue arrow, control; bicolored arrow: red: drought, green: rewatered. Abbreviations: Asn, asparagine; Asp, asparagine; Gaba, γ-aminobutyric acid; GB, glycine betaine; Gln, glutamine; Glu, glutamate; Ile, isoleucine; Leu, leucine; Val, valine; Phe, phenylalanine; Pro, proline; Pyro-Glu, pyroglutamate; Ser, serine; Trp, tryptophan; Tyr, tyrosine; UDPG-like, uridine diphosphate glucose-like; unk, unknown compound.

The PCA of both roots and shoots confirms that major stress-induced metabolic changes occurred during the final 3-5 d of progressive drought and lasted for another 3 d into the recovery period, which exactly mirrors the response of water relations (RWC, OP) and of membrane damage (EL, MDA) during the stress and the recovery phase. In both organs the rewatered samples showed a reversed trajectory (Figure 3-9 A, C) and rewatered samples clustered again with controls between d 16-17, indicating the transitory nature of the metabolic changes triggered by progressive drought. However, in roots, samples taken between d 23-25 showed a tendency to separate again from the control plants along PC1 (Figure 3-9 C), suggesting that after 10 DAR (d 23), roots were metabolically distinct from non-stressed conditions, whereas this did not seem to be the case in shoots.

3.5 DISCUSSION

3.5.1 Damage repair was important during recovery and involved glycine betaine

Drought stress triggers various physiological and biochemical responses in plants. For sugar beets, which have only a limited ability to regulate transpiration (Hanson and Hitz 1982), the adaptation of the metabolism after a drought spell is especially relevant. While drought induced metabolic changes have been extensively described (Bloch *et al.* 2006b; Choluj *et al.* 2008; Wu *et al.* 2014), little is known about the dynamics and completeness of metabolic recovery in Beta vulgaris. In the present study, young plants suffered from significant membrane damage and lipid peroxidation after 13 d of progressive drought before the onset of rewatering. Based on a previous study, sugar beets are severely, but not lethally stressed under these conditions (Wedeking *et al.* 2016).

The typical accumulation of primary metabolites such as soluble carbohydrates, organic and amino acids as well as amides was observed at the end of the drought period in both organs (Figure 3) and is consistent with other studies (Meyer *et al.* 2014). While after 12 d of rewatering physiological parameters had returned to control levels, metabolites, especially AAAs, recovered only slowly. This is not surprising, since many processes need to be rearranged under rewatering to reach a new balance, and metabolic adjustments are needed to coordinate investment of resources into damage repair and resumed growth (Sims *et al.* 2012). In addition, shoots ensure photosynthesis to maintain energy supply, while roots warrant water and nutrient uptake. This requires different sets of metabolites even under well-watered conditions, and during and after drought, resources need to be re-distributed to ensure efficient recovery strategies in each organ (Gargallo-Garriga *et al.* 2014). The distinct functions of shoots and roots likely result in different stress levels and consequently distinct dynamics of metabolic responses as outlined below.

Lipid peroxidation caused by reactive oxygen species (ROS) is commonly observed under severe drought. As functional membranes are indispensable for photosynthesis, nutrient and water uptake or respiration, it can be assumed that the repair of membranes has priority during recovery. However, detoxification of ROS is an energy consuming process and requires large amounts of reductive power for enzymatic and non-enzymatic scavenging (Pinheiro and Chaves 2011). The continued increase of EL in shoots during the first two days of rewatering and the slow recovery of MDA indicate that either the supply of reductants was not available or that ROS scavenging systems were not fully recovered shortly after the onset of rewatering.

Chen and Murata (2002) argue that the fate of cellular components under stress depends on the balance between damage and repair rather than the severity of the damage alone, and that elevated ROS levels hinder repair processes, even before the damage is measurable. They suggest that compatible solutes such as GB and proline protect the protein-synthesizing machinery from oxidative stress, thus maintaining conditions under which repair mechanisms occur at high rates. Compatible solutes thus fulfil a double role by conferring osmotic adjustment (OA) under drought, as well as contributing to a high rate of repair during recovery. In Beta vulgaris, GB is a constitutive cytoplasmic compatible solute, and can accumulate to considerable amounts under stress conditions (Chen and Murata 2011). It is likely that shoot membranes suffer more severe damage than those of roots, since a drought-induced imbalance between photosynthetic activity and growth results in an enhanced production of ROS. In the present study, both GB and proline increased in both organs very late during the drought period, and their accumulation was higher in shoots compared to roots. In summary this may indicate that they were involved in protection rather than OA during the final phase of drought, and enabled necessary repair mechanisms as suggested by Chen and Murata (2002).

Elevated GB levels in sugar beet roots could negatively affect sugar yield in two different ways. Firstly, GB reacts with sucrose during processing and thus impairs sugar crystallization (van der Poel *et al.* 1998) and secondly, its biosynthesis is energy consuming, since the synthesis of 1 mol GB requires approximately the same energy input as 1 mol sucrose (Hitz *et al.* 1982). Hence, energy and photosynthates used in this reaction are neither available for sucrose storage nor for other processes related to economic yield. In the present study GB concentrations returned to control levels within 12 d of rewatering, but it remains to be seen whether additional drought events might lead to maintained high GB concentrations and thus lower sugar yields.

3.5.2 Metabolic adjustment occurred at the expense of regrowth

Drought affects plant growth and yield and even short-term water deficits can induce significant yield losses in sugar beet, particularly when arising during early development (Brown *et al.* 1987). Here, plants resumed growth under rewatering, but maintained a lower growth rate in both organs until the end of the experiment, suggesting a need for allocating C to metabolic adjustment, continued energy supply and an efficient damage repair after cessation of the stress.

The transient increase in root biomass compared to controls during the final days of drought was mainly due to the progressive formation of a network of fine side roots, rather than an increase of the taproot (data not shown). A dense mat of side roots increases the soil volume that can be exploited for water, but redirection of resources into side roots occurs at the expense of taproot formation and ultimately reduced incorporation of sucrose (Hoffmann 2014). It is therefore likely that an early impairment of the taproot formation might contribute to sucrose yield losses at harvest (Brown et al. 1987), and it remains to be determined whether this can be compensated during development, especially if future drought spells arise.

3.5.3 Drought-induced carbon re-allocation is only partly reversed during rewatering

Under drought, C allocation patterns are changed in order to distribute resources to the sites where they are most needed during acclimation and, after stress release, restauration processes (Bohnert and Sheveleva 1998). Here, drought led to elevated levels of soluble sugars in shoots, which were paralleled by a decrease in starch. Decreasing starch levels in drought-stressed shoots have been previously observed in sugar beet (Fox and Geiger 1986) and other crops (Zrenner and Sitt 1991), and result from an inhibited starch biosynthesis (Geigenberger *et al.* 1997) or enhanced turnover to provide soluble sugars for OA (Usadel *et al.* 2008).

Rewatering reversed the drought induced changes of sucrose and starch, clearly indicating that photosynthesis quickly recovered after rewatering. Interestingly, starch levels reached and maintained values which were significantly higher than the controls throughout the second half of the rewatering period. Since growth resumed only after d 18 (5 DAR) and at reduced rates, it is possible that inhibited growth contributed to the observed accumulation of starch. It would be interesting to see whether starch concentrations return to control levels after a longer recovery period, or whether this is a long-lasting stress imprint affecting sugar metabolism throughout development. Alternatively, starch synthesis and degradation follow a circadian regulation, which can be compromised under drought (Greenham and McClung 2015). Under regular water supply, leaves accumulate starch during the day and remobilize it at night to support metabolism and growth (Zrenner & Sitt, 1991). It cannot be ruled out that drought-induced perturbations of the diurnal pattern of starch metabolism were involved in

the observed starch accumulation during rewatering, and further studies should include measurements of diurnal starch variations.

3.5.4 Amino acids accumulate during drought and respond differently to rewatering

The PCA indicates that AA represented the dominant loadings under severe stress in both roots and shoots (Figure 3-9). In other words, the increase in AA was indicative for the transition from mild to severe drought stress. Increasing AA concentrations, and especially AAAs and BCAAs, were frequently observed under drought in leaves and roots of several species (tomato: Semel *et al.* 2007; Arabidopsis: Binder 2010; barley: Bowne *et al.* 2012; maize: Witt *et al.* 2012). Due to their slow catabolism, these AA represent an excellent pool to rebuild proteins after the stress ends. The AA pool can be fed either by N assimilation, or by chlorophyll and protein turnover. Here, the increase in AA was accompanied by decreasing total protein concentrations in both organs, which might indicate enhanced proteolysis provoked by the stress in combination with a slow catabolism of AA (Araújo *et al.* 2011). However, the AA accumulation under drought was preceded by a significant drop in NO_3^- concentrations (Figure 3-6). Since NO_3^-supply and uptake into the root are likely inhibited under drought (Ruffel *et al.* 2014), such a drop in plant NO_3^- levels could be an indicator for continued N-assimilation, at least during the first days of drought and as long as the NO_3^- pool was not exhausted. Indeed, this would be an excellent valve to get rid of excess energy caused by drought-induced growth inhibition, while photosynthesis is still functioning. However, other studies indicate rapid inhibition of nitrate reductase (NR) activity under drought in different species (Foyer *et al.* 1998; Robredo *et al.* 2011). Additional experiments are under way to assess N-assimilation and NR activity in drought stressed sugar beet.

Under rewatering, levels of BCAAs and AAAs returned to control levels within several days, but more slowly in roots compared to shoots. Under conditions of limited resources, BCAAs as well as AAAs play a role in mitochondrial respiration (Araújo *et al.* 2011; Pires *et al.* 2016), and can be catabolized into the TCA cycle to contribute to the cellular energy metabolism (Galili *et al.* 2016). In addition, BCAA-derived metabolites such as fatty acids and acyl sugars contribute to plant growth, defense and flavor (Ding *et al.* 2012), which may be beneficial for the recovery process. The more rapid decrease of BCAA, aspartate, asparagine and phenylalanine levels in shoots during rewatering might indicate that these AAs were important in contributing to the energy supply in photosynthetic tissues, which were severely damaged by ROS formation, while newly assimilated C was first used to repair essential structures before being translocated to roots. Longer maintenance of elevated AA levels in roots might also be attributed to an overall slower recovery of protein synthesis and growth in belowground organs (roots).

Surprisingly, AAAs only transiently returned to control levels in shoots, and a second strong increase was evident towards the end of the rewatering period, which was not observed in roots. Aromatic AAs serve as precursors of secondary metabolites including anthocyanins, which in turn are precursors of lignin and suberin, and auxin, which plays a leading role in plant organ formation. At this point it can only be speculated that the second increase in AAAs in shoots could indicate an increased demand for these substances during the onset of regrowth or represents a stress imprint, which might confer a competitive advantage during future drought events (Crisp *et al.* 2016).

Another difference between roots and shoots was the stronger drought-induced increase of serine in roots. Serine is involved in various biological processes such as cell proliferation, C-1 metabolism, signaling and sphingolipid biosynthesis and serves as precursor for tryptophan biosynthesis (Benstein *et al*. 2013) Hence, sufficient serine concentrations are fundamental for all tissues to ensure plant development, and evidence for its involvement in abiotic and biotic stress responses is increasing (Galili *et al*. 2016). However, an explanation for the observed additional increase towards the end of the rewatering period is currently not known.

3.6 CONCLUSION

The untargeted ^{1}H-NMR metabolomic approach delivered a detailed metabolic picture of temporarily drought stressed Beta vulgaris plants. Drought-induced changes in primary metabolism as well as impairments of plant water status and membrane stability were mostly reversed within 12 d of recovery, but clearly different recovery dynamics were observed in roots and shoots, possibly related to the distinct functions and the need for efficient recovery strategies in each organ. This difference is reflected in the PCA results, which indicated that roots sampled at the end of the rewatering period were metabolically distinct from non-stressed plants, while this was not the case in shoots. Only in shoots we detected a second increase in AAAs towards the end of rewatering. At this point it remains unclear whether this indicates an increased demand for AAAs during the onset of regrowth, or whether it represents a stress imprint which might be beneficial during an upcoming drought spell.

Damage repair seemed to be particularly important during the initial recovery phase. The late increase of GB and proline towards the end of the drought period especially in shoots might indicate their protective function specifically for the maintenance of favorable conditions for cellular restauration.

Even though the targeted analysis of further metabolites such as nitrate indicated a continued N-assimilation at least during the initial days of drought, metabolic adjustments and repair processes during recovery occurred at the expense of growth for at least 12 days. Whether this reduced growth

rate or perturbation in the diurnal starch metabolism accounted for the observed significant increase in starch during the recovery period still awaits verification.

Overall, it can be concluded that drought and recovery are two distinct processes subject to different regulatory mechanisms actively driven by the plant. While progressive drought leads to acclimation processes required for a new metabolic steady-state under increasing water limiting conditions, rewatering results in a re-distribution of resources to ensure the recovery process, in an organ specific manner.

ACKNOWLEDGEMENTS

We thank MetaboHUB (ANR-11-INBS-0010 project) and PHENOME (ANR-11-INBS-012) projects for financing. This study was financially supported by the German Federal Ministry of Education and Research (BMBF 0315529) and the European Union for regional development (EFRE z1011bc001a) and is part of CROPSENSe.net, the competence network for phenotyping research. We would like to thank Katrin Kemmerling (INRES Plant Nutrition, University of Bonn) for her contribution of the analysis of the plant water status and the indicators of membrane damage, and Duyên Prodhomme (UMR1332 Biologie du Fruit et Pathologie, INRA, Bordeaux) for her contribution to the targeted metabolite analysis,

3.7 REFERENCES

Araújo W.L., Tohge T., Ishizaki K., Leaver C.J., Fernie A.R. (2011) Protein degradation – an alternative respiratory substrate for stressed plants. Trends in Plant Science 16, 489–498.

Benstein R.M., Ludewig K., Wulfert S., Wittek S., Gigolashvili T., Frerigmann H., Gierth M., Flügge U-I, Krueger S. (2013) Arabidopsis phosphoglycerate dehydrogenase1 of the phosphoserine pathway is essential for development and required for ammonium assimilation and tryptophan biosynthesis. The Plant cell 25, 1–20.

Bhargava S., Sawant K. (2013) Drought stress adaptation, metabolic adjustment and regulation of gene expression (R Tuberosa, Ed.). Plant Breeding 132, 21–32.

Binder S. (2010) Branched-chain amino acid metabolism in Arabidopsis thaliana. The Arabidopsis Book/ American Society of Plant Biologists 8, 1–14.

Bloch D., Hoffmann C.M., Märländer B. (2006a) Solute accumulation as a cause for quality losses in sugar beet submitted to continuous and temporary drought stress. Journal of Agronomy and Crop Science 192, 17–24.

Bloch D., Hoffmann C., Märländer B. (2006b) Impact of water supply on photosynthesis, water use and carbon isotope discrimination of sugar beet genotypes. European Journal of Agronomy 24, 218–225.

Bohnert H.J., Sheveleva E. (1998) Plant stress adaptations — making metabolism move. Current Opinion in Plant Biology 1, 267–274.

Bowne J.B., Erwin T.A., Juttner J., Schnurbusch T., Langridge P., Bacic A., Roessner U. (2012) Drought responses of leaf tissues from wheat cultivars of differing drought tolerance at the metabolite level. Molecular Plant 5, 418–29.

Bradford M.M. (1976) A rapid and sensitive method for the quantitation of microgram quantities of protein utilizing the principle of protein-dye binding. Analytical Biochemistry 72, 248–254.

Brown K.F., Messem A.B., Dunham R.J., Biscoe P.V. (1987) Effect of drought on growth and water use of sugar beet. The Journal of Agricultural Science 109, 421–435.

Chen T.H.H., Murata N. (2002) Enhancement of tolerance of abiotic stress by metabolic engineering Of betaines and other compatible solutes. Current Opinion in Plant Biology 5, 250–257.

Chen T.H.H., Murata N. (2011) Glycinebetaine protects plants against abiotic stress, mechanisms and biotechnological applications. Plant, Cell and Environment 34, 1–20.

Choluj D., Karwowska R., Ciszewska A., Jasińska M. (2008) Influence of long-term drought stress on osmolyte accumulation in sugar beet (Beta vulgaris L.) plants. Acta Physiologiae Plantarum 30, 679–687.

Crisp P.A., Ganguly D., Eichten S.R., Borevitz J.O., Pogson B.J. (2016) Reconsidering plant memory, Intersections between stress recovery, RNA turnover, and epigenetics. Science Advances 2, 1–14.

Cross J.M., von Korff M., Altmann T., Bartzetko L., Sulpice R., Gibon Y., Palacios N., Stitt M. (2006) Variation of enzyme activities and metabolite levels in 24 Arabidopsis accessions growing in carbon-limited conditions. Plant Physiology 142, 1574–1588.

Deborde C., Jacob D. (2014) MeRy-B, a Metabolomic Database and Knowledge Base for Exploring Plant Primary Metabolism BT Plant Metabolism, Methods and Protocols. In, Sriram G, ed. Totowa, NJ, Humana Press, 3–16.

Deborde C., Moing A., Roch L., Jacob D., Rolin D., Giraudeau P. (2017) Plant metabolism as studied by NMR spectroscopy. Progress in Nuclear Magnetic Resonance Spectroscopy 102–103, 61–97.

Ding G., Che P., Ilarslan H., Wurtele E.S., Nikolau B.J. (2012) Genetic dissection of methylcrotonyl CoA carboxylase indicates a complex role for mitochondrial leucine catabolism during seed development and germination. The Plant Journal 70, 562–577.

EEA (2015) Indicator assessment data and maps, Global and European temperature. Copenhagen.

Enz M., Dachler C. (1997) Compendium of growth stage identification keys for mono- and dicotyledonous plants – extended BBCH scale. BBA, BSA, IGZ, IVA, AgrEvo, BASF, Bayer, Novartis.

Fan T.W-M. (1996) Metabolite profiling by one- and two-dimensional NMR analysis of complex Mix turen. Progress in Nuclear Magnetic Resonance Spectroscopy 28, 161–219.

Ferry-Dumazet H., Gil L., Deborde C., Moing A., Bernillon S., Rolin D., Nikolski M., de Daruvar A., Jacob D. (2011) MeRy-B, a web knowledgebase for the storage, visualization, analysis and annotation of plant NMR metabolomic profiles. BMC Plant Biology 11, 104.

Flexas J., Barón M., Bota J., Ducruet J.M., Gallé A., Galmés J., *et al*. (2009) Photosynthesis limitations during water stress acclimation and recovery in the drought-adapted Vitis hybrid Richter-110 (V. berlandieri×V. rupestris). Journal of Experimental Botany 60, 2361–2377.

Fox T., Geiger D.R. (1986) Osmotic response of sugar beet leaves at CO2 compensation point. Plant Physiology 80, 239–241.

Foyer C.H., Valadier M-H., Migge A., Becker T.W. (1998) Drought-induced effects on nitrate reductase activity and mRNA and on the coordination of nitrogen and carbon metabolism in maize leaves. Plant Physiology 117, 283–292.

Galili G., Amir R., Fernie A.R. (2016) The regulation of essential amino acid synthesis and accumulation in plants. Annual Review of Plant Biology 67, 153–178.

Gargallo-Garriga A., Sardans J., Pérez-Trujillo M., Rivas-Ubach A., Oravec M., Vecerova K., *et al*. (2014) Opposite metabolic responses of shoots and roots to drought. Scientific Reports 4, 1–7.

Geigenberger P., Reimholz R., Geiger M., Merlo L., Canale V., Stitt M. (1997) Regulation of sucrose and starch metabolism in potato tubers in response to short-term water deficit. Planta 201, 502–518.

Gibon Y., Vigeolas H., Tiessen A., Geigenberger P., Stitt M. (2002) Sensitive and high throughput metabolite assays for inorganic pyrophosphate, ADPGlc, nucleotide phosphates, and glycolytic intermediates based on a novel enzymic cycling system. The Plant Journal for cell and molecular biology 30, 221–235.

Greenham K., McClung C.R. (2015) Integrating circadian dynamics with physiological processes in plants. Nature Reviews Genetics 16, 598–610.

Hanson A.D., Hitz W.D. (1982) Metabolic response of mesophytes to plant water deficits. Annual Review of Plant Physiology 33, 163–203.

Hendriks J.H.M., Kolbe A., Gibon Y., Stitt M., Geigenberger P. (2014) ADP-glucose pyrophosphorylase is activated by posttranslational redox-modification in response to light and to sugars in leaves of Arabidopsis and other plant species. Plant Physiology, 133, 838–849.

Hitz W.D., Ladyman J.A.R., Hanson A.D. (1982) Betaine synthesis and accumulation in barley during field water-stress. Crop Science 22, 47.

Hodges D.M., DeLong J.M., Forney C.F., Prange R.K. (1999) Improving the thiobarbituric acid-reactive-substances assay for estimating lipid peroxidation in plant tissues containing anthocyanin and other interfering compounds. Planta 207, 604–611.

Hoffmann C.M. (2010) Sucrose accumulation in sugar beet under drought stress. Journal of Agronomy and Crop Science, 243–252.

Hoffmann C.M. (2014) Adaptive responses of *Beta vulgaris* L. and *Cichorium intybus* L. root and leaf forms to drought stress. Journal of Agronomy and Crop Science.

Jones P.D., Lister D.H., Jaggard K.W., Pidgeon J.D. (2003) Future climate impact on the productivity of sugar beet (*Beta vulgaris* L.) in Europe. Climatic Change, 93–108.

Lyon D., Castillejo M.A., Mehmeti-Tershani V., Staudinger C., Kleemaier C., Wienkoop S. (2016). Drought and recovery -Independently regulated processes highlighting the importance of protein turnover dynamics and translational regulation in Medicago truncatula. Molecular & Cellular Proteomics 15, 1921–1937.

Meyer E., Aspinwall M.J., Lowry D.B., Palacio-Mejía J.D., Logan T.L., Fay P.A., Juenger T.E. (2014) Integrating transcriptional, metabolomic, and physiological responses to drought stress and recovery in switchgrass (Panicum virgatum L.). BMC Genomics 15, 527.

Moing A., Maucourt M., Renaud C. (2004) Quantitative metabolic profiling by 1-dimensional ^{1}H-NMR analyses, application to plant genetics and functional genomics. Functional Plant Biology 31, 889–902.

Monti A., Brugnoli E., Scartazza A., Amaducci M.T. (2006) The effect of transient and continuous drought on yield, photosynthesis and carbon isotope discrimination in sugar beet (*Beta vulgaris* L.). Journal of Experimental Botany 57, 1253–1262.

Morari F., Meggio F., Lunardon A., Scudiero E., Forestan C., Farinati S., Varotto S. (2015) Time course of biochemical, physiological and molecular responses to field-mimicked conditions of drought, salinity and recovery in two maize lines. Frontiers in Plant Science, 314.

Obata T., Fernie A.R. (2012) The use of metabolomics to dissect plant responses to abiotic stresses. Cellular and Molecular Life Sciences 69, 3225–3243.

Pinheiro C., Chaves M.M. (2011) Photosynthesis and drought, can we make metabolic connections from available data? Journal of Experimental Botany 62, 869–882.

Pires M.V., Pereira Júnior A.A., Medeiros D.B., Daloso D.M., Pham P.A., Barros K.A., *et al.* (2016) The influence of alternative pathways of respiration that utilize branched-chain amino acids following water shortage in Arabidopsis. Plant, Cell and Environment 39, 1304–1319.

van der Poel P.W., Schwieck H., Schwartz T. (1998) Sugar Technology - Beet and Cane Sugar Manufacture. Berlin, Bartens.

Robredo A., Pérez-López U., Miranda-Apodaca J., Lacuesta M., Mena-Petite A., Muñoz-Rueda A. (2011) Elevated CO_2 reduces the drought effect on nitrogen metabolism in barley plants during drought and subsequent recovery. Environmental and Experimental Botany 71, 399–408.

Ruffel S., Gojon A., Lejay L. (2014) Signal interactions in the regulation of root nitrate uptake. Journal of Experimental Botany 65, 5509–5517.

Semel Y., Schauer N., Roessner U., Zamir D., Fernie A.R. (2007) Metabolite analysis for the comparison of irrigated and non-irrigated field grown tomato of varying genotype. Metabolomics 3, 289–295.

Sims L., Pastor J., Lee T., Dewey B. (2012) Nitrogen, phosphorus and light effects on growth and allocation of biomass and nutrients in wild rice. Oecologia 170, 65–76.

Usadel B., Blasing O.E., Gibon Y., Retzlaff K., Hohne M., Gunther M., Stitt M. (2008) Global transcript levels respond to small changes of the carbon status during progressive exhaustion of carbohydrates in Arabidopsis rosettes. Plant Physiology 146, 1834–1861.

Wedeking R., Mahlein A-K., Steiner U., Oerke E-C., Goldbach H.E., Wimmer M.A. (2016) Osmotic adjustment of young sugar beets (Beta vulgaris) under progressive drought stress and subsequent rewatering assessed by metabolite analysis and infrared thermography. Functional Plant Biology 44, 119–133.

Wishart D.S., Jewison T., Guo A.C., Wilson M., Knox C., Liu Y., D…, Scalbert, A. (2013) HMDB 3.0—The Human Metabolome Database in 2013. Nucleic Acids Research 41, D801–D807.

Witt S., Galicia L., Lisec J., Cairns J., Tiessen A., Araus J.L., Palacios-Rojas N., Fernie A.R. (2012) Metabolic and phenotypic responses of greenhouse-grown maize hybrids to experimentally controlled drought stress. Molecular Plant 5, 401–417.

Wu G-Q., Wang C-M., Su Y-Y., Zhang J-J., Feng R-J., Liang N. (2014) Assessment of drought tolerance in seedlings of sugar beet (Beta vulgaris L.) cultivars using inorganic and organic solutes accumulation criteria. Soil Science and Plant Nutrition 60, 565–576.

Zrenner R., Sitt M. (1991) Comparison of the effect of rapidly and gradually developing water-stress on carbohydrate metabolism in spinach leaves. Plant, Cell and Environment 14, 939–946.

CONCLUDING REMARKS AND OUTLOOK

This thesis focused on the physiological and metabolic characterization of young sugar beets under progressive drought and during rewatering. One objective was to provide the chronology of physiological and metabolic changes under progressive drought and to demonstrate how these relate to a phenotypic approach using infrared thermal imaging. Further, the underlying metabolic mechanisms under rewatering of temporarily drought-stressed sugar beets were studied with special emphasis on differences between shoots and roots. Here, an untargeted ^{1}H-NMR approach in combination with targeted analyses of hexose-phosphates, starch, amino acids, nitrate and proteins, and physiological measurements including relative water content, osmotic potential, electrolyte leakage and malondialdehyde concentrations was performed. To reach these aims, an obligatory requirement was the development and implementation of a reliable and reproducible test system that allowed the controlled implementation of progressive drought and recovery during rewatering under greenhouse conditions as well as a sufficient, cost-effective and rapid analysis of physiological and metabolic changes.

The underling methodical and analytical setup is presented with detailed background information and can be used as a handbook for the daily laboratory work. One particular advantage of the targeted metabolite assays is that they can be used in small scale as well as for robotized metabolite analyses in high throughput systems.

The protocols of the enzyme based metabolite assays, that were primarily developed for the model plant *Arabidopsis thaliana*, were adapted to the different matrices of *B. vulgaris* and within the network project CROP.SENSe also to barley (*H. vulgaris*). However, it should be noted that the sample preparation of sugar beet roots was quite work intensive due to the high water content when it comes to the homogenization of the fresh plant material by mortar and pestle. An important outcome is here, that the use of an ultra-turrax® for the homogenization under liquid nitrogen is highly recommended. Besides a reduced manual work-load, sample preparation is accelerated and thus degradation processes can be reduced.

In case of the ethanolic extraction of freeze dried root material for the ^{1}H-NMR analysis it can be concluded that the dried and ground powder considerably expands upon addition of the extraction buffer. While this is easy to handle if samples are prepared „by-hand" this property is critical when using pipetting robots. Here, a test run and adjustment of the pipetting unit is highly recommended.

Although sample preparation and analysis of plant material for a metabolic approach by ^{1}H-NMR is time-consuming and more expensive in comparison to other metabolomics technologies such as GC-

MS or LC-MS, ^{1}H-NMR has an advantage regarding metabolites such as the quaternary ammonium compound glycine betaine, which are difficult or even impossible to detect by other technologies. Although the applied extraction provided detailed insights into of the metabolic changes in the primary metabolism, high amounts of glycine betaine in the shoot and the high sucrose content in the taproot partly hindered the characterization and identification of metabolites. Here, a previous purification step to get rid of sucrose and glycine betaine might improve the analysis.

By means of the invasive and non-invasive analysis of drought-stressed and rewatered sugar beets it was possible to characterize the dynamic development of distinct stress phases under drought and rewatering. Although IRT allowed the detection of the initial impairment of leaf transpiration within the first day of drought stress, only the destructive approach facilitate the differentiation of a phase of metabolic adjustment together with redirection of carbon flow into protective mechanisms and a subsequent phase of membrane destabilization and cellular damage caused by reactive oxygen species. Only the combination of destructive and non-destructive methods allowed the differentiation of the complete sequence of physiological changes induced by drought stress. This finding could be of special relevance for the selection of phenotypes that are adapted to early drought. Under rewatering, shoots of *B. vulgaris* rapidly re-established water relations, but membrane damage and partial stomatal closure persisted longer, which could have an impact on subsequent stress events. Taproots, however, required more time to recover the water status and to readjust primary metabolites than shoots.

The combined approach of the untargeted ^{1}H-NMR and targeted metabolite analysis together with physiological measurement of growth and the plant water status allowed the allowed the identification and characterization of major metabolites of the primary metabolism. While this revealed the metabolic strategy of the temporarily drought stressed sugar beets it was also shown that drought-induced changes in primary metabolism, changes of plant water status and membrane stability were mostly reversed within 12 days of recovery. In particular the clearly distinct recovery dynamics observed in roots and shoots, which were possibly related to the different functions of organs and their need for an efficient recovery. This was also emphasized by findings of the PCA, indicating that the roots sampled at the end of the rewatering period were metabolically distinct from control plants, while this was not the case in shoots. The second increase of AAAs at the end of the rewatering period was unique for shoots. However, it remains open whether this indicates an increased demand for these amino acids during the onset of regrowth, or whether it represents a stress imprint which might be beneficial during an upcoming drought stress event.

While the extent of membrane damage was demonstrated by microscopic investigations, damage repair of ROS induced injuries of membrane systems seemed to be of particular importance during

the early recovery phase. The late increase of glycine betaine and proline towards the end of the drought period especially in shoots might indicate the protective function of these metabolites specifically for the maintenance of favorable conditions for cellular restauration.

Even though the targeted analysis of further metabolites such as nitrate indicated a continued N-assimilation at least during the initial days of drought, metabolic adjustments and repair processes during recovery occurred at the expense of growth for at least 12 days. Whether this reduced growth rate or perturbation in the diurnal starch metabolism accounted for the observed significant increase in starch during the recovery period still awaits verification.

Finally, it can be concluded that the metabolism of young sugar beets can efficiently deal with severe transient drought stress and further, that drought and recovery are two distinct processes subjected to different regulatory mechanisms which are actively driven by the plant. This is underlined by the reaction of shoots and roots, reacting in a distinct physiological and metabolic manner.

While progressive drought leads to acclimation processes required for a new metabolic equilibrium under the increasing water deficit, rewatering results in a re-distribution of resources to ensure the recovery process, in an organ specific manner. This work provides tools to tailor phenotyping approaches for drought tolerance and underlying metabolic alteration in particular if invasive and non-invasive approaches such as IRT are combined.

Further work is on the way, where proteomic and transcriptomic issues are addressed with the aim to identify regulatory key mechanisms enabling sugar beets to rapidly react to episodic stress events. The first analysis of the leaf proteome revealed and induced protein adjustment and transcript analysis will hopefully reveal insights of the regulatory processes of stress endurance and the subsequent recovery process. Here, a complementary analysis of identified key enzymes of the primary metabolism is possible.